Report R-105

Report R-105

Research Contract between Euratom
and CISE
No. 060.61.7 - RDI

Liquid volume fraction in adiabatic two-phase vertical upflow-round conduit

by P. Alia, L. Cravarolo, A. Hassid, E. Pedrocchi

Topical Report No. 15

CISE Segrate (Milano), June 1965

DOCUMENTATION SERVICE

LIQUID VOLUME FRACTION IN ADIABATIC TWO-PHASE VERTICAL UPFLOW- ROUND CONDUIT

by

P. Alia, L. Cravarolo, A. Hassid, E. Pedrocchi

This work was performed in accordance with the provisions of the CAN-2 Program sponsored by the U.S.-EURATOM Joint Research and Development Board.

C. I. S. E. - Report R 105

June 1965

TABLES OF CONTENTS

Abstract

This report presents and discusses the results obtained at CISE under the CAN-2 Research Program on liquid volume fraction with vertical upward flow of two-phase (gas+liquid) mixtures in adiabatic conditions.

The experiments were carried out under the following conditions:

Geometry:	round conduits 1.5 and 2.5 cm I.D.
Fluids:	gas phase: argon
	liquid phase: water, ethyl alcohol
Gas flow rate:	15 ÷ 100 $g/cm^2 s$
Liquid flow rate:	20 ÷ 200 $g/cm^2 s$
Temperature:	$\sim$ 18-20 °C
Pressure:	up to 22 kg/cm^2

The experiments have been performed through various methods based on different principles which are briefly reviewed.

The results enable us to outline the dependences of liquid volume fraction upon the following parameters: specific mass flow rate, quality, gas density, surface tension, diameter.

An empirical correlation is discussed and compared with the available data in literature.

Foreword

This is the ninth topical report issued by CISE and devoted to the experimental work performed under the CAN-2 Research Program on the Hydrodynamics of two-phase adiabatic flow. It presents and discusses the results of liquid volume fraction.

The reports so far issued have been devoted respectively to the following subjects:

- CISE R-59: design and construction of a high pressure gas circulator for the new experimental facility.
- CISE R-53: pressure drop and film thickness data obtained with different channel geometries.
- CISE R-73: influence of some physical properties on pressure drop and film thickness.
- CISE R-75: design, construction and assembly of a high pressure experimental facility.
- CISE R-89: development of a new instrument for the investigation of the phase and velocity distribution in the region close to the wall.
- CISE R-82: development of a new instrument for the measurement of shear stress on the wall of a conduit and its application in mean density determination in two-phase flow.
- CISE R-92: development of a method for the measurement of the liquid volume fraction of two-phase two-component mixtures.
- CISE R-93: effect of entrance conditions and length on some hydrodynamics parameters.

Work on the hydrodynamics of two-phase flow was also carried out under the previous Research Program CAN-1: the results were presented and discussed in four topical reports (CISE R-26, R-35, R-41 and R-43) and in a special CISE Report ("A Research Program in Two-Phase Flow").

Acknowledgements

The authors are grateful to prof. M. Silvestri for his helpful suggestions and discussions throughout the work. They also wish to thank Mr. A. Colombo who carried out all the experimental work.

1. INTRODUCTION

1.1. In two-phase (gas+liquid) flow, the fraction of the conduit cross section occupied by either phase ($1-\alpha$ or α)-which will be hence forth referred to as liquid (or gas) volume fraction(°)-is in general different from the liquid (or gas) volume quality, derived from the volume flow rates as follows:

$$1 - X_v = \frac{Q_l}{Q_g + Q_l} = \frac{1}{1 + \frac{X}{1-X}\,\frac{\rho_l}{\rho_g}} \qquad (°)$$

This difference derives from two main reasons: (i) the local value of the component of the velocity in the flow direction for one phase (averaged over a suitable time interval) is different from that for the other and (ii) the phase distribution and velocity profiles are not uniform over the conduit cross section. In general the heavier phase is mostly concentrated in the region of low velocity and, as a consequence, the liquid volume fraction is larger than the liquid volume quality.

A useful parameter for representing the difference between $1-\alpha$ and $1-X_v$ is the ratio between the average actual velocity of each phase, i.e. slip ratio:

$$S = \frac{U_g}{U_l} \qquad (°)$$

(°) Unless otherwise stated, in the present report only quantities averaged over the cross section area of the conduit will be considered; therefore the indication of average will be omitted.

This parameter is correlated to the aforesaid quantities through the following relationship:

$$S = \frac{1 - \alpha}{\alpha} \quad \frac{X_v}{1 - X_v}$$

When slip ratio is equal to one, liquid volume fraction coincides with liquid volume quality and the flow can be considered as homogeneous. As regard this it is worthwhile mentioning that the condition of a flow, locally homogeneous - i.e. local values of S equal to 1 in every point of the test section - is not enough to lead to an overall slip ratio equal to one. In the case of local values of slip ratio equal to unity, overall slip ratio is equal also to unity, only if either the profile of velocity or phase distribution is uniform all over the cross section of the conduit.

In the specific case of a two-phase (gas + liquid) upward flow, slip ratio is in general larger than one and can take on values comprised broadly between 1 and 10 or even 100 and more in some cases, as for example with a pure annular flow pattern.

Another quantity related to the those above is the density of the mixture:

$$\rho = (1 - \alpha)\rho_l + \alpha \rho_g$$

which, according to the value of slip ratio, is in general different from the flow rate density, defined as follows:

$$\rho^* = (1 - X_v)\rho_l + X_v \rho_g$$

1.2. Knowledge of liquid volume fraction of two-phase (gas+liquid) mixtures is taking on greater and greater interest both from a fundamental point of view and for application purposes. In particular, for the utilization of steam-water mixtures as cooling agents for nuclear reactors, it is essential for the development of neutron statics and dynamics calculations to know the water content in the reactor core (i.e. the density of the mixture).

The problem of mean density determination in a boiling channel has been tackled both by collecting experimental data in various conditions and by developing theoretical models which could predict with a satisfactory approximation the experimental results and, eventually, the actual values in the case of a reactor boiling channel.

The experimental data so far collected by a number of authors are relevant to a large variety of conditions: as regards the mixture, components, geometry, heat transfer conditions, flow direction, etc. [2] to [16]. These results have been analysed only to a small extent and the conclusions to which they lead may even contrast with one another. In any case, among the data so far published, those obtained in a range of flow rates, quality, physical properties, geometries of interest for a reactor cooled by an evaporating steam-water mixture in forced convection (the so called "fog cooled reactor")[1] are very scarce. Furthermore the available experimental data are not enough to establish exactly the governing parameters or their influence: in particular the influence of flow rate, geometry, physical properties is far from clear.

The experimental data have been empirically and semi-empirically correlated in various ways. As far as adiabatic flow is concerned, the attempts of Lockhart-Martinelli[17], Martinelli-Nelson[18], Hughmark-Pressburg[19], Marchaterre[20], Von Glahn[21] can be men-

tioned. Among the analyses carried out in heat transfer conditions, the best known so far is that of Maurer[22].

Several attempts have been made also from a theoretical point of view. Starting from a number of hypothesis, some authors developed models which, in some cases, satisfactorily predicted the experimental values[23][24][25][26].

1.3. The scarcity of suitable experimental data and the need to check the existing correlations or to develop a new correlation in the range of interest for nuclear reactor design[1], led us to undertake a systematic experimental investigation under the CAN-2 Program.

However, due to the difficulties inherent in the measurements in heat transfer conditions at large pressure, it seemed appropriate to begin with experiments on the CISE existing facility[27] at room temperature, but at high pressure, with a two-phase two component mixture. Provided the influence of physical properties is determined, it would be possible to predict the $1-\alpha$ values relevant to steam-water mixtures in adiabatic conditions (par. 6.2). As will be discussed in more detail later (par. 6.3), the effect of heat addition should not be important at least in the annular-dispersed flow: therefore it would also be possible to predict the $1-\alpha$ values in conditions close to those foreseen for a nuclear reactor, in the portion of the evaporating channel where annular dispersed flow is established.

There are two advantages in such a procedure:

- the experiments in cold conditions are simpler and more accurate than in hot conditions and therefore a systematic investigation is possible without great difficulties to select the best measurement method for application to hot conditions;

- it is possible, with two-phase two componet mixtures to find out the influence of each physical property, while with steam-water mixture experiments it is not possible to differentiate the effect of the single parameters. In this case, in fact, only a dependence upon operating pressure can be found.

1.4. This report presents and discusses the experimental data obtained during the CAN-2 Research Progral and the various methods used for the measurements. An empirical correlation is proposed for liquid volume fraction whiqh is also compared with the few experimental data available in the literature. A discussion is given about its eventual application in the case of a reactor evaporating channel.

The measurements have been carried aut on the experimental loop already described in[27] and whose schematic flow-sheet is presented in Fig. 1. The two-phase mixture is formed in a tee-mixer[27] with the gas entering the run side, the liquid is injected through an annular slot with an adjustable aperture. After passing through a calming section (50 cm long) the mixture enters the vertical test section (300 cm long). At the top the test section leads into a high efficiency separator out of which each separated phase returns to its own circuit.

1.5. The experimental data described in the present report are relevant only to circular tubes with vertical upward flow: the flow regimes investigated were mostly annular-dispersed flow[°] and, to a

---

(°) As it has been recently defined[28] the annular-dispersed flow consists of two main regions: the central region of the the duct characterized by a continuous gas phase and a discontinuous liquid phase; the region close to the walls where exactly the opposite situation exists.

lesser extent, the bubble flow. The flow patterns were identified visually: the regions investigated are outlined on the Baker plot[42] in Fig. 2.

The effect of the following parameters are analysed:

- quality X (or any quantity related to it as $1-X_v$)
- mass flow rate G (or any quantity related to it as G_g or G_l)
- gas density ρ_g
- surface tension γ
- diameter D

The effects of the other parameters, namely liquid density, gas and liquid viscosity were not investigated experimentally but are analysed on the basis of the already available data and of the experimental evidence so far achieved at CISE.

The mixtures investigated were argon-water and argon-pure ethyl alcohol at various operating pressures and at a temperature of 18-20° C. In this way the influence of surface tension and gas density could be outlined(°).

The physical properties of the various mixtures are tabulated in Table I for the operating temperatures and pressures. The range of the variables investigated are reported in Table II.

(°) The difference (Table I) between the values of density and viscosity of water and ethyl alcohol should have a negligible effect on the results since the difference is small compared to that of surface tension and, moreover, since the influence of these two quantities, as will be dealt with later (see par. 4.4.), should be small.

TABLE I

PHYSICAL PROPERTIES

Fluid	Θ °C	P kg/cm^2(a)	ρ g/cm^3	μ poise	γ dyne/cm
Water	18	up to 22	1.000	1.06×10^{-2} (2)	73.0 (2)+
Ethyl Alcohol*	20	" " 22	0.789 (1)	1.20 " (1)	22.5 (1)
Argon	18	21.8	36.1×10^{-3}	2.27×10^{-4} (3)	
"	18	16.8	27.7 "	2.26 " (3)	
"	18	11.5	18.8 "	2.25 " (3)	
"	18	6.15	10.0 "	2.24 " (3)	

* Alcohol Aethylicus anhydricus 99.9% by vol. - Carlo Erba - Milano

\+ At atmospheric pressure

(1) International Critical Tables -Mc Graw-Hill Book Compagny - New York 1933

(2) Handbook of Chemistry and Physics - C.D. Hodgman Ed. 40th, 1958-59

(3) Nuclear Engineering Handbook - H. Etherington Ed. 1st, 1958

TABLE II

MIXTURES	GEOMETRY: ROUND TUBE	GAS DENSITY	EXPERIMENTS AT G_g and G_l CONSTANT		EXPERIMENTS AT G and X COSTANT	
			G_g	G_l	G	X
		g/cm^3	g/cm^2 s	g/cm^2 s	g/cm^2 s	
Argon-water	2.5 cm I.D.	36.1×10^{-3}	16 + 94	22.1 + 206	100 + 200	0.015 + 0.15
"	"	27.7×10^{-3}			50 + 200	0.015 + 0.50
"	"	18.8×10^{-3}			50 + 200	0.010 + 0.37
Argon-water	1.5 cm I.D.	36.1×10^{-3}	27.8 + 94	22.1 + 177	100 + 250	0.016 + 0.172
"	"	27.7×10^{-3}	27.5 + 95	22.1 + 157		
"	"	18.8×10^{-3}	27.5 + 47.5	22.1 + 119		
Argon-ethyl alcohol	2.5 cm I.D.	36.1×10^{-3}	16 + 94	22.1 + 177	100 + 200	0.015 + 0.15
"	"	18.8×10^{-3}	16 + 27.7	22.1 + 66.5	100 + 150	0.015 + 0.05
"	"	10.0×10^{-3}	8.5 + 14.7	22.1 + 66.5		

2. MEASUREMENT METHODS

2.1. A number of methods, briefly described in a preceding report[29] have been developed by the various authors for the measurement of liquid volume fraction and of the related quantities. At CISE four methods, based on various operating principles, have been utilized in order to find out a simple and reliable method which could be systematically used for the determination of $1 - \alpha$ in the conditions and range that interest us. Furthermore, through a comparison of the results obtained in various ways, it has been possible to confirm indirectly the estimated accuracy of the experimental data.

The four methods, which have been extensively described in previous reports, are the following:

a) Measurement of the attenuation of a β radiation produced by a small Sr^{90} source moveable along a diameter of the conduit. The density of the mixture was worked out by integrating the measured distribution of material along a diameter[30][2]. These measurements have been performed with argon-water at $\rho_g = 36.1 \times 10^{-3}$ g/cm^3 and on a 2.5 cm circular conduit, at a distance from the inlet equal to 150 cm(°).

b) Measurement of the phase distribution profiles over a conduit cross section determined by means of two isokinetic sampling probes especially designed for investigating both the central region of the conduit[2][27] and that close to the wall[31]. The profiles obtained in this way are integrated to give the overall liquid

---

(°) These measurements were made under the CAN-1 Research Program on the experimental loop provided with a test-section 150 cm long[2].

volume fraction. The measurements have been made with various mixtures, on a 2.5 cm. I.D. circular conduit at a distance from the inlet equal to $\sim$ 350 cm.

c) From the momentum balance equation, provided the momentum variation along flow direction is negligible with respect to the weight term, by measuring shear stress[33][34] and pressure drop. In this case it can be written in fact:

$$\rho = \frac{1}{g} \left[\frac{\Delta P}{\Delta Z} - \tau \frac{4}{D} \right]$$

The measurements have been made with various mixtures, on a 2.5 cm I.D. circular conduit at a distance[°] from the inlet equal to $\sim$ 350 cm.

d) Direct measurement of the liquid hold-up value over a length L of the conduit, through the determination of the liquid level variation in a burette connected to the liquid line of the circuit in correspondence with the following two conditions: two-phase flow and single-phase (gas) flow in the test element[29]. The length of conduit over which the liquid hold up is determined is comprised between two sections respectively 130 and 400 cm distant from the mixer.

2.2. Before comparing the results obtained through the various methods it is necessary to recall that phase distribution and velocity profiles, hence liquid volume fraction can undergo a significant

---

(°) The measurements of τ are performed over a tube length equal to $\sim$8 cm and can therefore be considered as local measurements.

variation along flow direction even in the case of adiabatic flow[32][35]. In annular-dispersed flow in the conditions relevant to the present experiments, this variation is negligible at the low flow rates and increases mainly with increasing liquid[°][32]. However the experimental evidence is that at the top of the test element ($\sim$350 cm apart from the mixing section) the flow configuration should be quite close to the fully developed flow even at the largest flow rates investigated.

To carry out a significant comparison it is necessary therefore to consider only measurements performed at the same position along flow direction if the data obtained even at the largest mass flow rates are taken into account; otherwise the comparison must be limited to experiments at low flow rates.

2.3. For sake of simplicity, all the comparisons are carried out against the results obtained with method (d), with which most of the data have been collected. As stated, this method gives an average value of liquid volume fraction over a length L; at the low flow rates this value should be practically equal to that relevant to fully developed flow[32]. On the contrary, at the largest mass flow rates, there is a certain difference which, as has been discussed earlier[29], should not be larger in any case than 5 - 10%. On the whole the measurement error of this method, which increases at low values of $1 - \alpha$, has been estimated as $\pm$ 10% [29].

(°) In particular it has been found that:
- for liquid flow rates smaller than 80 g/cm^{2}s the variation of $1 - \alpha$ along flow direction is negligible whatever the gas flow rate;
- at larger liquid rates, at least in the annular-dispersed flow region, $1 - \alpha$ decreases asymptotically along flow direction; the variation between L = 150 cm and L = 350 cm is practically independent of the gas flow rate and increases with increasing G_l (up to 20% at most).

2.3.1. Data obtained with method (a): The results given by this method suffer from an error[30] mainly due to the assymetry of the profiles of material distribution over the conduit cross section at the measurement position. This assymetry is very low at the low flow rates (gas and liquid) and increases with the increase of these parameters. This and the fact that at the large liquid rates there should be a difference due to the variation along flow direction render the comparison at large flow rates meaningless.

The comparison is presented in table III ($\rho_g = 36.1 \times 10^{-3}$ g/cm^3 argon-water mixtures); as expected, at high flow rates there is a noticeable discrepancy, while at the low flow rates the agreement is quite satisfactory.

2.3.2. Data obtained with method (b): The results given by this method are affected by the error inherent in the integrating procedure as well as the inherent measurement error of the isokinetic probes. Since in the present case the phase distribution profile is known on almost the whole cross section, the error should not be larger than 10 ÷ 15%; the worst case being that of the largest total flow rate and quality. It is worth mentioning, on the other hand, that in the position where these measurements have been performed, the assymmetry of the profiles is unappreciable, hence its impact on the total error.

As far as the data with argon-water mixtures are concerned, the agreement is always within ± 15% (Table IV). It is worse for argon-alcohol mixtures because in this case the profiles are less regular than those experienced with argon-water mixtures: nevertheless, the agreement between the two sets of results is still quite satisfactory except for one point for which the value given by method (b) is much larger than the other one.

TABLE III

G_g	G_l	$(1-\alpha)'$	$(1-\alpha)''$	$(1-\alpha)'/(1-\alpha)''$
g/cm^2s	g/cm^2s			
24	25.5	0.107	0.115	0.93
"	45.1	0.155	0.163	0.95
"	78	0.229	0.215	1.065
"	135	0.234	0.280	0.84
32	25.5	0.092	0.088	1.045
"	45.1	0.126	0.130	0.97
"	78	0.190	0.173	1.10
"	135	0.174	0.225	0.77
55	25.5	0.063	0.052	1.21
"	45.1	0.083	0.076	1.09
"	78	0.095	0.105	0.90
"	135	0.169	0.150	1.13
73	25.5	0.045	0.037	1.215
"	45.1	0.054	0.054	1.00
"	78	0.071	0.077	0.92
"	135	0.146	0.116	1.26

$(1-\alpha)'$ = values obtained from attenuation of a β radiation (method "a")

$(1-\alpha)''$ = values obtained from direct measurement of the liquid hold-up (method "d")

TABLE IV

MIXTURES	GEOMETRY: ROUND TUBE	GAS DENSITY g/cm^3	G_g g/cm^2s	G_l g/cm^2s	$(1-\alpha)'$	$(1-\alpha)''$	$(1-\alpha)'/(1-\alpha)''$
Argon-water	2.5 cm I.D.	36.1×10^{-3}	24.0	25.5	0.115	0.115	1.00
"	"	"	"	135	0.277	0.280	0.99
"	"	"	73	25.5	0.0301	0.0375	0.80
"	"	"	"	135	0.102	0.117	0.87
"	"	"	82	206	0.127	0.124	1.02
Argon-ethyl alcohol	"	"	24.1	25.5	0.108	0.115	0.94
"	"	"	24.3	135	0.280	0.289	0.97
"	"	"	73	25.5	0.0303	0.0183	1.66
"	"	"	"	135	0.098	0.098	1.00

$(1-\alpha)'$ = values obtained from integration of phase distribution profiles (method "b")

$(1-\alpha)''$ = values obtained from direct measurement of the liquid hold-up (method "d")

The reason for this discrepancy is still not clearly understood: on the one hand the phase distribution profile is somewhat irregular (Fig. 3) and this could lead to a considerable error in the integration; on the other hand, as will be discussed throughly later (see par.4.4), method (d) gives, in this range, liquid volume fraction values that are quite low and for these values the error with method (d), as stated, can be quite large. The matter therefore is still obscure and further experiments are thus needed to get a definite answer to this question.

2.3.3. Data obtained with method (c): As has been discussed throughly in a previous report[34], the data obtained with this method can be affected by quite large errors with increasing quality and total flow rate. This is due to two reasons:

- A given error on τ and $\Delta P/\Delta Z$ gives rise to an error on $1-\alpha$, derived through the above mentioned equation (page 10), which increases with increasing τ and $\Delta P/\Delta Z$, i.e. with increasing total flow rate and quality (appendix A).

- In addition, increasing these two parameters, the momentum variation along flow direction (ΔM) increases. In the above equation a term equal to $\frac{1}{\Omega} \frac{\Delta M}{\Delta Z}$ should have been introduced; the error on ρ ($\Delta\rho/\rho$) due to neglecting this term depends on the quantity $\frac{1}{\Omega} \frac{\Delta M}{\Delta Z}$[34] which increases with the increase of both G and X[32][34]. Thus, even if the measurements were carried out at a large distance from the mixer, the data are reliable only in a restricted range at low flow rate and quality.

As shown (Fig. 4)[(°)], the liquid volume fraction values obtained

(°) The points for which the probable error is larger than 20-30%, even if the term $\frac{1}{\Omega} \Delta M/\Delta Z$ were negligible, are omitted.

with this method are always larger than those obtained with method (d), and this difference, as stated, increases with the increase of both flow rates. As an example, we indicate, (for argon-water mixtures at $\rho_g = 36.1 \times 10^{-3}$ g/cm^3) for each gas flow rate, the liquid rate above which the discrepancy is larger than 10%:

G_g (g/cm^2 s)	G_l (g/cm^2 s)
16	206
21	206
27	206
35	91
47	91

The same trend, but more pronunced (especially as far as gas flow rate is concerned) is found for argon-alcohol mixtures (Fig. 4);this is due to the larger momentum variation with these mixtures[32].

At the lowest flow rates, however, in this case, too, the agreement is satisfactory.

2.4. From the considerations so far discussed, it can be stated that for the whole range of flow rates, the results given by the various methods agree satisfactorily. Hence this conclusion can be considered as a further confirmation of the reliability of the results presented in this report which, as stated, has been evaluated,for method (d), at $\pm$ 10%.

3. EXPERIMENTAL RESULTS

3.1. The experimental results of liquid volume fraction obtained during the present investigation are presented in Appendix B. On the whole approximately 300 points have been taken with the various methods.

As stated, most of the points have been obtained with method (d), described in par. 2.1. In the low quality range, corresponding approximately to the region of bubble flow, the data have been obtained through method (c) which, in this range, has a large accuracy.

In the following table the points obtained with each method are presented:(°)

method	(a)	16 points
method	(b)	13 "
method	(c)	70 "
method	(d)	223 "

(°) Experimental data obtained with method (a) are presented in [2][30].

4. ANALYSIS OF EXPERIMENTAL DATA

4.1. The choice of the quantity to be analysed among the three which are usually taken into account (i.e. density of the mixture (ρ), overall liquid or gas volume fraction ($1-\alpha$ or α), overall slip ratio (S)) is closely related to the utilization required for this parameter. For nuclear reactor calculations it is necessary to determine the overall water content in the reactor (under the form both of liquid and gas phase), and, in particular in a single channel[1]. This quantity is closely linked to the density of the mixture and this parameter should therefore be the one that is analysed and eventually correlated with a sufficient approximation.

A parameter which is as useful as density since it presents the same degree of approximation over the whole range(°) is liquid volume fraction. By contrast, gas volume fraction (or void fraction as it has been frequently and rather improperly called) which has so far received the largest attention, can be quite useful in the case of very low quality mixtures (where ρ is close to ρ_1) but loses some of its importance when dealing with high quality mixtures since the error with which is affected can lead to very large errors on ρ.(°)

(°) By definition:

$$\rho = (1-\alpha)\,\rho_1 + \alpha\,\rho_g$$

so that

$$\left|\frac{d\rho}{\rho}\right| = \left|\frac{d(1-\alpha)}{1-\alpha}\right| \left(1 - \frac{\rho_g}{\rho}\right)$$

$$\left|\frac{d\rho}{\rho}\right| = \left|\frac{d\alpha}{\alpha}\right| \left(\frac{\rho_1}{\rho} - 1\right)$$

Another parameter which has been taken into consideration is slip ratio, a parameter which would surely be suitable also from a fundamental point of view. Unfortunately, however, in general it cannot be measured directly and the values derived from measurement of other quantities usually sufer from a very large scattering so that they cannot be analysed or correlated satisfactorily. Furthermore this parameter can give the water content in a channel only through a calculation of density,(°) or liquid volume fraction: it therefore seems useless to have recourse to such a parameter.

In the following, attention will be given mostly to liquid volume fraction since, as stated, such a choice does not lead to any drawback in the determination of ρ and because it is the quantity we have measured directly.

4.2. Strictly speaking, liquid volume fraction should depend in vertical upflow in adiabatic (fully developed) conditions upon the following parameters:

- gas and liquid flow rates through various couples of the related quantities (G and X, G_g and G_l, U^* and X_v(°°), ect), the choice of a given couple depending upon theoretical or practical considerations;
- gas and liquid density ρ_g, ρ_l;
- gas and liquid viscosity μ_g, μ_l;

(°) $$\rho = \frac{S(1 - X_v)}{S(1-X_v) + X_v} (\rho_l - \rho_g) + \rho_g$$

(°°) A definition of these quantities is given in the nomenclature.

- surface tension σ;

- a characteristic geometrical parameter which, for circular conduit, is the diameter of the conduit D.

In heat transfer conditions liquid volume fraction should depend also, a priori, upon heat flux or/and total power given to the channel.

The effect of the aforesaid parameters depends in general upon the established flow pattern. In the present experiments attention has been given mostly to the bubble and annular-dispersed flow, as it has been visually observed and confirmed by the Baker's prediction[42] (Fig. 2). In this regard it can be mentioned that with most of the flow rates investigated ($G > 100$ g/cm^{2}s at $\rho_g = 36.1 \times 10^{-3}$ g/cm^3) there is a smooth transition (at constant flow rate) from the bubble flow into the annular-dispersed flow region in correspondence with a volume quality equal, as a rule of thumb, to $1-X_v \simeq 0.5 \div 0.7$ (Fig. 5). (This is more or less in agreement with what Baker's map, as shown in Fig. 6, predicts).

4.3. Effect of flow rates

4.3.1. The effect of flow rates is outlined in Figs. 7 and 8, relevant to the $1-\alpha$ data with argon-water mixtures at $\rho_g = 36.1 \times 10^{-3}$ g/cm^3 which is the condition that has been most investigated.

From Fig. 8 it appears that two main regions can be distinguished: a region corresponding to $1-X_v \lesssim 0.65$, for which liquid volume fraction is larger than $1-X_v$ and a second one, corresponding to $1-X_v \gtrsim 0.65$, in which the liquid volume fraction coincides, within the measurement errors, with the liquid volume quality. The transition between the two regions corresponds approximately, to the transition between annular-dispersed and bubble flow.

In Figs. 7 and 8 the parameters taken into consideration are X, $1-X_v$ and G. As far as quality is concerned it appears that $1-\alpha$ is closely related to $1-X_v$, as was also expected from a physical point of view, and therefore any analysis should start from this parameter. As far as flow rates are concerned the parameters could have been G_g or G_l or U^* : none of these however would have been so easy to handle as G, when dealing with evaporating two-phase mixtures, which is constant along the channel length.

4.3.2. In the region for which $1-X_v \lesssim 0.65$, the ratio between $1-\alpha$ and $1-X_v$ at constant G increases with the increase of quality (or decrease of $1-X_v$) and can reach even quite large values ($\frac{1-\alpha}{1-X_v} \simeq 3 \div 4$) at the largest qualities. This is shown clearly by the following relationship which is quite satisfactory in the region $1-X_v \lesssim 0.2$:

$$1 - \alpha = k\,(1-X_v)^{0.8}$$

Correspondingly slip ratio increases with quality (Fig. 9). The large values for slip ratio are a consequence of the fact that in annular dispersed flow a substantial portion of the liquid flows close to the wall where the velocity is low; thus, even if the local slip ratio is equal to unity - as actually it is in annular-dispersed flow[28] - the overall slip ratio can be larger.

The influence of total mass flow comes out clearly in the above figures: in the low quality region ($1-X_v \gtrsim 0.35$) it is negligible (in any case its seems that $1-\alpha$ increases with G); with greater quality, $1-\alpha$ decreases with the G increase and in the range of high quality ($1 - X_v \lesssim 0.2$) such a dependence can be written as follows:

$$1 - \alpha = k/G^{0.3}$$

The same trend has been found for all the conditions investigated. It must be mentioned however that in the region of low $1 - X_v$ the dependence upon G decreases with diameter (Figs. 8 and 10) and with the increase of surface tension (Figs. 8 and 11).

4.3.3. The influence of these parameters has been studied by various authors; however while the influence of quality has been widely analysed and there is a good agreement between the conclusions drawn by the various authors, the same cannot be said about flow rate.

As far as the influence of quality is concerned the general conclusion is that, in agreement with the trend outlined in the previous paragraph, the ratio $\frac{1-\alpha}{1-X_v}$ increases with quality at the same G. As an example we can mention the experimental data obtained by Marchaterre et al.[36], Semenov et al.[8], Kosterin et al.[9], Hewitt et al.[11], Haywood[6] et al. The same trend is given by the correlations proposed by Lockart-Martinelli[17], Martinelli-Nelson[18], Marchaterre-Hoglund[20], Hughmark-Pressburg[19], Bankoff[25].

The agreement about the influence of flow rate is far less clear. This is probably due to the fact that the range investigated by the various authors is different; in fact, as shown in the previous paragraph, in the high quality region this influence is clear, whereas in the low quality region it is very small and rather obscure. Thus, as might be expected, most results collected by the above researches, showed a trend, in the high quality region, similar to the present data (see for example the data presented by Marchaterre et al.[36], Semenov et al.[8], Hewitt et al.[11]. On the contrary if most of the data are collected in the low quality region, the influence of G is found to be negligible (see for example the data of Isbin[4], Haywood[6], SNECMA[15]).

As a consequence even the available correlations in the literature do not agree with each other:

- Martinelli-Nelson[18], Lockhart-Martinelli[17], Bankoff[25], correlations do not take into account any influence of flow rate;
- the Marchaterre-Hoglund[20], Hughmark-Pressburg[19] correlations state that liquid volume fraction decreases with the G increase.

4.4. Effect of physical properties

4.4.1. Gas density. The dependence of $1-\alpha$ upon ρ_g has been established at the same $1-X_v$, to which $1-\alpha$ is closely related. Similarly, from a physical point of view, it should be better to carry out the analysis at constant velocity instead of at constant specific mass flow rate. In this regard, however, it must be kept in mind that the range of gas density investigated is not large enough to establish whether G or U^* is the governing parameter; furthermore, as stated, the choice of such a parameter would lead to some difficulties in the density calculations in a power channel. Thus, we preferred to analyse the data at constant G.

The dependence upon gas density is outlined in Fig. 12 where, for simplifying purposes, only some of the data obtained with argon-water mixtures at ρ_g = 36.1 and 18.8 x 10^{-3} g/cm^3 have been plotted against $1-X_v$ at two different G; as shown, $1-\alpha$ decreases in general with the increase of ρ_g; this effect which is negligible at small qualities ($1-X_v \lesssim 0.20$) increases with the increase of quality, i.e. going into the annular dispersed flow region, for which we can write:

$$1-\alpha = k(1/\rho_g)^{0.2} \quad \text{(at the same } 1-X_v \text{ and G)}$$

Such a dependence, which has been shown only for a given case (Fig. 12), is also valid for the argon-alcohol mixture and for the other geometry investigated.

A confirmation of such a dependence from the data available in the literature is quite difficult: most of these data were in fact obtained at various pressures with steam-water mixtures[6][8][9][36], for which cases it is not possible to distinguish the effect due to the variation of gas density from that of surface tension which can be quite important.

On the other hand the best known correlations for two-component systems foresee an influence of gas density which has been shown in Fig. 13.

The Lockhart-Martinelli correlation[17] (which apparently does not hold for $1-X_v \gtrsim 0.3 \div 0.4$ since it gives $1-\alpha$ values smaller than $1-X_v$) predicts a dependence upon ρ_g which is quite similar to that of the present experiments; the same conclusion is given by the Hughmark-Pressburg correlation[19]. The Marchaterre-Hoglund correlation[20] does not outline any appreciable influence of ρ_g: this is due to the fact that this correlation can be utilized only in the range of large $1-X_v$, where, as stated, the influence of ρ_g is very small.

4.4.2. Surface tension: the influence of surface tension can be derived from a comparison of the data obtained respectively with argon-alcohol (Fig. 11) and with argon-water mixtures (Fig. 8) (at the same gas density $\rho_g = 36.1 \times 10^{-3}$ g/cm^3) (Fig. 14). Qualitatively the dependence upon $1-X_v$ and G (Figs. 8 and 11) is the same in the two cases i.e. $\frac{1-\alpha}{1-X_v}$ increases with the decrease of $1-X_v$ and the decrease of G; however, from a quantitative point of view the fol-

lowing difference can be observed:

- In the range of large $1-X_v$ ($1-X_v \gtrsim 0.3$), the values of $1-\alpha$ with alcohol are slightly larger than those found with water; in other words the value of $1-X_v$ above which $1-\alpha$ coincides with $1-X_v$ is larger than that found with water as the liquid phase.
- In the range $0.05 \lesssim 1-X_v \lesssim 0.30$ (these limits are approximate and vary according to the flow rates) the values obtained with alcohol are lower than those obtained with water at the same $1-X_v$; in this range it can be observed that the influence of G and $1-X_v$ is larger than with water as the liquid phase (Figs. 11 and 14).
- In the range $1-X_v \lesssim 0.05$, $1-\alpha$ decreases abruptly with $1-X_v$ and even becomes equal to $1-X_v$ at the lower values of this parameter. As a consequence the trend of slip ratio is to increase with quality (with decreasing $1-X_v$), to reach a maximum which can be high as 1.5÷2.5 according to the flow rates, and then to decrease again down to a value equal to one. This trend appears especially at the largest mass flow rate ($G > 100 \div 150$ g/cm^{2}s) (Fig. 15).

In this regard, it is worth mentioning that the existing correlations do not predict slip ratio values equal to 1 in this range of quality. However the available experimental data are very scarce and are not enough to confirm or not the trend found in the present experiments(°). On the other hand there is no evidence, as stated, of any

---

(°) In particular the results obtained by Russian authors[8] relevant to steam-water mixtures even at large pressure (up to 120 Kg/cm^2) i.e. with very low surface tension, do not show any similar trend, since they investigated quite a different range; at G 100 g/cm^{2}s the smallest $1-X_v$ investigated is 0.06÷0.09 while data relevant to the range $1-X_v \lesssim 0.05$ were obtained only with lower G where the said effect has been found to be rather small in the present investigation.

measurement error; moreover in the region for which such trend is observed, also the pressure drop shows an abnormal trend (Fig. 16) thus confirming that the phenomenon should be intrinsic to the flow. In any case, this effect being so far unknown, for the sake of prudence any attempt to correlate and analyse the points obtained with alcohol will be limited only to the region for which $1-X_v > 0.05$ where the trend is confirmed by other data.

In the range $0.05 \leq 1-X_v \leq 0.3$, the dependence upon γ can be expressed, in a first approximation, as follows:

$$1 - \alpha = k \gamma^{0.3}$$

In the range $1-X_v \geq 0.3$ the dependence is the contrary, as stated, but much lower than in the annular-dispersed flow range.

Experimental data obtained with various liquids with a view to determine the influence of surface tension, could not be found in the existing literature. Data are available only for steam-water mixtures[6][8][9] at various pressures but in these cases it is difficult to distinguish the effect of the variation of surface tension from that of other parameters (in particular ρ_g) (see par. 4.4.1.).

The only correlation for two-phase two component mixtures which takes into account the influence of surface tension is that of Hughmark and Pressburg[19] who, on the basis of experiments carried out with various liquids, predicts, in the range of annular-dispersed flow, qualitatively the same dependence as has been found in the present experiments (Fig. 17). It is worth mentioning in this regard that the influence of γ in this correlation is almust the same over the range $0.01 \leq 1-X_v \leq 1$ which is in contrast with the present experimental evidence.

The correlations valid for steam-water mixtures indicate[8][18][20] that $1-\alpha$, at the same $1-X_v$, decrease with the increase of pressure: this effect however must be partly due to the effect of gas density (par. 4.4.1). An example is given in Fig. 18 which shows the influence of pressure according to the Martinelli-Nelson correlation between the two values: P=38 kg/cm^2 abs. and P=70 kg/cm^2 abs. The effect of gas density only, as we observed experimentally at constant γ and other parameters, is shown in the same figure: appearently in the former case the effect is larger than in the latter probably due to the influence of the surface tension variation.

4.4.3. Other physical properties. The effect of the other physical properties has not been studied in the present work. However previous experiments[2][38] indicate indirectly that gas and liquid viscosity should have a negligible effect, at least in the annular-dispersed flow regime.

As far as gas viscosity is concerned, experiments[38] with argon (μ_g = 2.21 x 10^{-4} poise) and nitrogen (μ_g = 1.8 x 10^{-4} poise) as the gas phase, have shown that the influence of μ_g on film thickness and pressure drop, at least in this range, is negligible. Since liquid volume fraction is closely related to film thickness[2] $1-\alpha$ too should depend hordly at all on μ_g. No experiments have been carried out to ascertain this to the authors' knowledge: the only indication is that of the existing correlations for two-component mixtures. As concerns this, while the Lockhart-Martinelli correlations confirms that the influence of μ_g should be negligible ($1-\alpha \equiv \mu_g^{-0.04}$), that of Hughmark and Pressburg indicates an important dependence which can be represented as $1-\alpha \equiv \mu_g^{1.3}$. This trend however derives from a comparison between the results obtained with low pressure steam-

water mixtures and with air-water mixtures at atmospheric pressure under two quite different experimental conditions; it might be that the difference between these two sets of data should be attributed to effects different from that of μ_g.

The influence of liquid viscosity has been studied indirectly by observing its influence on film thickness[2]: the variation of liquid viscosity ($0.7 < \mu_l < 1.4 \times 10^{-2}$ poise) was achieved with water as liquid phase by varying the test section temperature from 16°C to 37°C. Similarly as for μ_g, the influence has been found negligible both on film thickness and pressure drop, at least in this range.

The influence of μ_l has been throughly investigated by Fohrman[37] (with liquids having $0.75 < \mu_l < 500$ centipoise), who proposed the correlation

$$S = 80 \mu_l^{0.30} X^{0.77}$$

It is worth mentioning however that this correlation has been derived from data relevant to two component mixtures at low velocity flowing in a horizontal thin rectangular channel with μ_l values much larger than those relevant to the present experiments (1 centipoise) and contitions quite different from those taken into consideration in the present experiments.

Similarly Hughmark Pressburg[19] on the basis of data relevant to various liquids ($1 < \mu_l < 29$ poise) found that $1-\alpha$ increases with μ_l but to a smaller extent than that observed by Fohrman[37].

The Lockhart-Martinelli correlation[17], on the other hand, foresees quite a negligible dependence upon μ_l which is equal (in a contrary sense) to that of μ_g.

The effect of μ_l, therefore, is still obscure and must be furtherly studied since the variation of liquid viscosity, in the field concerned

is quite large and it should be therefore taken into account. In this regard, however, it must be mentioned that all the investigations were performed at viscosities larger than 1 cp. Little can be stated on the basis of these results in the range $\mu_l < 1$ cp.

No experiment has been performed in order to outline the dependence upon liquid density; even in the literature information is very scarce. The existing correlations on the other hand foresee that the influence of this parameter should (in a contrary sense) be approximately equal to that of gas density (for example that of Lockhart-Martinelli[17], Hughmark and Pressburg[19]), as would be expected.

4.5. Effect of geometry

As stated, in the present experiments only two circular tubes with a diameter of 2.5 and 1.5 cm I.D. have been tested. The following results have been obtained (Fig. 19):

- In the annular-dispersed flow region ($1-X_v \lesssim 0.2$) liquid volume fraction increases with the decrease of diameter, at the same specific mass flow rates, quality and other physical properties. The influence of diameter, which in any case is relatively small, can be roughly written in the following form in this range:

$$1 - \alpha = k\, D^{-0.2} \quad \text{(at the same G, } 1-X_v\text{, physical properties)}$$

- In the region for which $1-X_v \gtrsim 0.2 \div 0.4$, according to flow rate, the influence of diameter changes its sense (Fig.19). The reason for this is not clear and in any case this trend must be confirmed with proper experiments with different diameters since the range of diameters investigated is quite small.

The information available in the literature as regards the effect of diameter is very scarce. Data obtained with air-water mixtures at atmospheric pressure[15] with three circular tubes respectively 1.0; 2.0; 3.0 cm I.D. (Fig. 20) do not outline any influence of the diameter within the measurement inaccuracy. The data relevant to steam-water mixtures at 600 psig reported in[14][36], obtained with two circular tubes 2" I.D. and 0.622" I.D. respectively, show a dependence ($1-\alpha$ decreases with D) which does not contrast with our results since all these experiments were performed in a range of $1-X_v$ in correspondence to which in our case as well the dependence on diameter is contrary to that in the low $1-X_v$ range (Fig. 21).

A trend different from that outlined in the present experiments (for $1-X_v \lesssim 0.2$) has also been found by Semenov and Tochigin[8], who operated with steam-water mixtures in two circular tubes 3.0 cm and 1.7 cm I.D. in a range of G corresponding to that of the present investigation (par. 5.4.4.) (Fig. 22). It must be observed however that these authors operated in such a way (namely at constant Froude number) that the data relevant to the two diameters correspond to $1-X_v$ ranges which overlap only for $1-X_v$ that are generally larger than 0.1. Therefore, again in this case, these data are not strictly in contrast with the present ones. Moreover most of the Russian data were collected with the 3.0 cm I.D. tube and in this case the method utilized (a γ - ray attenuation method) was checked successfully with a quick closing valve system. By contrast no check is reported with the 1.7 cm I.D. for which only the γ - ray attenuation method seems to have been utilized; furthermore the data relevant to the 1.7 cm tube are very few (in particular only one pressure was investigated) and it is therefore difficult to extrapolate the observed trend to the other uninvestigated conditions.

Most of the existing correlations do not take into account any influence of geometry: neither the Lockhart-Martinelli[17] and Martinelli-Nelson correlations[18], nor the Hughmark-Pressburg correlation[19]. The Marchaterre-Hoglund correlation[20] predicts that $1-\alpha$ decreases with D: this is due to the fact that the correlation is probably based on the results reported in Fig. 21 as above discussed.

The disagreement between the correlations, again in the case of the influence of D, is due mainly to the different range investigated, thus preventing any firm conclusion. For the time being we assume, therefore, the trend outlined in the present investigation to be valid since it is practically the only source of data in the annular-dispersed flow region(°).

(°) Data obtained recently with a round tube 1.0 cm I.D. confirm, at least qualitatively, the trend of the results presented here.

5. LIQUID VOLUME FRACTION CORRELATION

5.1. The importance of liquid volume fraction for nuclear reactor design suggested the derivation of an empirical relationship which could predict in a satisfactory way the influence of the various parameters involved, as has been determined experimentally. The empirical correlation ought to be as simple as possible so as to be handled without great difficulty and, at the same time, to have the largest possible range of applications.

As discussed in the previous paragraphs, the existing correlations fail to predict the influence of all the parameters involved; in some cases, the correlation is given in a graphical form which is uncomfortable to handle mathematically. Some of them, furthermore, predict slip ratio smaller than unity when they are utilized for predicting $1-\alpha$ in some two-phase systems (par.6.2).

5.2. From the examination of all the experimental data obtained during the present investigation the following relationship has been derived(°):

$$1-\alpha = (1-X_v)\left[1+\frac{1.35\ X_v^n}{1+0.335\ \frac{G}{\gamma}D^{1/2}}\left(\frac{1}{\rho_g}\right)^{1/4}\right] \qquad \text{(C G S Units)}$$

where

$$n = 0.9 + 0.05\gamma \qquad \text{(C G S Units)}$$

(°) In reference[40] the data have been correlated through a relationship different from the above one. That relationship was derived straight-forwardly from the dependences outlined in the previous chapter and in the range of validity of the present correlation does not quantitatively differ from the present one. It was however much more complicated since three formulas were necessary (for the three regions $1-X_v \leqslant 0.15$; $0.15 \leqslant 1.X_v \leqslant 0.65$ and $1-X_v \geqslant 0.65$) instead of only one.

This relationship takes into account the dependence of the parameters involved as derived in the previous chapter.

5.3. The validity of the proposed correlation is checked in Figs.23-28 against the experimental data obtained during the present investigation. The following remarks can be made:

- The data obtained with ethyl alcohol have been satisfactorily correlated only for $1-X_v > 0.05$. Outside this range the experimental values are largely overestimated: the trend of the experimental data, however, has still to be confirmed (see par. 4.4.2).
- The larger influence of G with lower surface tension liquids and with larger diameter is shown through the ratio $\frac{G}{\sigma} D^{1/2}$.
- The influence of diameter is satisfactorily expressed only for the region for which $1-X_v < 0.2 \div 0.4$. In the region for which $1-X_v > 0.2 \div 0.4$ the dependence upon diameter has been found actually to be opposite to that predicted by the correlation: however since the available data in this range are scarce and since in this range the effect of diameter in the correlation is negligible, for simplicity's sake, the former dependence has been left in the correlation.
- The same can be stated for the mass flow rate G.
- In order to take into account the influence of surface tension in the region of large $1-X_v$, which is opposite to that in the range of low $1-X_v$ (par. 4.4.2), a further dependence upon σ has been inserted in the exponent n .

If the data with argon–alcohol mixtures, for which $1-X_v < 0.05$ are excluded, 70% of all the experimental data are correlated with the above formula within an approximation of $\pm$ 10%, and 83% within $\pm$ 15%.

5.4. In this paragraph the data available in the literature are compared with those predicted by the proposed correlation. The line followed was to exclude in general the data obtained in conditions very different from those considered in the present investigation, in particular:

- those obtained with a flow direction different from vertical upward;
- those obtained in pure annular flow or in slug flow or, with regard to bubble flow, those obtained at very low flow rate (free convection system);
- those obtained with geometries different from the circular one;
- those obtained in heat transfer conditions.

Thus the available data are the following:

5.4.1. SNECMA data[15]: a number of data have been collected at atmospheric pressure with three circular tubes 1.0, 2.0, 3.0 cm I.D.; the experimental range in the following:

$$G = 200\text{-}600 \ g/cm^2 s$$
$$1-X_v = 0.07 \div 0.8$$
$$\rho_g = 1.2 \div 3.3 \times 10^{-3} \ g/cm^3$$

As shown in Fig. 29, the experimental data are underestimated on the average of approximately 15%. Since the range of G and $1-X_v$ is the same as that thoroughly investigated in our experiments, the discrepancy with the values predicted by the correlation should be attributed to the gas density whose influence is probably taken into a good account only in our range of ρ_g. By slightly varying the exponent of ρ_g in the above correlation the discrepancy disappears.

5.4.2. Harwell data[11][43]: the data collected by the British team at Harwell are relevant to air-water mixtures at nearly atmospheric pressure with one circular tube 1 1/4" I.D.; the experimental range is the following:

$$G = 3\text{-}30 \ g/cm^2s$$

$$1-X_v < 0.008$$

$$\rho_g = 1.2 \div 2.3 \times 10^{-3} \ g/cm^3$$

As shown in Fig. 30, the experimental data are all underestimated. This may be due both to the high gas volume quality range investigated (in fact the experimental points tend to be closer to the correlation as $1-\alpha$ increases) and the gas density, the effect of which, as already stated, is not taken into a good account in this range. It must be mentioned, as regard this, that a number of these data are relevant to pure annular flow where the influence of the various parameters might be different.

5.4.3. University of Cambridge data[6]: these data have been obtained with steam-water mixtures with a circular tube 3.81 cm I.D. in the following experimental range:

$$G = 60 \div 150 \ g/cm^2s$$

$$1-X_v = 0.2 \div 1$$

at the following pressures:

$$P = 18 - 42 - 88 - 148 \ kg/cm^2 \ abs.$$

The data obtained in adiabatic conditions are compared in Fig. 31 with the values predicted by the correlation. As shown, the correlation predicts the data quite satisfactorily 95% of them are predicted within $\pm$ 10%.

5.4.4. Russian data[8][9]: these data have been obtained with steam-water mixtures with two circular tubes 1.7 cm and 3.0 cm I.D. in adiabatic conditions. The experimental range with the 3.0 cm I.D. element is the following:

$$G = 20 \div 600 \text{ g/cm}^2\text{s}$$
$$1-X_v = 0.01 \div 0.9$$

at the following pressures:

$$P = 20 - 40 - 70 - 120 \text{ kg/cm}^2 \text{ abs.}$$

These points agree well with those that can be derived from the correlation (about 72% of the data are predicted within $\pm$ 10%) (Figs. 32, 33). If the points with $G < 30$ g/cm^{2}s, indicated in the Fig. 32 by an appropriate symbol, are excluded, 83% of the data are predicted within $\pm$ 10%.

With the 1.7 cm I.D. test element the experimental range is the following:

$$G = 20 \div 500 \text{ g/cm}^2\text{s}$$
$$1-X_v = 0.03 \div 0.80$$
$$P = 40 \text{ kg/cm}^2 \text{ abs.}$$

The agreement in this case is worse, due to the effect of diameter found by the Russians which is opposite to that predicted by the correlation (see par. 4.5). About 67% of the data are predicted within $\pm$ 10% (Fig.34).

5.4.5. ANL data[14][36]: these data have been obtained with steam-water mixtures with two circular tubes 2" and 0.622" I.D. in adiabatic conditions and P = 600 psig.

The experimental range is:

- for the 2" tube $G = 53.2\ g/cm^2s$

$$0.25 < 1-X_v < 0.8$$

- for the 0.622" tube $G = 67.5\ g/cm^2s$

$$0.2 < 1-X_v < 0.55$$

The points for the 2" tube are satisfactorily predicted by the correlation; the 0.622" I.D. tube data are, in contrast, overpredicted (see par. 4.5). The discrepancies, as stated, are still due to the effect of diameter which could not be taken into satisfactory account in this $1-X_v$ region (Fig. 35).

5.5. The range of validity of the present correlation can be derived from the analysis of experimental data so far performed. The following limits can be assumed:

- Mass or volume quality: the correlation satisfactorily represents the experimental data, at least, in the following range:

$$1-X_v \gtrsim 0.05$$

At lower values the correlation fails in representing the data relevant to argon-alcohol mixture, i.e. at low surface tensione, while there is still a good agreement with those obtained with cold water as the liquid phase.

In this regard it is noteworthy that even with cold water as the liquid phase the correlation does not hold any longer when $1-X_v$ is so small that the flow pattern is probably pure annular: see for example the Harwell data (par. 5.4.2. and Fig. 30).

- Mass flow rate: at constant other conditions, the correlation indicates that $1-\alpha$ decreases with the increasing of G and becomes equal

to $1-X_v$ for $G \rightarrow \infty$ which is not a physically inconsistent condition. However, systematic experiments in the range $G > 250$ g/cm^{2}s are not available, so that such a trend cannot be confirmed. In any case we can state for the time being:

$$G < 250 \text{ g/cm}^2\text{s}$$

A statement about the lower limit is somewhat problematic since it is likely to depend upon the value for gas density. The correlation, in fact, has been derived from data obtained in the annular-dispersed and bubble flow regimes and it is likely to fail for other flow regimes (see for example the comparison with Harwell data). Thus, since the minimum mass flow rate value for which annular-dispersed flow and bubble flow can be established decreases with gas density, the same should happen for the said limit.

The available data, however, are not enough to make a reliable statement about this; it can only be said that in the range of ρ_g = $= 10 \div 40 \times 10^{-3}$ g/cm^3 approximately

$$G > 30 \div 40 \text{ g/cm}^2\text{s}$$

- Gas and liquid density: the influence of gas density is taken into satisfactory account only in the range:

$$10 < \rho_g < 40 \times 10^{-3} \text{ g/cm}^3$$

The comparison performed in par. 5.4.1., 5.4.2. with data obtained at lower densities suggests that the exponent of ρ_g should be increased in this range.

However a detailed analysis of the influence of gas density is necessary before reaching a final conclusion on this subject.

On the other hand, it is very improbable that only gas density has an effect on $1-\alpha$; it seems therefore more reliable to state that the influence of these two parameters should be expressed through a ratio $(\frac{\rho_l}{\rho_g})$ or $(\frac{\rho_l - \rho_g}{\rho_g})$.

However, the available experiments are not enough to derive any quantitative indication; in any case the correlation should hold satisfactorily since the range of liquid density variation, in the field of interest, is rather small and the dependence upon ρ_l, is probably small too (par. 4.4.3.).

- Surface tension: the range of validity of the correlation, as it has been derived from the experiments presented in this report is

$$23 < \sigma < 73 \quad \text{dyn/cm}$$

However, as shown by the comparison with the steam-water data at various pressures, the lower limit can be lowered to $\sim$ 10 dyn/cm. As regards this, it is worth mentioning that at other constant conditions, the correlation indicates that for $\sigma = 0$, the liquid volume fraction coincides with the liquid volume quality which a priori is not physically inconsistent.

- Gas and liquid viscosity: nothing can, with any certainty, be stated about the influence of these two parameters. Nevertheless, the experiments mentioned in par. 4.4.3. seem to indicate that in the range of application of the present correlation (steam- water mixtures at various pressures) the μ_g effect should not play any appreciable role (μ_g in fact undergoes very small variation and remains almost equal to the value investigated with argon and nitrogen).

The influence of μ_l is much less known, as already mentioned. In any case it must be small since the correlation would satisfactorily predicts the data relevant to steam-water mixtures and it would be

quite a surprising coincidence if an erroneously predicted influence of ρ_g, and γ accounted for the dependence upon μ_l.

- Geometry: The influence of geometry is taken into account in the following range:

$$1.5 < D < 3.0 \text{ cm}$$

However, the existence of an opposite trend to that of the correlation as outlined by other authors (par. 4.5.) suggests that further systematic experiments in a larger range should be carried out (see footnote page 31).

5.6. The value of slip ratio can easily be derived from the correlation which, for simplifying purposes is written as follows:

$$\frac{1-\alpha}{1-X_v} = 1+\varepsilon \text{ where } \varepsilon = \frac{1.35\, X_v^n}{1+0.355\, \frac{G}{\gamma}\, D^{1/2}} \left(\frac{1}{\rho_g}\right)^{1/4}; \quad n=0.9+0.05\gamma$$

Thus slip ratio is equal to:

$$S = \frac{1}{1 - \frac{\varepsilon}{X_v(1+\varepsilon)}}$$

Slip ratio increases monotonausly from 1, when quality is zero, to a finite value larger than one when quality reaches the limiting value for which $1-X_v = 0.05$.

6. APPLICATION TO STEAM WATER MIXTURES

6.1. As already discussed, the aim of the present investigation was to derive a relationship suitable for design reactor calculations, which could predict the $1-\alpha$ values with steam-water mixtures in conditions applicable in a "fog-cooled reactor". For this purpose it has been necessary (1) to check its validity for steam-water mixtures in the case of adiabatic conditions and (2) to determine, on the basis of the available experimental data, the influence of heat addition.

6.2. Adiabatic conditions

The correlation developed in the previous chapter gives values which agree well with the few available data obtained with steam-water mixtures in adiabatic conditions. Thus, while waiting for further systematic results, the correlation can be considered satisfactory for the time being.

It is interesting to compare the correlation with those derived by other authors so as to show, for example for steam-water mixture at 70 kg/cm^2 (a condition considered as interesting for the fog-cooled reactor[1]) the discrepancy between the various correlations.

The correlations analysed are the following:

- Martinelli-Nelson[18]
- Bankoff[25]
- Bankoff modified[26]
- Hughmark-Pressburg[19]
- Marchaterre-Houglund[20]

The result of the comparison is outlined in Figs. 36-37 where the values of $1-\alpha$ are plotted against mass and volume quality in the range of interest for reactor design. The following comments can be made:

- Martinelli-Nelson correlation: the slope of $1-\alpha$ vs. $1-X_v$ is maller than that of the present correlation so that the resulting $1-\alpha$ values are higher in the low $1-X_v$ region and smaller in the high $1-X_v$ region; moreover in this region the Martinelli-Nelson correlation can give $\frac{1-\alpha}{1-X_v}$ values smaller than one, which is a condition that should be physically inconsistent, at least in adiabatic flow.

- Bankoff correlation: the correlation gives $1-\alpha$ values which agree completely with those derived from the present correlation only in the high $1-X_v$ region. In the low $1-X_v$ region the values are much larger: this discrepancy should be attributed to the fact that the values of the constant appearing in the correlation have been derived on the basis of experimental data obtained in the low quality region.

- Bankoff modified correlation: the modification suggested by Hughmark to the previous correlation improves the resulting values but not enough to make them agree with the correlation presented in this report. This may be due to the fact that both correlations (Bankoff and Bankoff modified) correlate α instead of $1-\alpha$ so that in the low $1-X_v$ region even a small error on α gives rise to a large error on $1-\alpha$.

- Hughmark-Pressburg correlation: this correlation gives $1-\alpha$ values which disagree with those obtained from the present correlation. In the low quality region it gives rise to a physically inconsistent situation since it leads to values of overall slip ratio smaller than unity. Such discrepancies should be attributed to the fact that the correlation, although based on a number of experimental data, does not take into account properly the influence of physical properties.

- Marchaterre-Hoglund correlation: this correlation agrees most closely of all with the one proposed here, especially as regards the influence of quality. The only discrepancy is that the influence of diameter is the contrary in the two correlations (par. 4.5.): this difference leads to a larger discrepancy between the two correlations as the diameter gets smaller. The two correlations give the same $1-\alpha$ values with a circular conduit 4.5 cm I.D. (at G = 50 $g/cm^2 s$) as shown in Fig. 38. However a drawback of the Marchaterre-Hoglund correlation is that it is restricted to low G values (with 1.5 cm I.D. tube, P = 70 kg/cm^2 G is at most 50 $g/cm^2 s$) (Fig.37).

6.3. Heat transfer conditions

The problem has been widely dealt with in literature but a definite conclusion cannot yet be drawn. The results so far achieved can be summariwed as follows:

- low quality region ($1-X_v > 0.6$)(°): the influence of heat addition can be quite important (12)(13)(22). Liquid volume fraction, at constant quality, decreases with the increasing of heat flux; this effect is larger the smaller the specifc mass flow rate, at constant other conditions (22);
- high quality region ($1-X_v < 0.6$): the influence of heat addition seems to be negligible as shown by the experiments of Egen et al. (13) and Rouhani at al. (7) and as assumed in the treatment of Maurer (22), which is based on previous experimental data.

(°) As stated, this limit corresponds broadly to the boundary, provided specific mass flow rate is large enough, between bubble flow and annular-dispersed flow.

As regards this the experiments carried out with steam-water mixtures at 51 kg/cm^2 with an isokinetic probe moveable along a diameter of the cross section conduit (a circular tube 2.5 cm I.D.)[41] indicated that at a given position along the test section, at the same quality and specific mass flow rate, the $1-\alpha$ profile in the core region was steeper with power than in adiabatic conditions (Fig. 39). This led to an overall slip ratio in the region investigated ($0 < r < 1.04$ cm) larger with heat transfer than in adiabatic conditions; however from these data it is not possible to infer any conclusion about the overall slip ratio (over the whole cross section) since in the remaining region ($1.04 < r < 1.25$ cm) the phase distribution could be such as to reverse the partial result in the core.

6.4. Conclusions

Although the influence of heat transfer has so far not been well established, thus requiring further experimental studies, the general evidence is that, at least in the portion of the evaporating channel where $1-X_v < 0.6$, this influence should be rather limited. Thus in this region the correlation proposed here should give, as has been shown, values not far from the actual ones. In the low quality portion of the channel, approximated procedures, such as that suggested by Maurer, should be followed.

Overall measurements in heat transfer conditions, now being carried out at CISE, will contribute substantially to resolving the problem.

APPENDIX A

Density of two-phase mixture has also been derived from the measured value of $\frac{\Delta P}{\Delta Z}$ and τ (over a small enough, length ΔZ) when the momentum variation along the flow direction was negligible. The following momentum balance equation has in fact been utilized:

$$\rho = \frac{1}{g}\left[\frac{\Delta P}{\Delta Z} - \frac{4}{D}\tau\right] \qquad (1)$$

As shown, the density is derived from the difference between two terms and can therefore be affected, in some conditions, by quite a large error: as is well known, with the increasing of quality and total flow rate both $\frac{\Delta P}{\Delta Z}$ and τ increase, while ρ decreases.

Assuming that the errors are composed as the square root of the sum of the squares of the single terms the measurement error on ρ will be given by the following equation derived from eq. (1):

$$\left|\frac{\Delta\rho}{\rho}\right| = \sqrt{\left(\frac{1}{g}\,\frac{\Delta P/\Delta Z}{\rho}\right)^2 \left|\frac{\Delta(\Delta P/\Delta Z)}{\Delta P/\Delta Z}\right|^2 + \left(\frac{4\tau}{gD\rho}\right)^2 \left|\frac{\Delta\tau}{\tau}\right|^2} \qquad (2)$$

From eqs. (2) and (1), we have:

$$\left|\frac{\Delta\rho}{\rho}\right| = \sqrt{\left(1 + \frac{4\tau}{gD\rho}\right)^2 \left|\frac{\Delta(\Delta P/\Delta Z)}{\Delta P/\Delta Z}\right|^2 + \left(\frac{4\tau}{gD\rho}\right)^2 \left|\frac{\Delta\tau}{\tau}\right|^2}$$

The term $\frac{(\Delta P/\Delta Z)}{\Delta P/\Delta Z}$, as has been discussed in an earlier report[2], amounts approximately to about 2%. The term $\frac{\Delta\tau}{\tau}$ has been evaluated, too, in a previous report[34], and is strictly dependent on the characteristics of the measurement system, in addition, of course, to flow rate, quality etc. For the evaluation of $\frac{\Delta\rho}{\rho}$ the

measurement error $\Delta\tau/\tau$ has been derived from ref.[34], where this term has been dealt with throughly.

The trend of $\frac{\Delta\rho}{\rho}$ obtained from experimental data of τ and ρ is shown in Fig. A-1

Apparently the error increases with mass quality and mass flow rate.

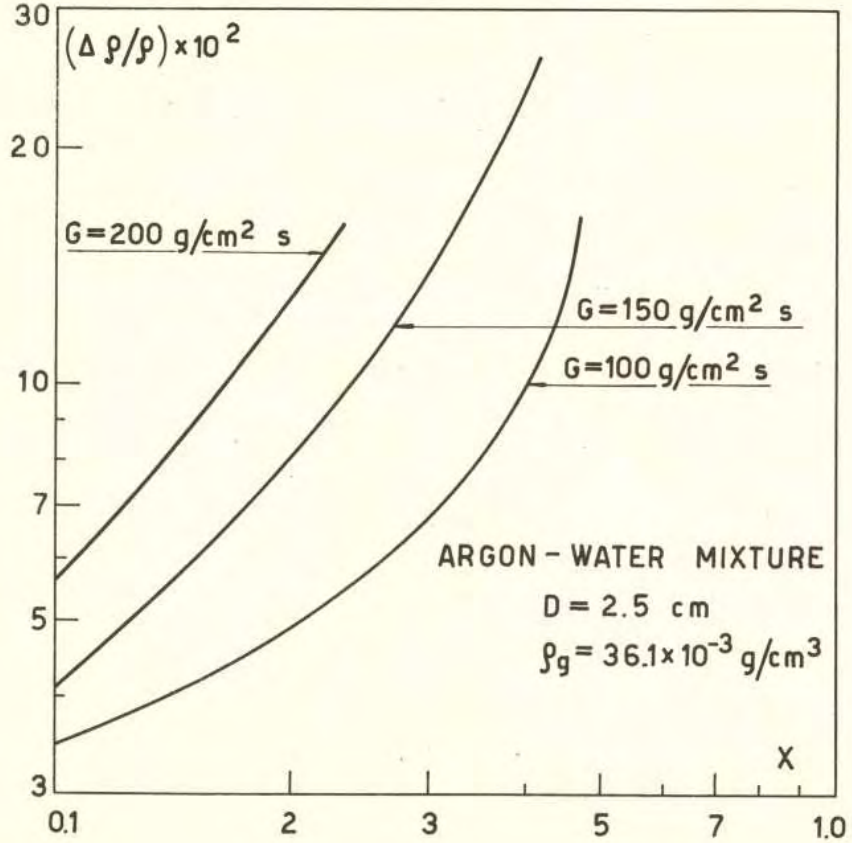
30
20
10
7
5
3
$(\Delta \rho/\rho) \times 10^2$
G=200 g/cm² s
G=150 g/cm² s
G=100 g/cm² s
ARGON - WATER MIXTURE
D = 2.5 cm
$\rho_g = 36.1 \times 10^{-3}$ g/cm³
X
0.1
2
3
5
7
1.0

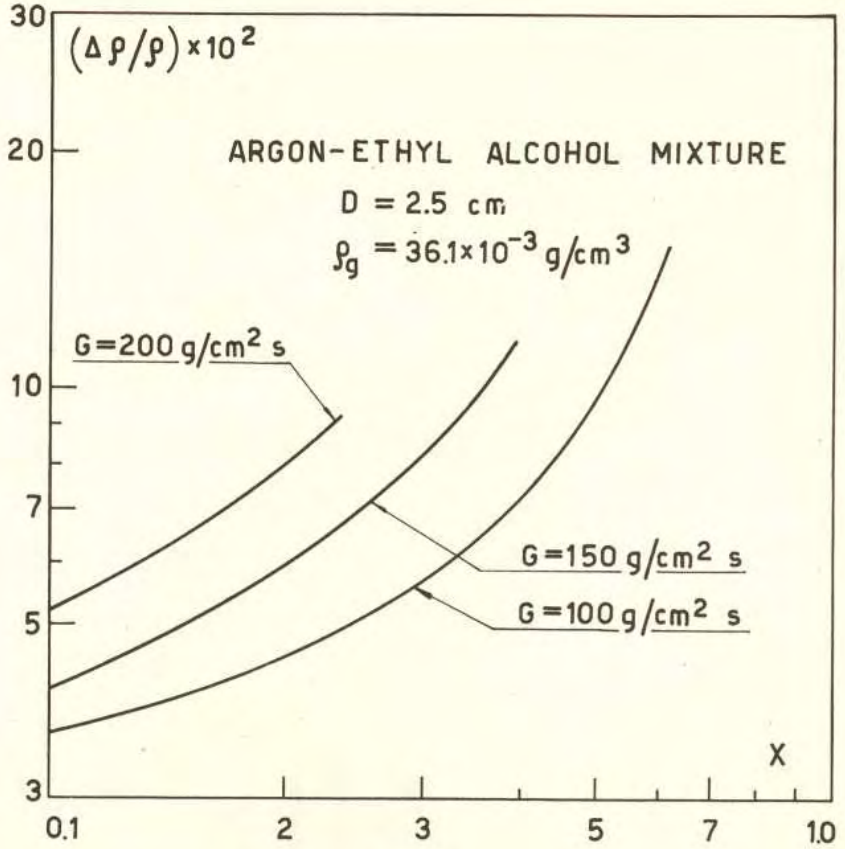
30
20
10
7
5
3
$(\Delta \rho/\rho) \times 10^2$
ARGON-ETHYL ALCOHOL MIXTURE
D = 2.5 cm
$\rho_g = 36.1 \times 10^{-3}$ g/cm³
G=200 g/cm² s
G=150 g/cm² s
G=100 g/cm² s
X
0.1
2
3
5
7
1.0

Fig. A1

APPENDIX B

LIQUID VOLUME FRACTION – SLIP RATIO

Gas phase : argon

Liquid phase : water

Element : round tube 2.5 cm I.D

TABLE I

Gas density : 36.1 $\times 10^{-3}$ g/cm^3

Press. (a): 21.8 kg/cm^2 – Temp. 18 °C

G_g g/cm^2 s	G_l g/cm^2 s	$1-X_v$	$1-\alpha$	S
16.0	22.1	0.0475	0.156	3.70
"	38.2	0.079	0.209	3.06
"	66.5	0.130	0.269	2.45
"	91	0.171	0.312	2.20
"	119	0.212	0.355	2.05
"	157	0.262	0.385	1.76
"	206	0.317	0.400	1.43
21.4	22.1	0.0359	0.117	3.55
"	38.2	0.060	0.165	3.06
"	66.5	0.101	0.224	2.57
"	91	0.133	0.260	2.28
"	119	0.167	0.295	2.08
"	157	0.209	0.325	1.81
"	206	0.258	0.335	1.45
27.8	22.1	0.0279	0.092	3.52
"	38.2	0.0473	0.128	2.95
"	66.5	0.079	0.177	2.48
"	91	0.104	0.209	2.23
"	119	0.134	0.232	1.95
"	157	0.170	0.260	1.72
"	206	0.211	0.270	1.38
35.1	22.1	0.0222	0.075	3.57
"	38.2	0.0378	0.106	3.01
"	66.5	0.064	0.143	2.43
"	91	0.086	0.167	2.14
"	119	0.109	0.195	1.97
"	157	0.139	0.215	1.69
"	206	0.175	0.227	1.38
46.9	22.1	0.0167	0.054	3.35
"	38.2	0.0286	0.078	2.87
"	66.5	0.0403	0.110	2.43
"	91	0.065	0.131	2.15
"	119	0.084	0.160	2.07
"	157	0.108	0.182	1.84
"	206	0.136	0.188	1.46
62.5	22.1	0.0126	0.0420	3.43
"	38.2	0.0216	0.057	2.76
"	66.5	0.0298	0.080	2.26
"	91	0.0491	0.101	2.13
"	115	0.064	0.124	2.05
"	157	0.083	0.149	1.93
"	206	0.107	0.162	1.62
73	22.1	0.0108	0.0350	3.31
"	38.2	0.0191	0.048	2.66
"	66.5	0.0315	0.067	2.18
"	91	0.0422	0.085	2.06
"	119	0.054	0.107	2.03
"	157	0.072	0.127	1.87
"	206	0.092	0.140	1.59
81	22.1	0.0098	0.0315	3.29
"	38.2	0.0174	0.042	2.57
"	66.5	0.0285	0.059	2.11
"	91	0.0381	0.077	2.05
"	119	0.049	0.094	1.95
"	157	0.063	0.112	1.80
"	206	0.084	0.126	1.57
94	22.1	0.0084	0.0265	3.20
"	38.2	0.0147	0.0350	2.47
"	66.5	0.0250	0.0495	2.03
"	91	0.0334	0.0665	2.03
"	119	0.0424	0.082	1.95
"	157	0.055	0.096	1.76
"	206	0.072	0.105	1.48

TABLE II

Gas density : 36.1 $\times 10^{-3}$ g/cm^3

Press. (a): 21.8 kg/cm^2 – Temp. 18 °C

G g/cm^2 s	X	$1-X_v$	$1-\alpha$	S
100	0.0200	0.64	0.65 +	1.00
"	0.0300	0.54	0.57 +	1.12
"	0.050	0.407	0.474 +	1.33
"	0.100	0.245	0.390 +	1.93
"	0.150	0.172	0.310 +	2.19
150	0.0150	0.705	0.70 +	1.00
"	0.0200	0.64	0.65 +	1.05
"	0.0300	0.54	0.55 +	1.07
"	0.050	0.407	0.484 +	1.36
"	0.100	0.245	0.400 +	2.05
"	0.150	0.172	0.317 +	2.26
200	0.0100	0.775	0.78 +	0.99
"	0.0200	0.64	0.65 +	1.05
"	0.0300	0.54	0.58 +	1.17
"	0.050	0.407	0.51 +	1.53
"	0.100	0.245	0.386 +	1.93

TABLE III

Gas density : 27.7 $\times 10^{-3}$ g/cm^3

Press. (a): 16.8 kg/cm^2 – Temp. 18 °C

G g/cm^2 s	X	$1-X_v$	$1-\alpha$	S
50	0.200	0.100	0.239	2.83
"	0.350	0.0490	1.146	3.32
"	0.50	0.0270	0.092	3.66
100	0.0200	0.57	0.60 +	1.12
"	0.0300	0.470	0.52 +	1.20
"	0.050	0.342	0.474 +	1.71
"	0.100	0.200	0.339 +	2.06
"	0.150	0.137	0.263 +	2.27
"	0.200	0.100	0.211	2.41
"	0.350	0.049	0.132	2.95
"	0.50	0.0270	0.080	3.15
150	0.0150	0.65	0.65 +	1.03
"	0.0200	0.575	0.59 +	1.04
"	0.0300	0.470	0.51 +	1.16
"	0.050	0.343	0.445 +	1.52
"	0.100	0.200	0.362 +	2.27
"	0.150	0.137	0.292 +	2.63
200	0.0100	0.73	0.74 +	1.04
"	0.0200	0.575	0.59 +	1.07
"	0.0300	0.470	0.54 +	1.32
"	0.050	0.343	0.472 +	1.70
"	0.100	0.200	0.362 +	2.27
"	0.200	0.100	0.176	1.93
"	0.350	0.049	0.1015	2.19
"	0.50	0.0270	0.056	2.14

TABLE IV

Gas density : 18.8 $\times 10^{-3}$ g/cm^3

Press. (a): 11.5 kg/cm^2 – Temp. 18 °C

G g/cm^2 s	X	$1-X_v$	$1-\alpha$	S
50	0.150	0.096	0.240	2.96
"	0.260	0.050	0.167	3.74
"	0.370	0.0302	0.111	3.89
75	0.150	0.096	0.227	2.74
"	0.260	0.050	0.143	3.11
"	0.370	0.0302	0.102	3.55
100	0.0200	0.478	0.54 +	1.31
"	0.0300	0.375	0.50 +	1.63
"	0.050	0.261	0.427 +	2.09
"	0.150	0.096	0.210	2.49
"	0.260	0.050	0.124	2.64
"	0.370	0.0302	0.090	3.08
150	0.0150	0.55	0.57 +	1.10
"	0.0200	0.478	0.53 +	1.21
"	0.0300	0.375	0.491 +	1.585
200	0.0100	0.65	0.67 +	1.095
"	0.0200	0.478	0.54 +	1.30
"	0.0300	0.375	0.492 +	1.66

+ Data obtained from shear stress measurements

LIQUID VOLUME FRACTION – SLIP RATIO

Gas phase : argon
Liquid phase : water
Element : round tube 1.5 cm I.D.

TABLE V

Gas density : 36.1 $\times 10^{-3}$ g/cm^3

Press. (a): 21.8 kg/cm^2 – Temp. 18 °C

G_g g/cm^2 s	G_l g/cm^2 s	$1-X_v$	$1-\alpha$	S
27.8	22.1	0.0279	0.099	3.83
"	38.2	0.0473	0.137	3.20
"	66.5	0.079	0.187	2.68
"	91	0.106	0.217	2.34
"	119	0.134	0.255	2.22
"	157	0.169	0.286	1.96
"	177	0.187	0.291	1.79
35.0	22.1	0.0223	0.078	3.72
"	38.2	0.0379	0.113	3.24
"	66.5	0.064	0.158	2.75
"	91	0.086	0.182	2.37
"	119	0.109	0.218	2.27
"	157	0.139	0.246	2.01
"	177	0.154	0.253	1.86
47.5	22.1	0.0165	0.058	3.67
"	38.2	0.0282	0.079	2.95
"	66.5	0.0480	0.124	2.82
"	91	0.064	0.156	2.67
"	119	0.083	0.183	2.48
"	157	0.107	0.209	2.21
"	177	0.119	0.215	1.88
62.5	22.1	0.0126	0.0400	3.26
"	38.2	0.0216	0.067	3.23
"	66.5	0.0368	0.095	2.75
"	91	0.050	0.115	2.47
"	119	0.064	0.145	2.46
"	157	0.083	0.170	2.26
"	177	0.093	0.173	2.05
72	22.1	0.0110	0.0343	3.20
"	38.2	0.0188	0.054	2.99
"	66.5	0.0321	0.086	2.82
"	91	0.0436	0.099	2.41
"	119	0.056	0.123	2.34
"	157	0.073	0.154	2.31
"	177	0.082	0.155	2.07
82	22.1	0.0096	0.0276	2.92
"	38.2	0.0165	0.0466	2.91
"	66.5	0.0284	0.070	2.60
"	91	0.0385	0.089	2.45
"	119	0.0498	0.105	2.23
"	157	0.0645	0.133	2.22
"	177	0 072	0.143	2.14
95	91	0.0334	0.084	1.01
"	119	0.0432	0.099	2.43
"	157	0.056	0.120	2.29
"	177	0.063	0.141	2.44

TABLE VI

Gas density : 36.1×10^{-3} g/cm^3

Press. (a): 21.8 kg/cm^2 –Temp. 18 °C

G g/cm^2 s	X	$1-X_v$	$1-\alpha$	S
100	0.172	0.150	0.266	2.06
"	0.098	0.250	0.363	1.71
"	0.062	0.350	0.451	1.52
"	0.0389	0.471	0.535	1.29
150	0.172	0.150	0.258	1.97
"	0.098	0.250	0.343	1.57
"	0.062	0.350	0.436	1.43
"	0.0348	0.500	0.56	1.26
"	0.0268	0.58	0.605	1.10
200	0.172	0.150	0.257	1.96
"	0.098	0.250	0.383	1.87
"	0.062	0.350	0.470	1.65
"	0.0348	0.500	0.59	1.44
"	0.0237	0.60	0.63	1.15

TABLE VI

Gas density : 36.1×10^{-3} g/cm^3

Press. (a): 21.8 kg/cm^2 –Temp. 18 °C

G g/cm^2 s	X	$1-X_v$	$1-\alpha$	S
250	0.172	0.150	0.250	1.89
"	0.098	0.250	0.360	1.69
"	0.062	0.350	0.481	1.72
"	0.0348	0.500	0.62	1.62
"	0.0156	0.70	0.75	1.28

TABLE VII

Gas density : 27.7 $\times 10^{-3}$ g/cm^3

Press. (a): 16.8 kg/cm^2 – Temp. 18 °C

G_g g/cm^2 s	G_l g/cm^2 s	$1-X_v$	$1-\alpha$	S
27.5	22.1	0.0225	0.082	4.00
"	38.2	0.0370	0.120	3.54
"	66.3	0.063	0.167	3.01
"	119	0.107	0.226	2.43
47.5	22.1	0.0131	0.051	4.20
"	38.2	0.0225	0.075	3.65
"	66.3	0.0373	0.111	3.25
"	119	0.065	0.154	2.63
"	157	0.084	0.187	2.51
71.5	22.1	0.0085	0.0380	4.09
"	38.2	0.0153	0.0476	3.38
"	66.5	0.0254	0.071	2.97
"	119	0.0441	0.105	2.56
"	157	0.057	0.119	2.22
95	22.1	0.0064	0.0286	4.56
"	38.2	0.0109	0.0372	3.47
"	66.5	0.0200	0.052	2.86

TABLE VIII

Gas density : 18.8 $\times 10^{-3}$ g/cm^3

Press. (a): 11.6 kg/cm^2 – Temp. 18 °C

G_g g/cm^2 s	G_l g/cm^2 s	$1-X_v$	$1-\alpha$	S
27.5	22.1	0.0149	0.059	4.15
"	38.2	0.0254	0.098	4.16
"	66.5	0.0434	0.142	3.65
"	119	0.075	0.206	3.19
47.5	22.1	0.0089	0.0380	4.52
"	38.2	0.0147	0.060	4.22
"	66.5	0.0256	0.089	3.74
"	119	0.0450	0.151	3.79

TABLE IX

Gas density : 10.0×10^{-3} g/cm^3

Press. (a): 6.15 kg/cm^2 – Temp. 18 °C

G_g g/cm^2 s	G_l g/cm^2 s	$1-X_v$	$1-\alpha$	S
15.9	22.1	0.0138	0.060	4.56
"	38.2	0.0233	0.089	4.09
"	63.2	0.0399	0.131	3.63
"	119	0.069	0.190	3.17

LIQUID VOLUME FRACTION – SLIP RATIO

Gas phase : argon

Liquid phase : ethyl alcohol

Element : round tube 2.5 cm I.D.

TABLE X

Gas density 36.1×10^{-3} g/cm³

Press. (a): 22.0 kg/cm² – Temp. 20 °C

G_g g/cm² s	G_l g/cm² s	$1-X_v$	$1-\alpha$	S
16.0	22.1	0.060	0.169	3.21
"	66.5	0.167	0.294	2.18
"	119	0.261	0.353	1.59
"	177	0.330	0.409	1.36
21.3	38.2	0.076	0.158	2.29
"	91	0.169	0.265	1.85
"	157	0.259	0.364	1.70
"	177	0.280	0.352	1.43
27.7	22.1	0.0355	0.082	2.42
"	66.5	0.099	0.186	2.07
"	119	0.170	0.232	1.54
"	177	0.233	0.297	1.45
35.0	22.1	0.0285	0.0493	1.77
"	66.5	0.080	0.149	2.02
"	119	0.138	0.181	1.42
"	157	0.175	0.238	1.53
"	177	0.194	0.255	1.48
46.7	38.2	0.0360	0.056	1.58
"	91	0.082	0.129	1.66
"	177	0.152	0.167	1.16
62.5	22.1	0.0159	0.0206	1.29
"	38.2	0.0286	0.0295	1.08
"	66.5	0.046	0.059	1.30
"	91	0.062	0.084	1.37
"	119	0.079	0.103	1.32
"	157	0.103	0.141	1.14
71.5	22.1	0.0130	0.0185	1.33
"	38.2	0.0240	0.0278	1.17
"	66.5	0.0410	0.0469	1.16
"	91	0.054	0.0725	1.34
"	119	0.070	0.092	1.34
"	157	0.090	0.110	1.24
81	22.1	0.0110	0.0149	1.22
"	38.2	0.0210	0.0223	1.06
"	66.5	0.0365	0.0358	0.99
"	91	0.0482	0.060	1.26
"	119	0.062	0.071	1.14
"	157	0.080	0.096	1.22
94	22.1	0.0107	0.0114	1.07
"	38.2	0.0178	0.0167	0.91
"	66.5	0.0313	0.0320	1.03
"	91	0.0420	0.0465	1.11
"	119	0.054	0.067	1.26
"	157	0.070	0.082	1.18

TABLE XI

Gas density : 36.1×10^{-3} g/cm³

Press. (a): 22.0 kg/cm² – Temp. 20 °C

G g/cm² s	X	$1-X_v$	$1-\alpha$	S
100	0.02	0.70	0.74 +	1.25
"	0.03	0.60	0.65 +	1.26
"	0.05	0.463	0.57 +	1.52
"	0.10	0.293	0.413 +	1.71
"	0.15	0.211	0.336 +	1.95
150	0.015	0.76	0.80 +	1.31
"	0.02	0.70	0.74 +	1.26
"	0.03	0.60	0.66 +	1.29
"	0.05	0.463	0.55 +	1.40
"	0.10	0.293	0.412 +	1.70
"	0.15	0.211	0.276 +	2.11
200	0.05	0.463	0.54 +	1.34
"	0.10	0.293	0.41 +	1.65

TABLE XII

Gas density : 18.8×10^{-3} g/cm³

Press. (a): 11.6 kg/cm² – Temp. 20 °C

G_g g/cm² s	G_l g/cm² s	$1-X_v$	$1-\alpha$	S
16.0	22.1	0.0332	0.124	4.27
"	38.2	0.055	0.146	2.99
"	66.5	0.091	0.207	2.62
21.2	22.1	0.0252	0.069	2.98
"	38.2	0.0430	0.109	2.85
"	66.5	0.071	0.153	2.42
27.7	22.1	0.0195	0.0380	2.08
"	38.2	0.0330	0.086	2.86
"	66.5	0.055	0.145	2.96

TABLE XIII

Gas density : 18.8×10^{-3} g/cm³

Press. (a): 11.6 kg/cm² – Temp. 20 °C

G g/cm² s	X	$1-X_v$	$1-\alpha$	S
100	0.02	0.54	0.62 +	1.39
"	0.03	0.441	0.57 +	1.70
"	0.05	0.312	0.464 +	1.91
150	0.015	0.62	0.66 +	1.24
"	0.02	0.54	0.60 +	1.31
"	0.05	0.312	0.54 +	1.54

TABLE XIV

Gas density : 10.0×10^{-3} g/cm³

Press. (a): 6.2 kg/cm² – Temp. 20 °C

G_g g/cm² s	G_l g/cm² s	$1-X_v$	$1-\alpha$	S
8.5	22.1	0.0312	0.133	4.65
"	38.2	0.052	0.216	4.84
"	66.5	0.089	0.256	3.47
11.3	22.1	0.0232	0.118	5.4
"	38.2	0.0400	0.150	4.12
"	66.5	0.067	0.209	3.54
14.7	22.1	0.0182	0.067	3.80
"	38.2	0.0312	0.107	3.64
"	66.5	0.052	0.156	3.22

+ Data obtained from shear stress measurements

TABLE XV

DATA OBTAINED FROM MEASUREMENTS OF PHASE DISTRIBUTION PROFILES (method "b")

- MIXTURE: ARGON-WATER
- GEOMETRY: ROUND TUBE 2.5 cm I.D.
- GAS DENSITY: 10.0×10^{-3} g/cm^3

G_g	G_l	$1-X_v$	$1-\alpha$	s
g/cm^2 s	g/cm^2 s			
6.7	25.5	0.0365	0.168	5.3
"	135	0.166	0.287	2.02
20.1	25.5	0.0126	0.054	4.47
"	135	0.063	0.147	2.56

NOMENCLATURE

Latin symbols

D	diameter
g	acceleration due to gravity
G	total specific mass flow rate ($G = \frac{\Gamma_g + \Gamma_l}{\Omega}$)
G_g	gas specific mass flow rate ($G_g = \frac{\Gamma_g}{\Omega}$)
G_l	liquid specific mass flow rate ($G_l = \frac{\Gamma_l}{\Omega}$)
P	Pressure
Q	volume flow rate ($Q_g = \frac{\Gamma_g}{\rho_g}$; $Q_l = \frac{\Gamma_l}{\rho_l}$)
S	overall slip ratio
U	average linear velocity ($U_g = \frac{\Gamma_g}{\alpha \Omega}$; $U_l = \frac{\Gamma_l}{(1-\alpha)\Omega}$)
U^*	average superficial velocity ($U^* = \frac{Q_g+Q_l}{\Omega}$)
W	power
X	mass flow rate quality (or mass quality) ($X = \frac{\Gamma_g}{\Gamma_g + \Gamma_l}$)
$1-X_v$	liquid volume flow rate quality (or liquid volume quality) ($1-X_v = \frac{Q_l}{Q_g+Q_l}$)
y	distance from the wall of the conduit

Greek symbols

α	overall gas volume fraction
$1-\alpha$	overall liquid volume fraction

γ	surface tension
Γ	mass flow rate
$\Delta P/\Delta Z$	pressure gradient
Θ	temperature
μ	viscosity
ρ	density
ρ^*	flow rate density ($\rho^* = \rho_g X_v + \rho_l (1-X_v)$
τ	shear stress
Ω	cross sectional area of the test section

Subscripts

a	air
abs	absolute
calc	calculated
exp	experimental
g	gas
in	inlet
l	liquid
o	outlet
tot	total

REFERENCES

(1) Casagrande I. "Preliminary remarks on the fog cooling of a power reactor" Energia Nucleare 10, 11, 585 (1963).

(2) "A research program in two-phase flow" CISE Report (January 1963).

(3) H.S. Isbin, N.C. Sher, K.C. Eddy: "Void fractions in two-phase steam-water flow" A.I. Ch. E. Journal, 3, 1, 136 (1957).

(4) H.S. Isbin, H.A. Rodriguez, H.C. Larson, B.A. Pattie: "Void Fractions in two-phase flow", A.I. Ch. E. Journal 5, 1, 427 (1959).

(5) H.C. Larson: "Void Fractions of two-phase Steam-Water Mixture" N.S. Thesis, University of Minnesota, Minneapolis, Minnesota (1957).

(6) Haywood R.W., Knights G.A., Middleton G.E. and Thom J.R.S.: "Experimental study of the flow conditions and pressure drop of steam-water mixtures at higt pressures in heated and unheated tubes" The Institution of Mechanical Engineers, 175, 13, 669 (1961).

(7) S.Z. Rouhani, K.M. Becker: "Measurements of Void Franctions for Flow of Boiling Heavy Water in a vertical Round Duct", AE-106 (1963).

(8) Semenov N.I., Tochigin A.A.: "Steam volume fraction in steam-water flow in vertical unheated pipes", Eng. Physics Journal IV, 7,30 (1961).

(9) Kosterin S.I., Semenov N.I., Tochigin A.A.: "Relative velocities of steam-water flow in vertical unheated pipes" Teploenergetika 1, 58 (1961).

(10) V.E. Shrock, G. Angelino, G. Possa, J.B. Van Erp: "Density measurements in a boiling channel" Energia Nucleare 10, 10, 525 (1963).

(11) Hewitt G.F., King I., Lovegrove P.C.: "Hold-up and pressure drop measurements in the two-phase annular flow of air-water" AERE-R 3764 (1961).

(12) J.J. Foglia, F.G. Peter, H.M. Epstein, R.O. Wooton, D.A. Dingee, J.W. Chastain: "Boiling-Water void Distribution and Slip Ratio in Heated Channels" BMI-1517 (1961).

(13) R.A. Egen, D.A. Dingee, J.W. Chastain: "Vapor formation and behaviour in boiling heat transfer" BMI-1163 (1957).

(14) P.A. Lottes, M. Petrick, J.F. Marchaterre: "Lecture notes on heat extraction from boiling water power reactors" ANL-6063 (1959).

(15) Private comunication from M.C. Moussez (SNECMA).

(16) T.A. Hughes, W. Markert, Jr.: "Steam-water mixtures studies in a vertical pipe at high pressures". The Babcock & Wilcox Co. (Dic 1960).

(17) Lockhart R.W., Martinelli R.C.: "Proposed correlation of data for isothermal two-phase, two component flow in pipes". Chem. Eng. Progress 45, 1, 39 (1949).

(18) Martinelli R.C., Nelson D.B.: "Prediction of pressure drop during forced circulation boiling of water", Trans. ASME, 70, 695 (1948).

(19) Hughmark G.A., Pressburg B.S.: "Holdup and Pressure Drop with Gas-liquid Flow in a Vertical Pipe", A.I.Ch.E. Journal 7, 4, 677 (1961).

(20) Marchaterre J.F., Hoglund B.M.: "Correlation for Two-Phase Flow" Nucleonics (August 1962).

(21) U.H. von Glahn: "An empirical relation for predicting void fraction with two-phase, steam-water flow", NASA TN D-1189 (1962).

(22) G.M. Maurer: "A Method of Predicting Steady-State Boiling Vapor fractions in Reactor Coolant Chanels" WAPD-BT-19 (June 1960).

(23) S. Levy: "Steam Slip-Theoretical Prediction from Momentum Model" Trans. ASME, Journal of Heat Transfer, series C. 82 113, (1960).

(24) S. Levy: "Prediction of Two-phase pressure Drop and Density Distribution from Mixing Length Theory", Trans. ASME, Journal of Heat Transfer (May 1963).

(25) S.G. Bankoff: "A Variable Density Single-Fluid Model for Two-Phase Flow with Particular Reference to Steam-Water Flow", Trans. ASME, Journal of Heat Transfer (November 1960).

(26) G.A. Hughmark: "Holdup in gas-liquid flow", Chem. Eng. Progress 58, 4, 62 (1962).

(27) N. Adorni, L. Cravarolo, A. Giorgini, A. Hassid, E. Pedrocchi: "Design and construction of a high pressure facility for hydrodynamics experiments on two-phase flow - Instrumentation - Preliminary tests in single and two-phase flow". CISE R-75 (1963).

(28) L. Cravarolo, A. Hassid: "Phase and velocity distribution in two-phase adiabatic dispersed flow". CISE N-98 (1963).

(29) P. Alia, L. Cravarolo, A. Hassid, E. Pedrocchi, M. Silvestri: "A volume displacement method for the measurement of the liquid volume fraction in two-phase adiabatic flow". CISE R-92 (1964).

(30) L. Cravarolo, A. Hassid, S. Villani: "A beta-ray attenuation method for density measurements of liquid-gas mixtures in adiabatic flow", Energia Nucleare 8, 12, 751 (1961).

(31) N. Adorni, P. Alia, L. Cravarolo, A. Hassid, E. Pedrocchi: "An isokinetic sampling probe for phase and velocity distribution measurements in two-phase flow near the wall of the conduit". CISE R-89 (1963).

(32) L. Cravarolo, A. Hassid, E. Pedrocchi: "Further investigation on two-phase adiabatic annular-dispersed flow: effect of length and of some inlet conditions on flow parameters", CISE R-93 (1964).

(33) N. Adorni, L. Cravarolo, A. Hassid, E. Predocchi and M. Silvestri: "Measurement of shear stress on the wall of a conduit and its application to the void fraction determination in two-phase flow", Review of Scientific Instr. 34, 8, 937 (1963).

(34) L. Cravarolo, A. Giorgini, A. Hassid, E. Pedrocchi: "A device for the measurement of shear stress on the wall of a conduit. Its application in the mean density determination in two-phase flow. Shear stress data in two-phase adiabatic vertical flow". CISE R-82 (1964).

(35) L.E. Gill, G.F. Hewitt, J.W. Hitchon: "Sampling probe studies of the gas core in annular two-phase flow". Part I-AERE R 3954 (1962).

(36) J.F. Marchaterre, M. Petrick: "The prediction of steam volume fractions in boiling systems", Nuclear Science and Eng. 7, 525 (1960).

(37) M.J. Fohrman: "The effect of the liquid viscosity in two-phase, two-component flow", ANL-6256 (1960).

(38) I. Casagrande, L. Cravarolo, A. Hassid, E. Pedrocchi: "Adiabatic dispersed two-phase flow: Further results on the influence of physical properties on pressure drop and film thickness" CISE R-73 (1963).

(39) N. Adorni, I. Casagrande, L. Cravarolo, A. Hassid, E. Pedrocchi, M. Silvestri: "Further investigations in adiabatic dispersed two-phase flow: Pressure drop and film thickness measurements with different channel geometries. Analysis of the influence of geometrical and physical parameters". CISE R-53 (1963).

(40) M. Silvestri, N. Adorni, S. Bertoletti, I. Casagrande, L. Cravarolo G.P. Gaspari, A. Hassid, C. Lombardi, E. Pedrocchi, G. Peterlongo: "Basic Heat transfer and hydrodynamics studies in two-phase flow" Geneva Conference P/867 (1964)

(41) N. Adorni, G. Peterlongo, R. Ravetta, F.A. Tacconi: "Phase and velocity distribution measurements in a round vertical tube". CISE R-91 (1964).

(42) O. Baker: "Simultaneous flow of oil and gas", The Oil and Gas Journal (July 1954).

(43) G.F. Hewitt, P.C. Lovegrove: "Comparative film thickness and holdup measurements in vertical annular flow". AERE-M 1203 (1963).

(44) "Research into boiler circulation carried out at the University of Cambridge for the Water Tube Boilermaker Association during the years 1952-59".

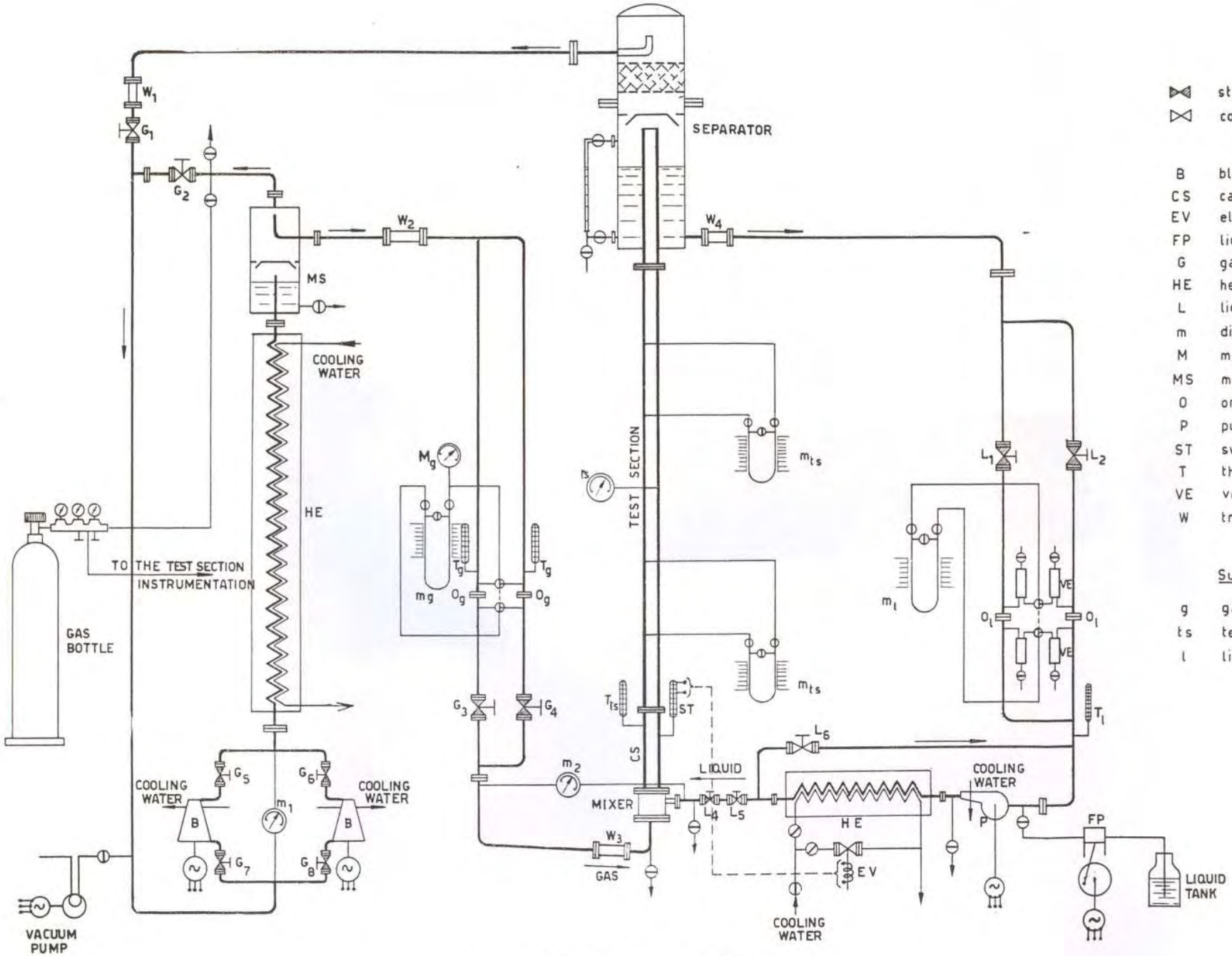

stop valve
control valve

B	blower
CS	calming section
EV	electromagnetic valve
FP	liquid feeding pump
G	gas line valve
HE	heat exchanger
L	liquid line valve
m	differential manometer
M	manometer
MS	moisture separator
O	orifice
P	pump
ST	switch thermometer
T	thermometer
VE	vent
W	transparent window

Subscripts

g	gas
ts	test section
l	liquid

Fig. 1 - Schematic flow sheet of the circuit.

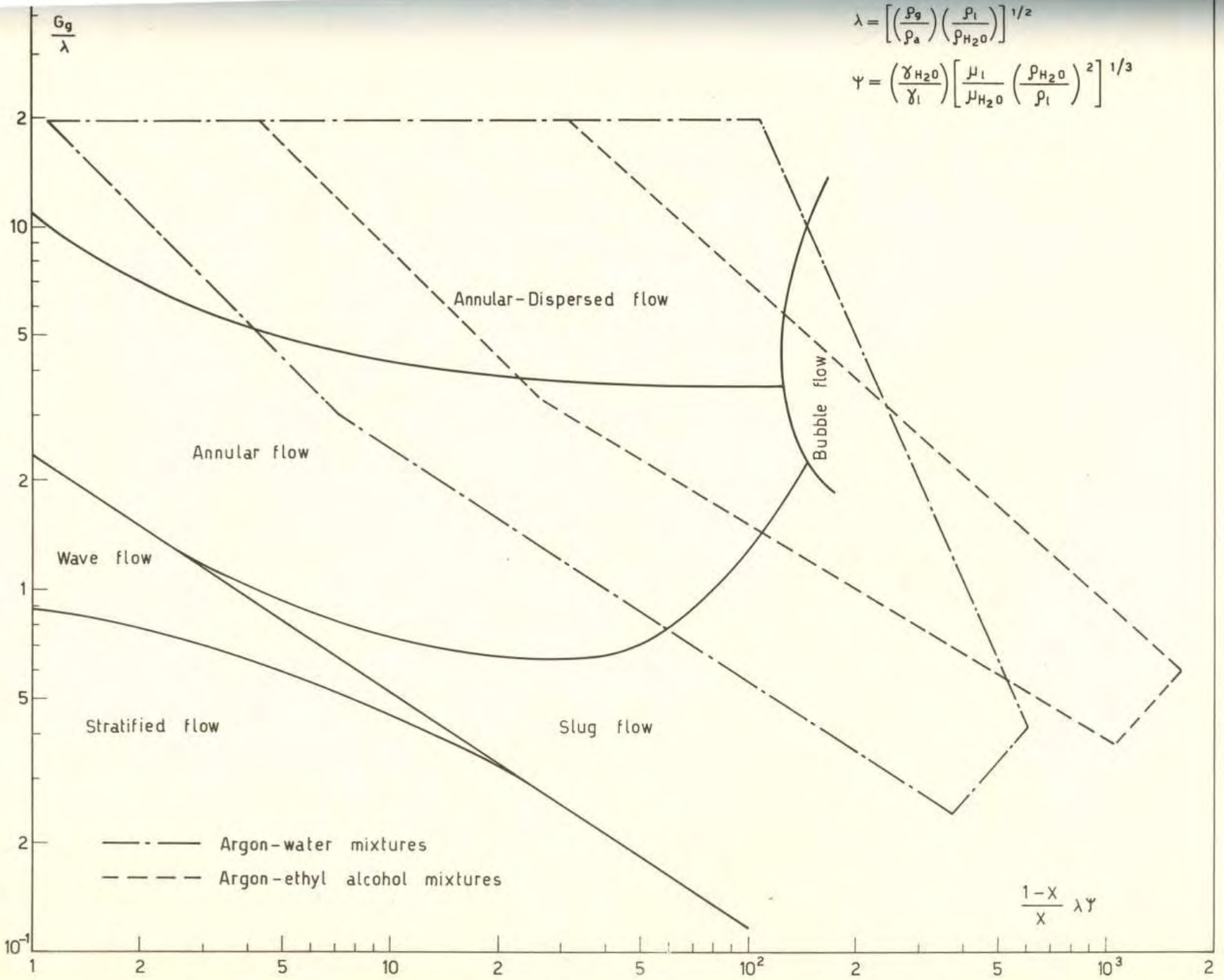

Fig. 2 - Experimental range on the Baker's map for argon-water and argon-ethyl alcohol mixtures at various ρ_g.

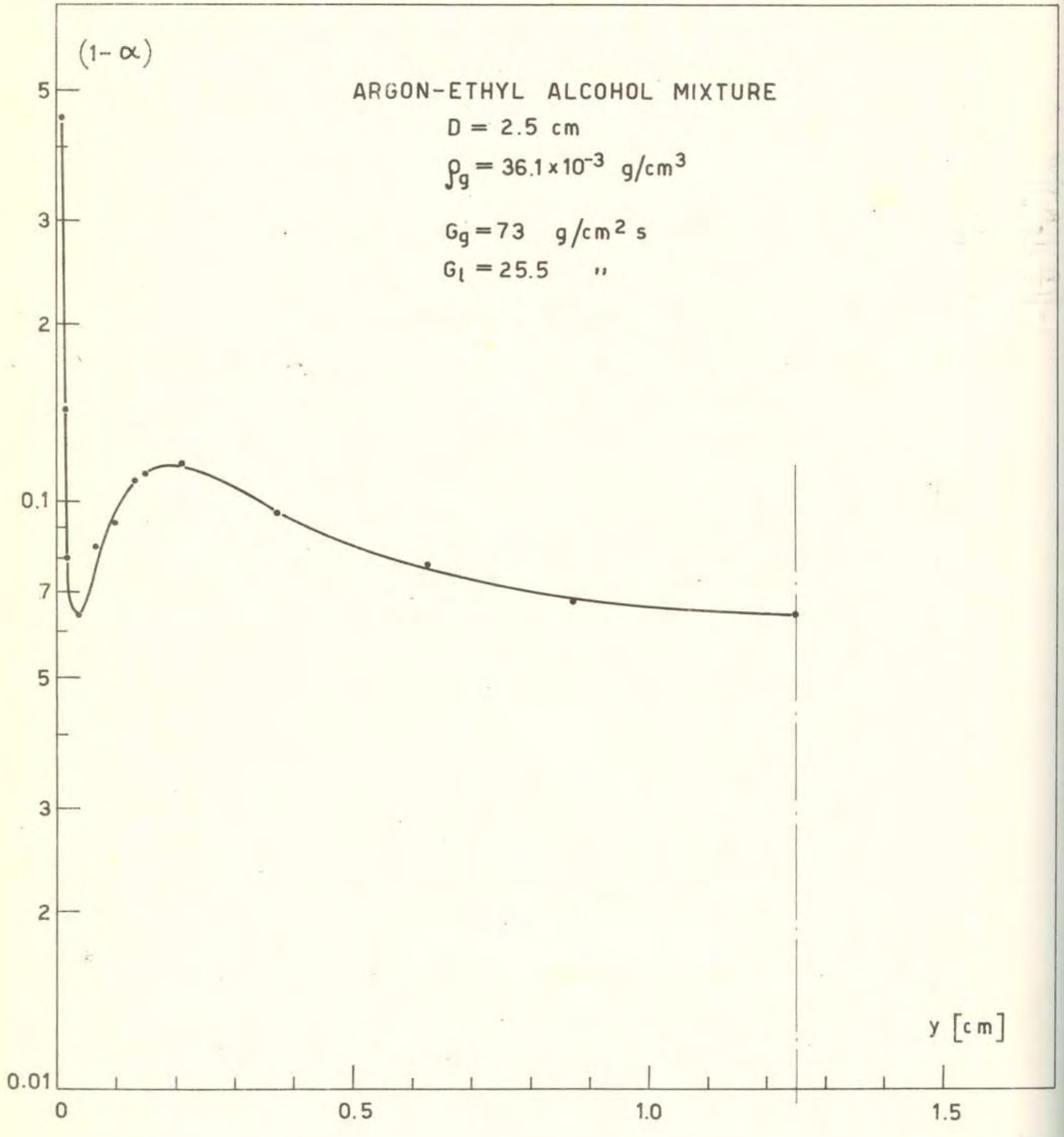

Fig. 3 - Phase distribution profile over the conduit cross-section vs. distance from the wall.

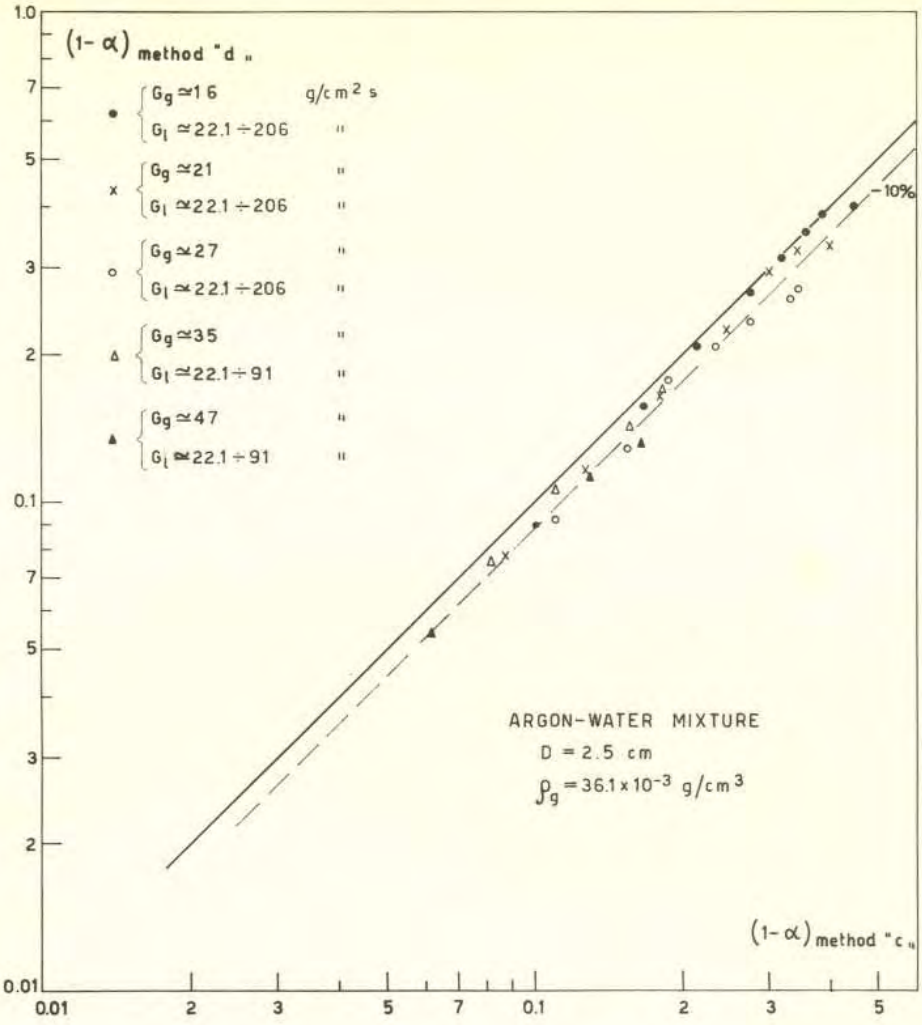

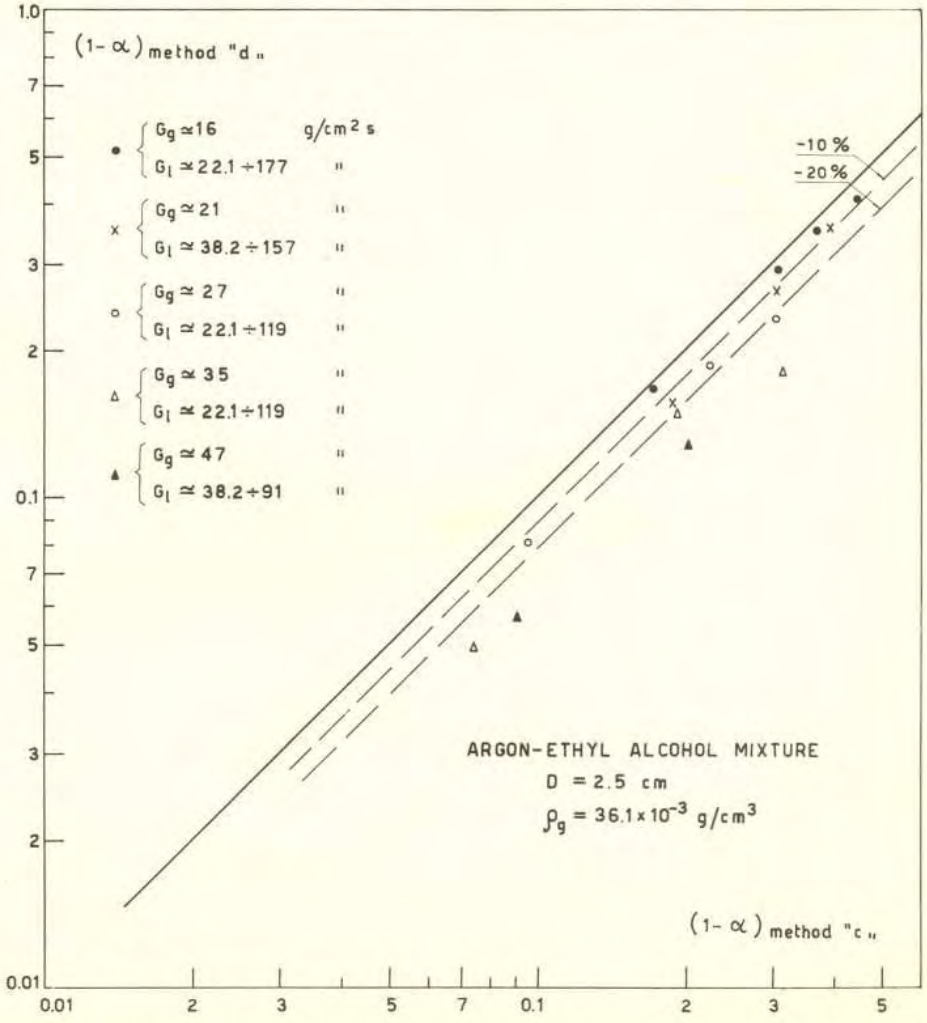

Fig. 4 - Comparison of liquid volume fraction data obtained from method "d" and method "c".

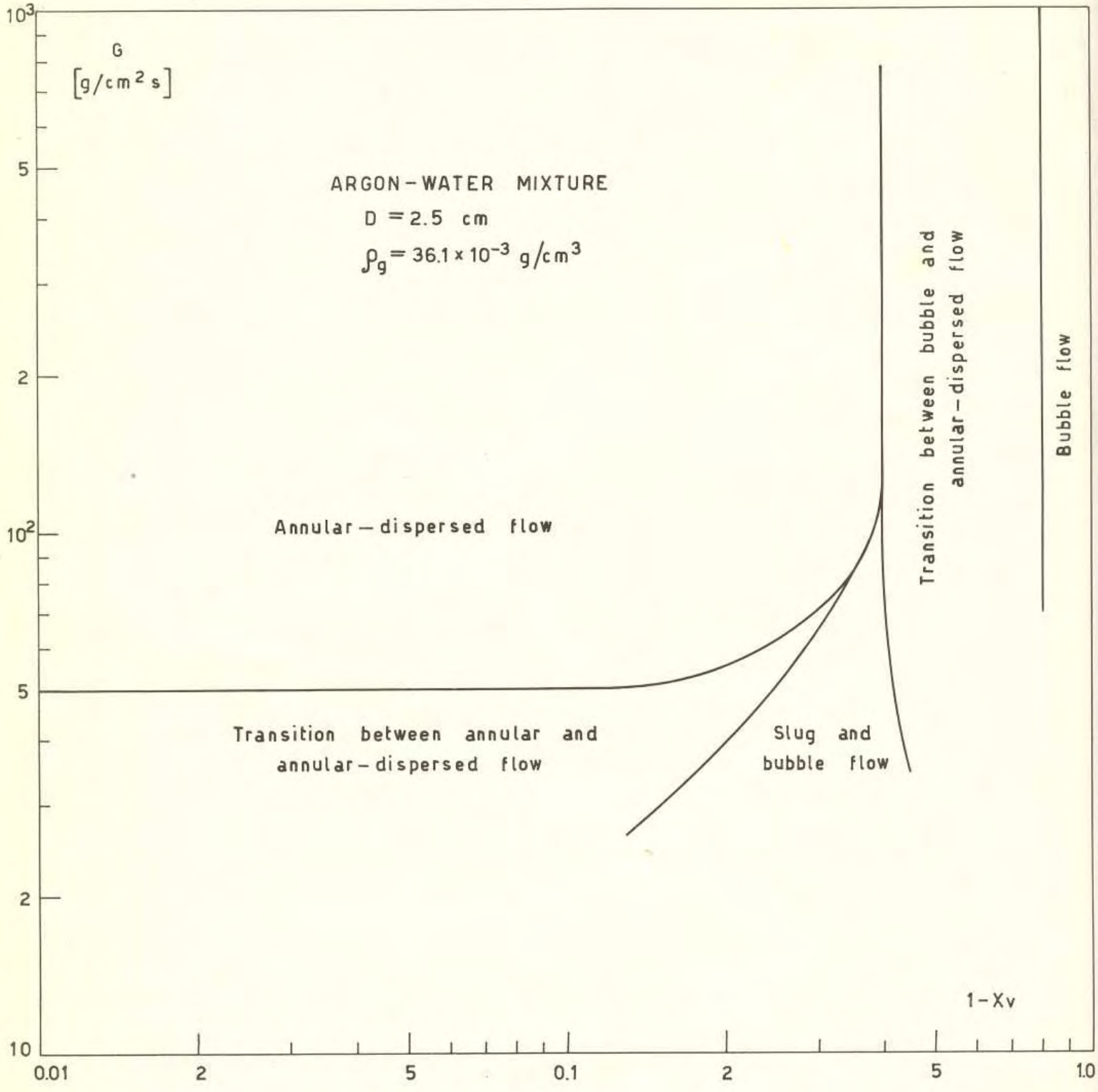

Fig. 5 - Flow patterns from visual observation.

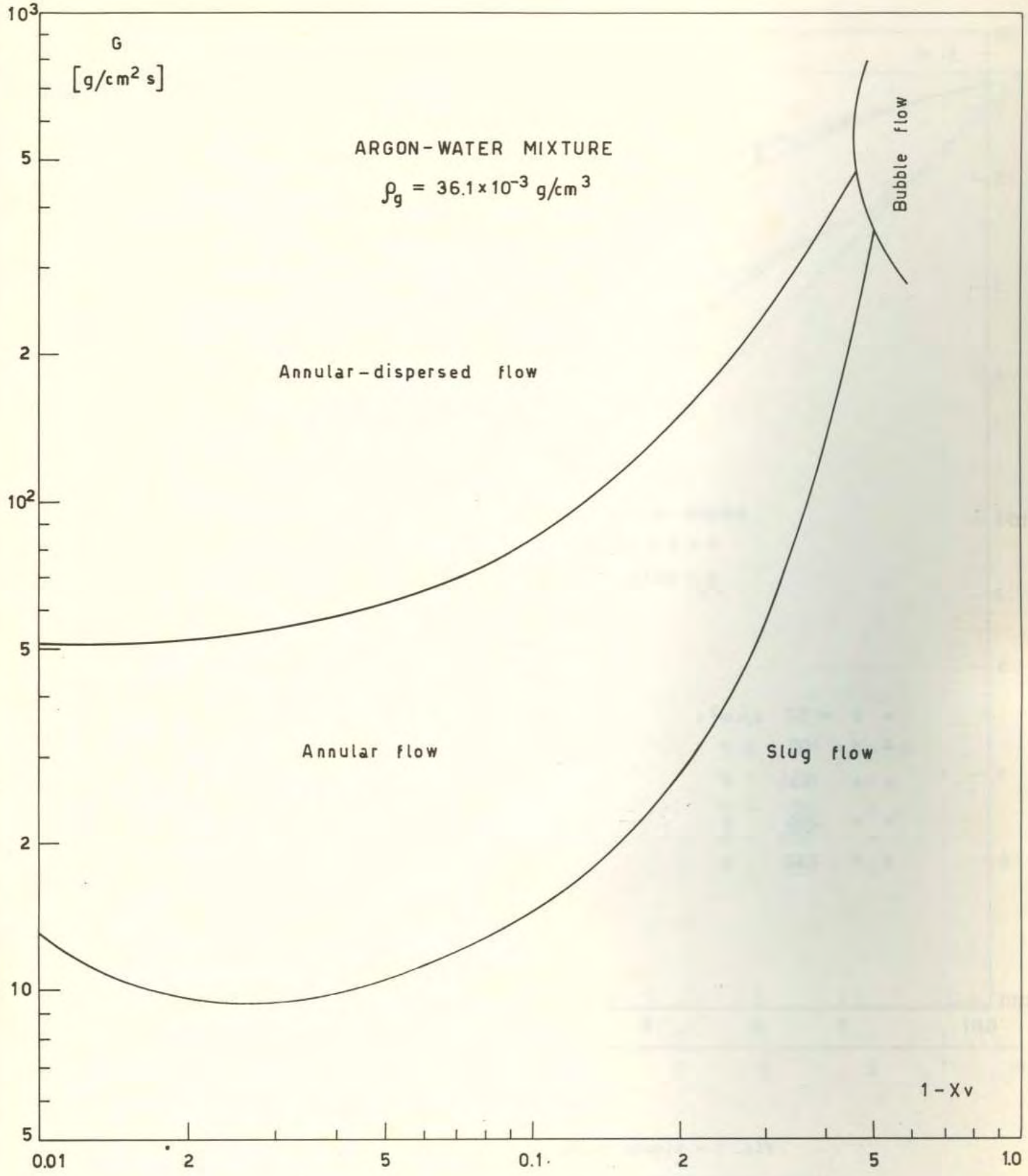

Fig. 6 - Flow patterns according to Baker's prediction.

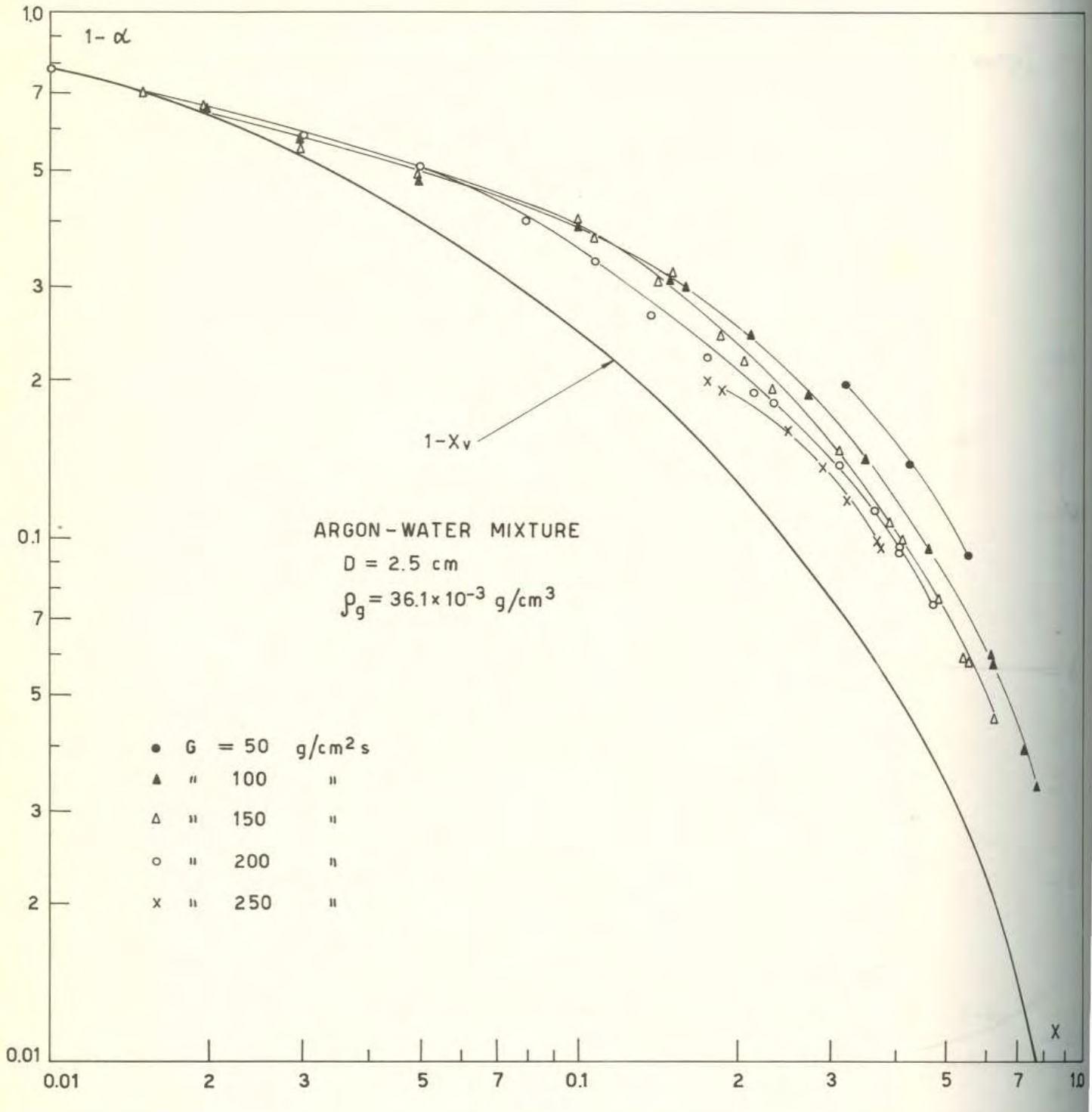

Fig. 7 - Liquid volume fraction data vs. mass quality.

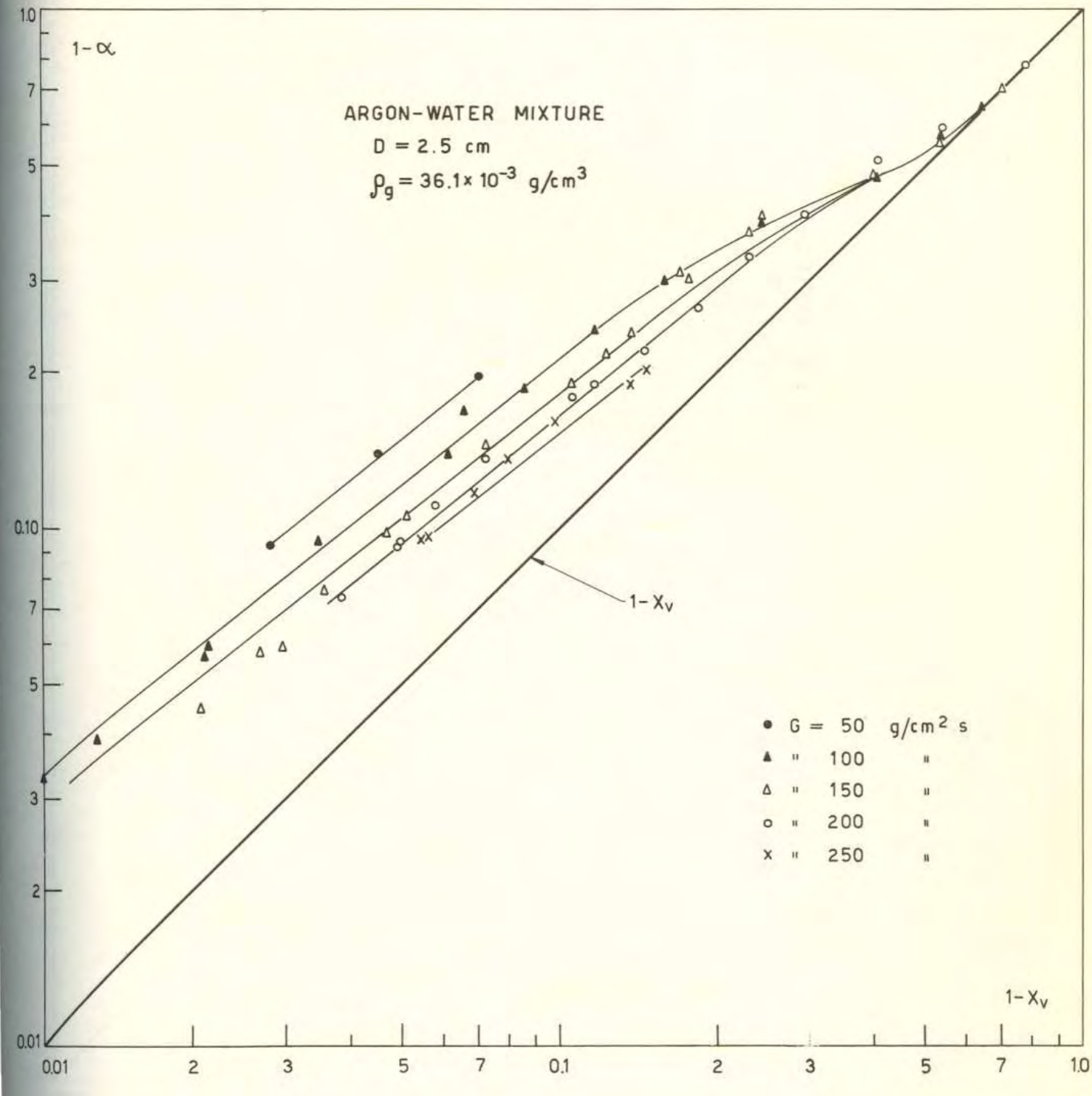

Fig. 8 - Liquid volume fraction data vs. liquid volume quality.

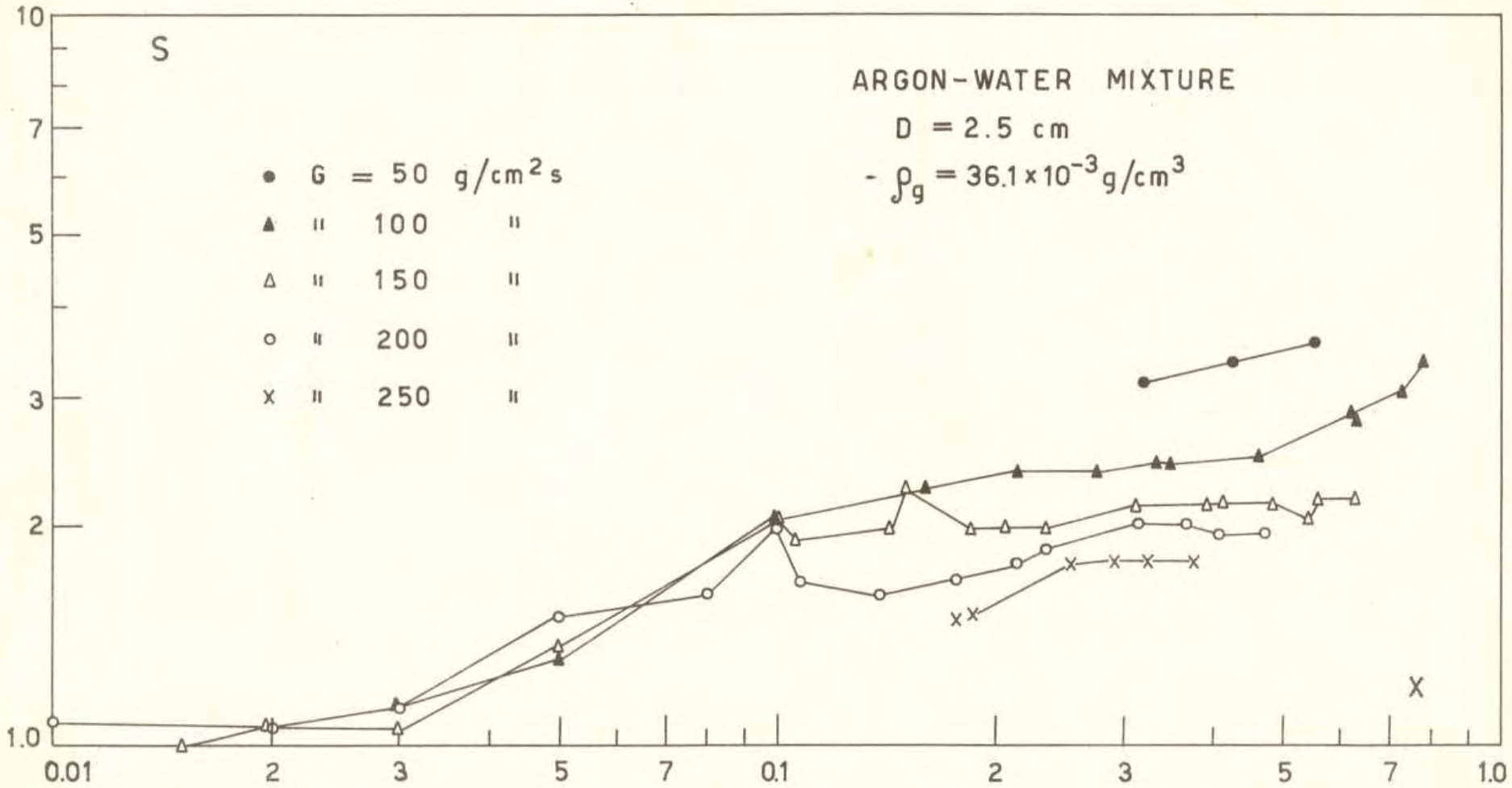

Fig. 9 - Slip ratio vs. mass quality.

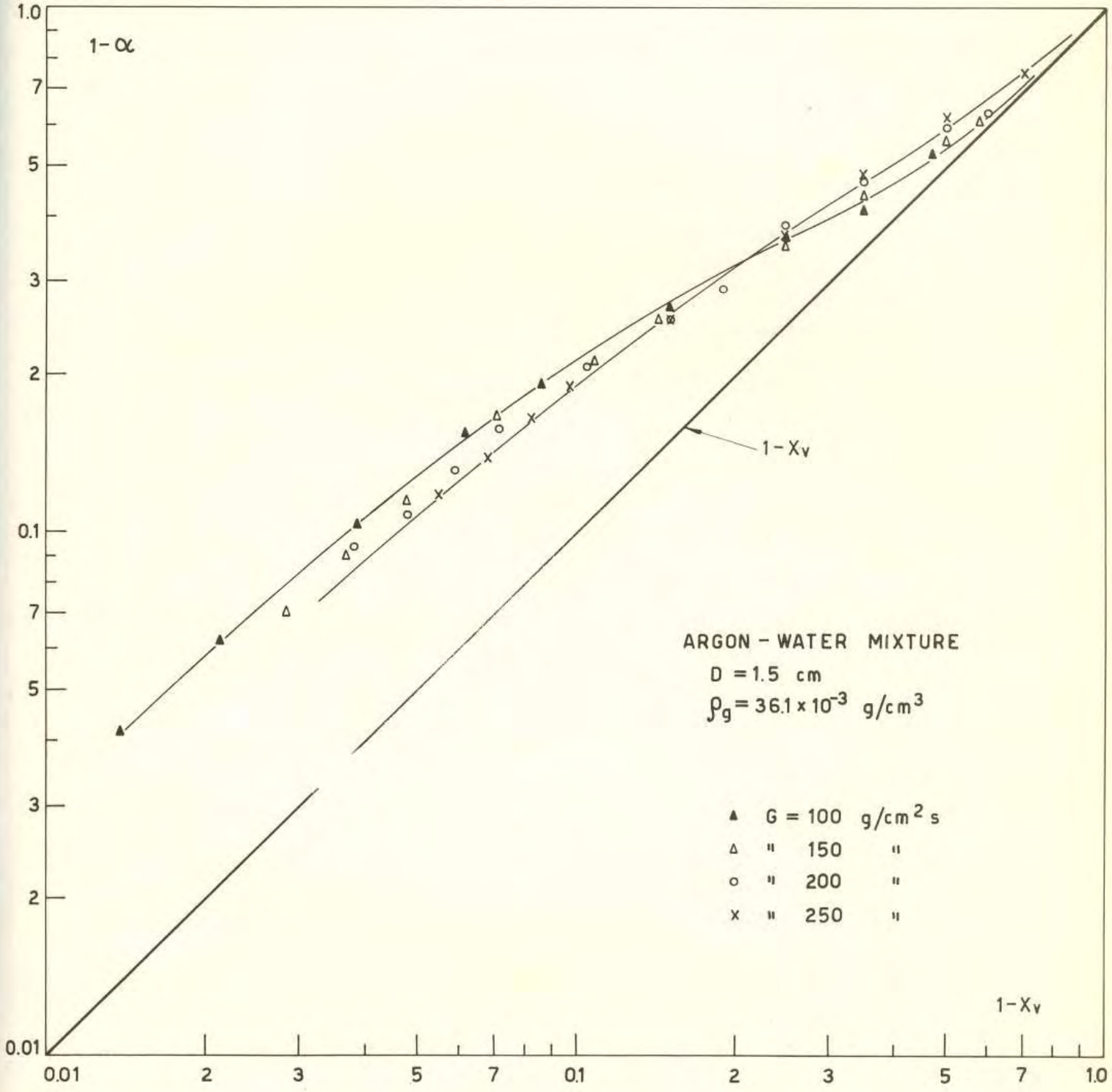

Fig. 10 - Liquid volume fraction data vs. liquid volume quality.

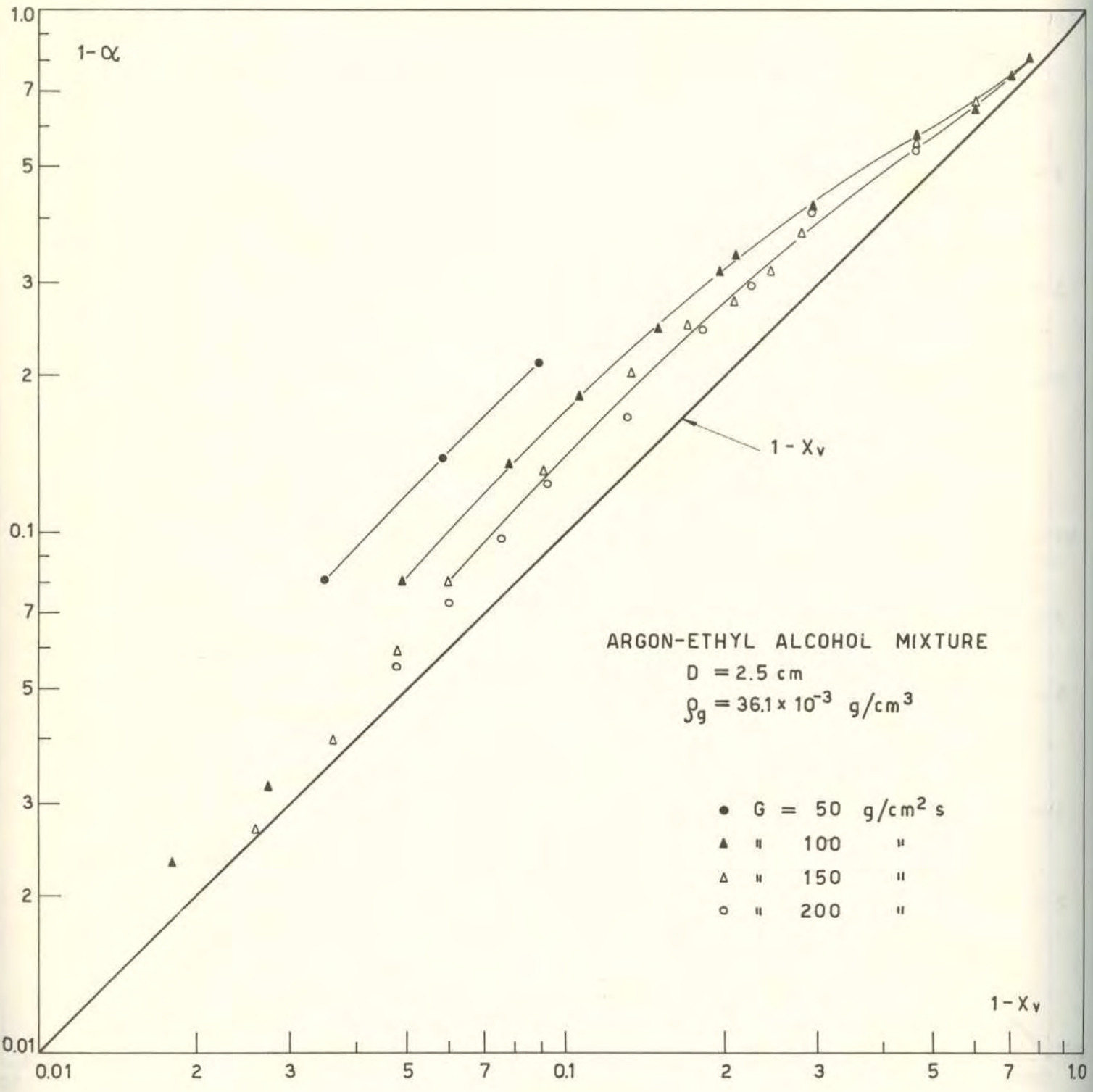

Fig. 11 - Liquid volume fraction data vs. liquid volume quality.

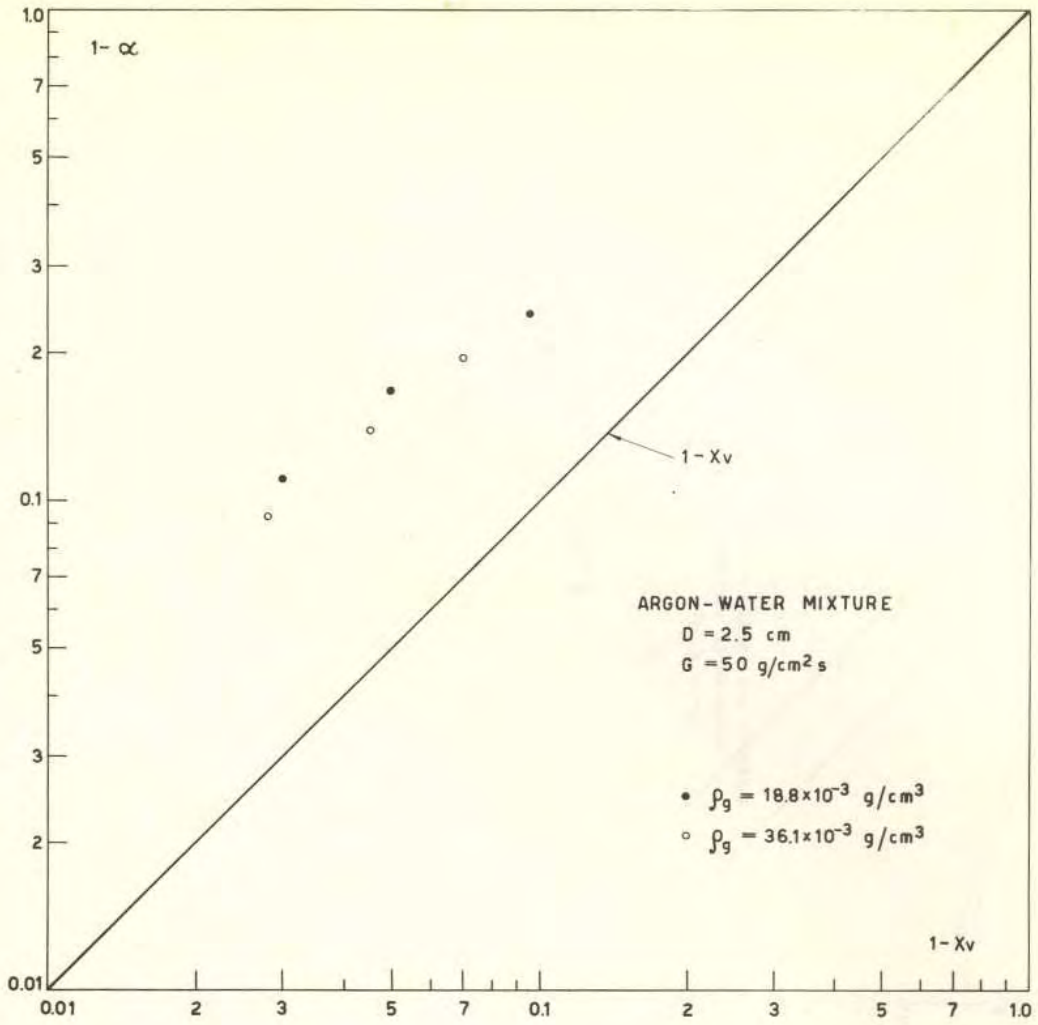

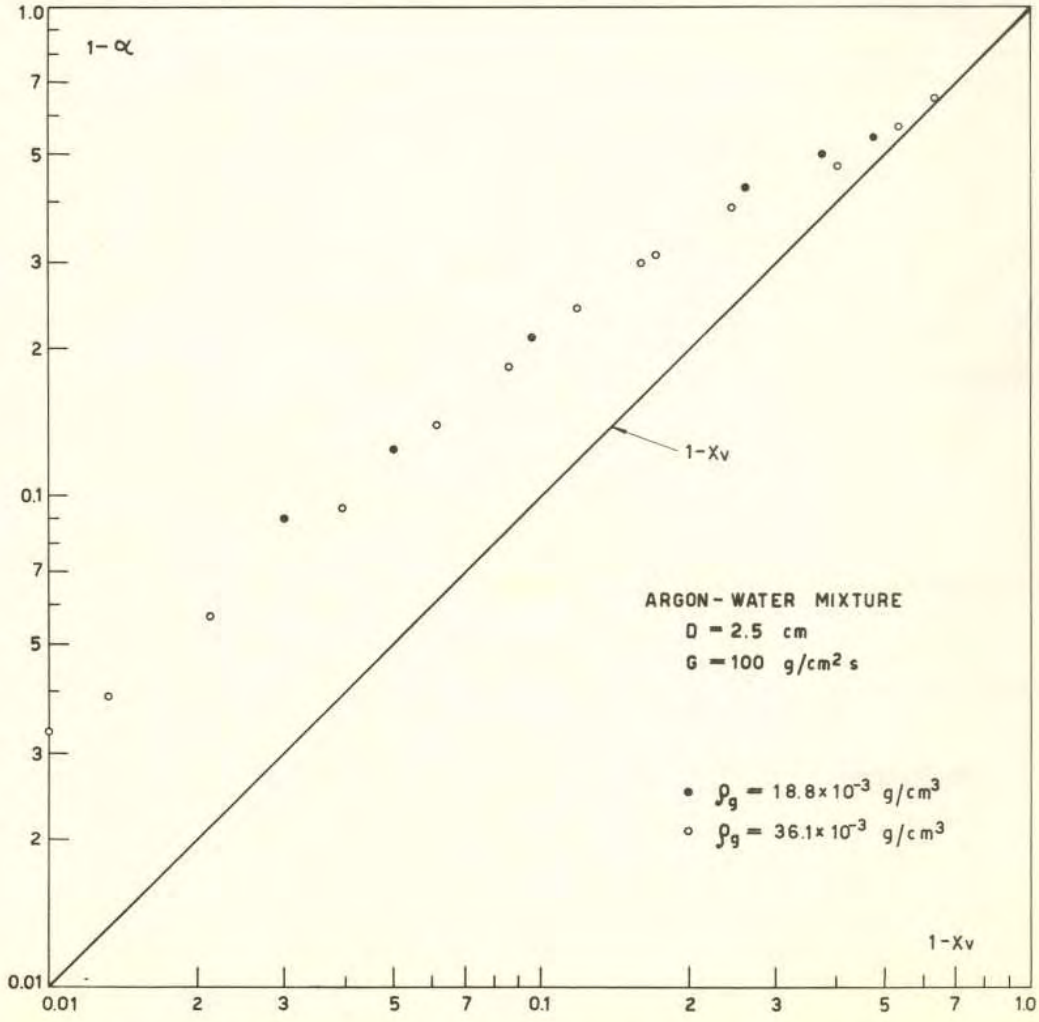

Fig. 12 - Influence of gas density on liquid volume fraction.

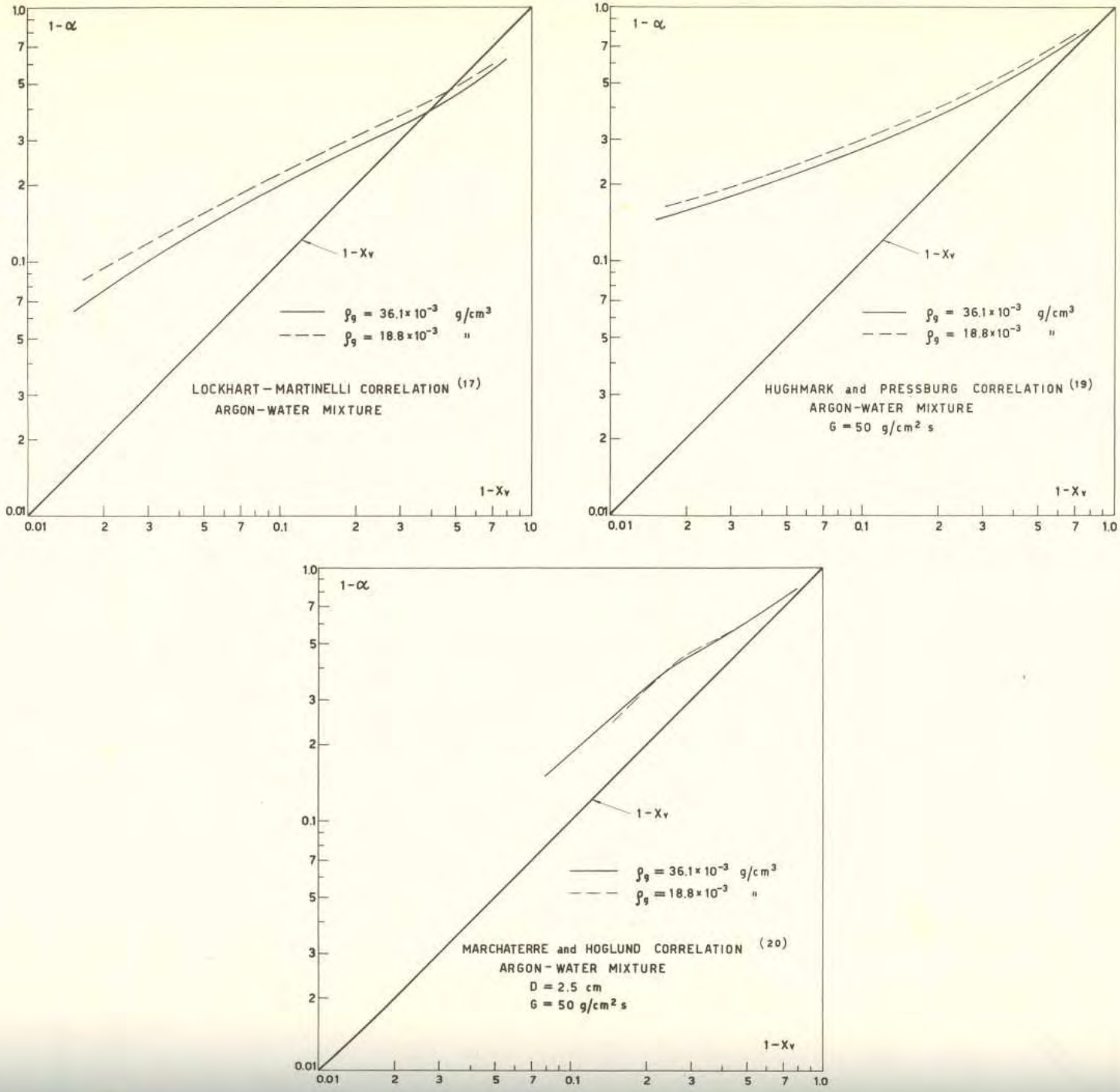

Fig. 13 - Influence of gas density on liquid volume fraction as predicted by various correlations.

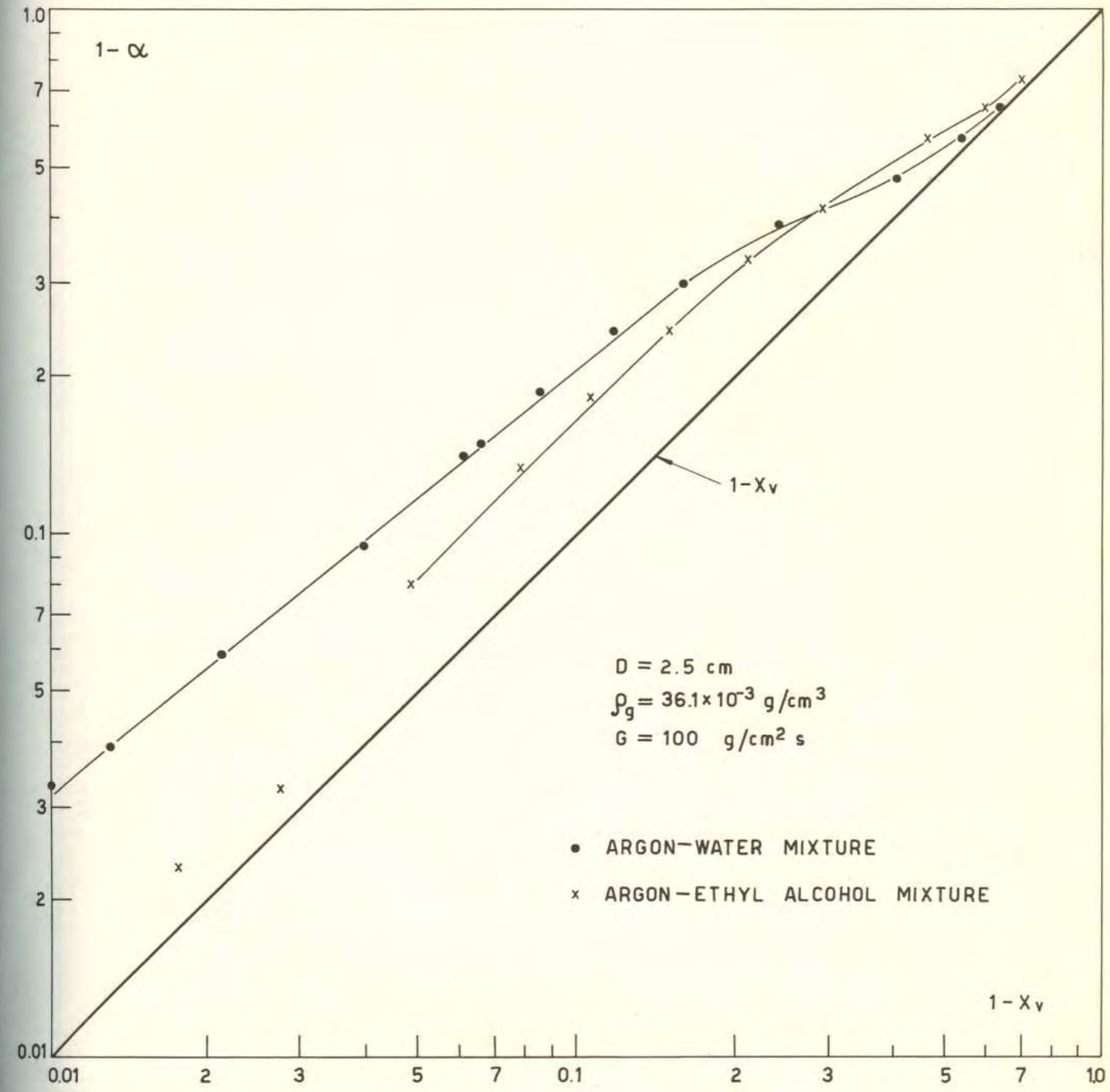

Fig. 14 - Influence of surface tension on liquid volume fraction.

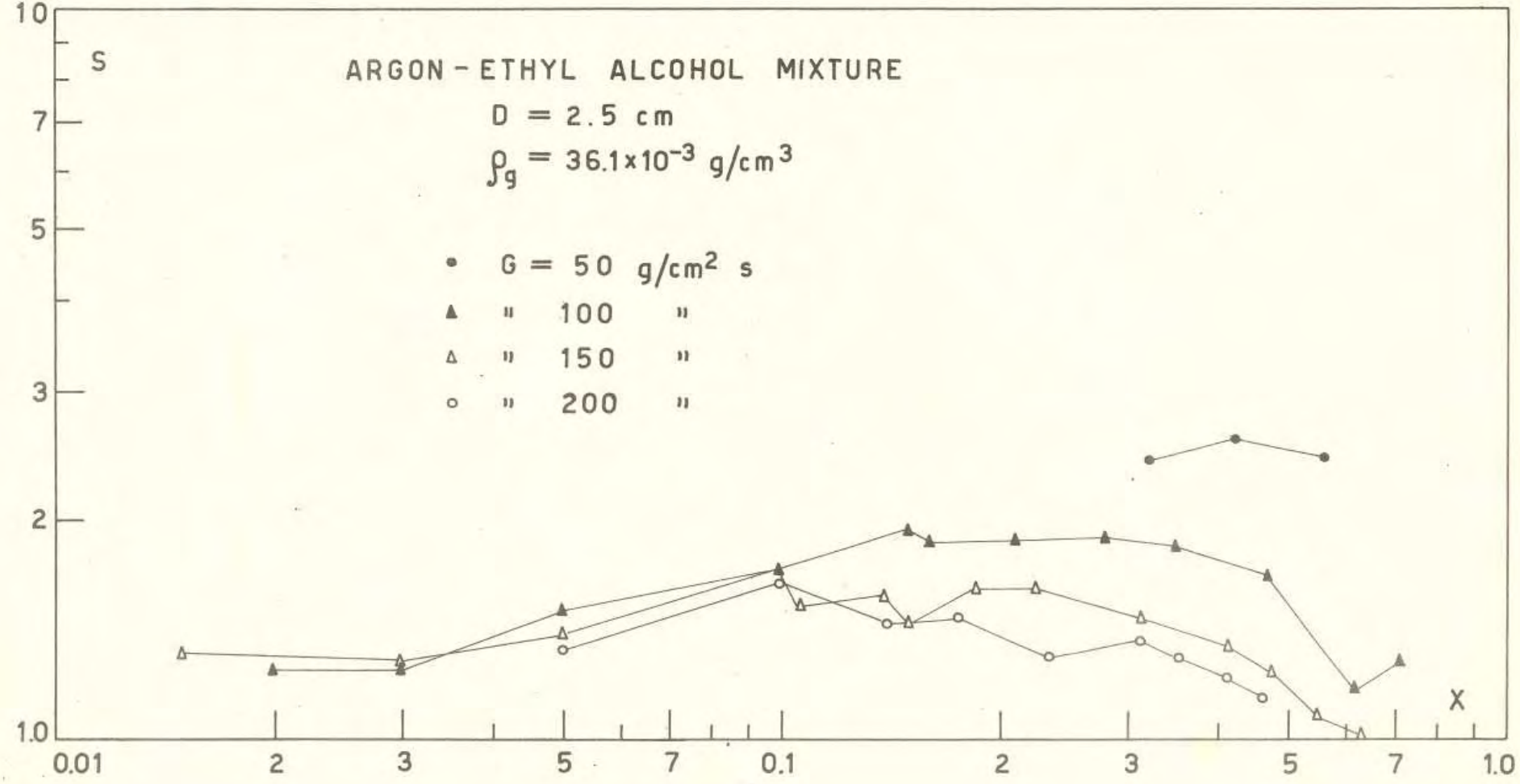

Fig. 15 - Slip ratio vs. mass quality.

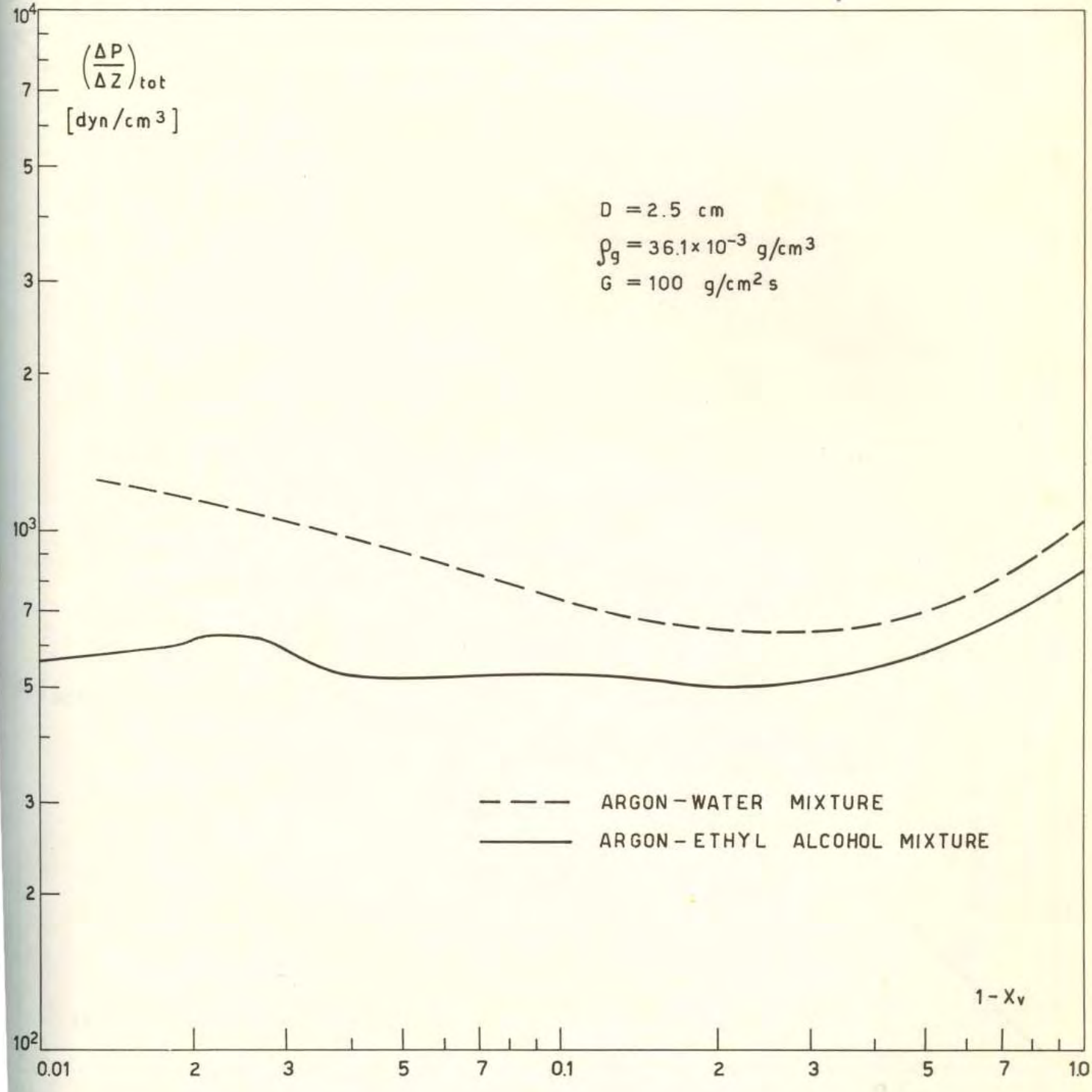

Fig. 16 - Pressure gradient vs. liquid volume quality.

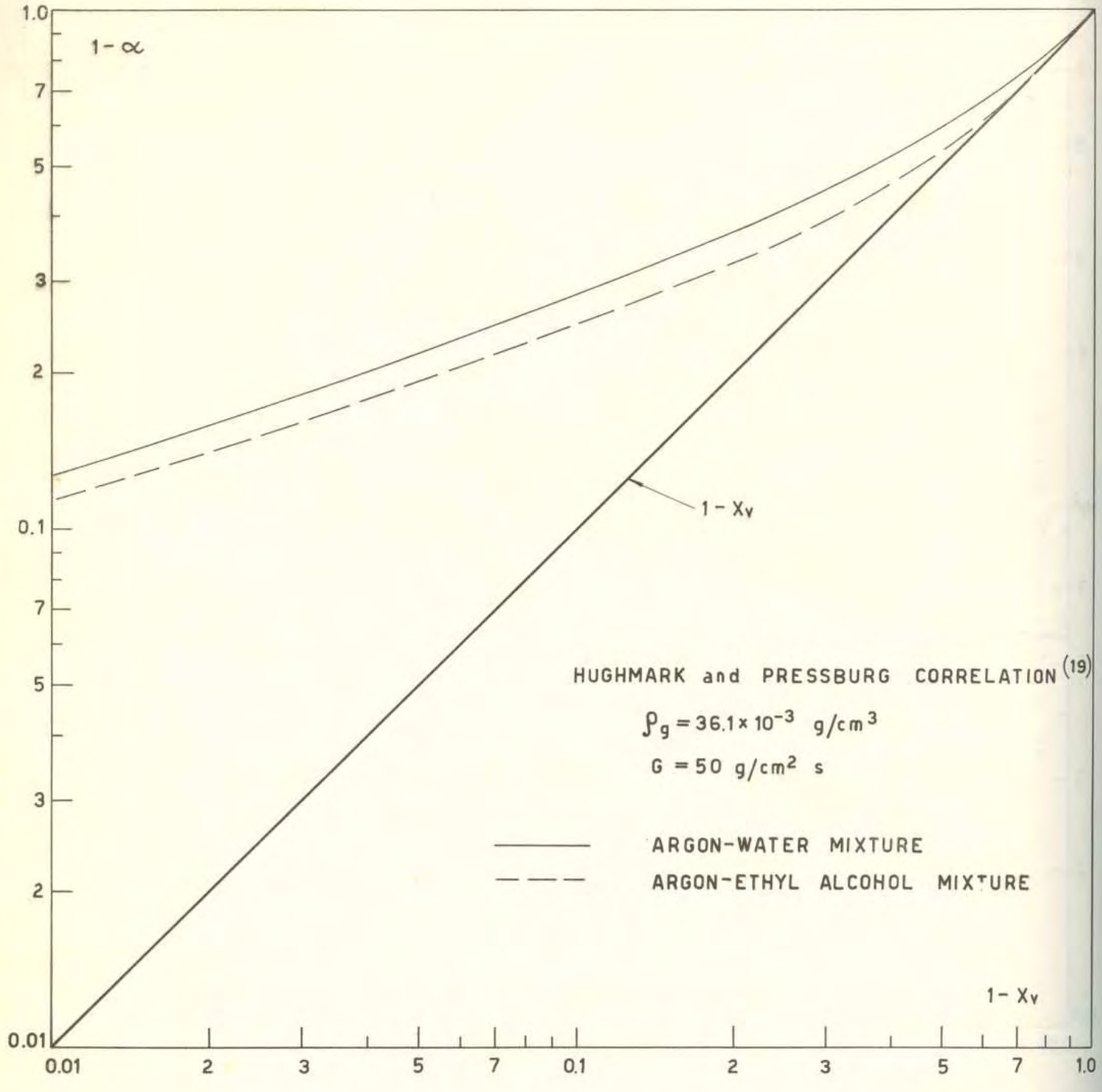

Fig. 17 - Influence of surface tension on liquid volume fraction as predicted by Hughmark and Pressburg correlation.

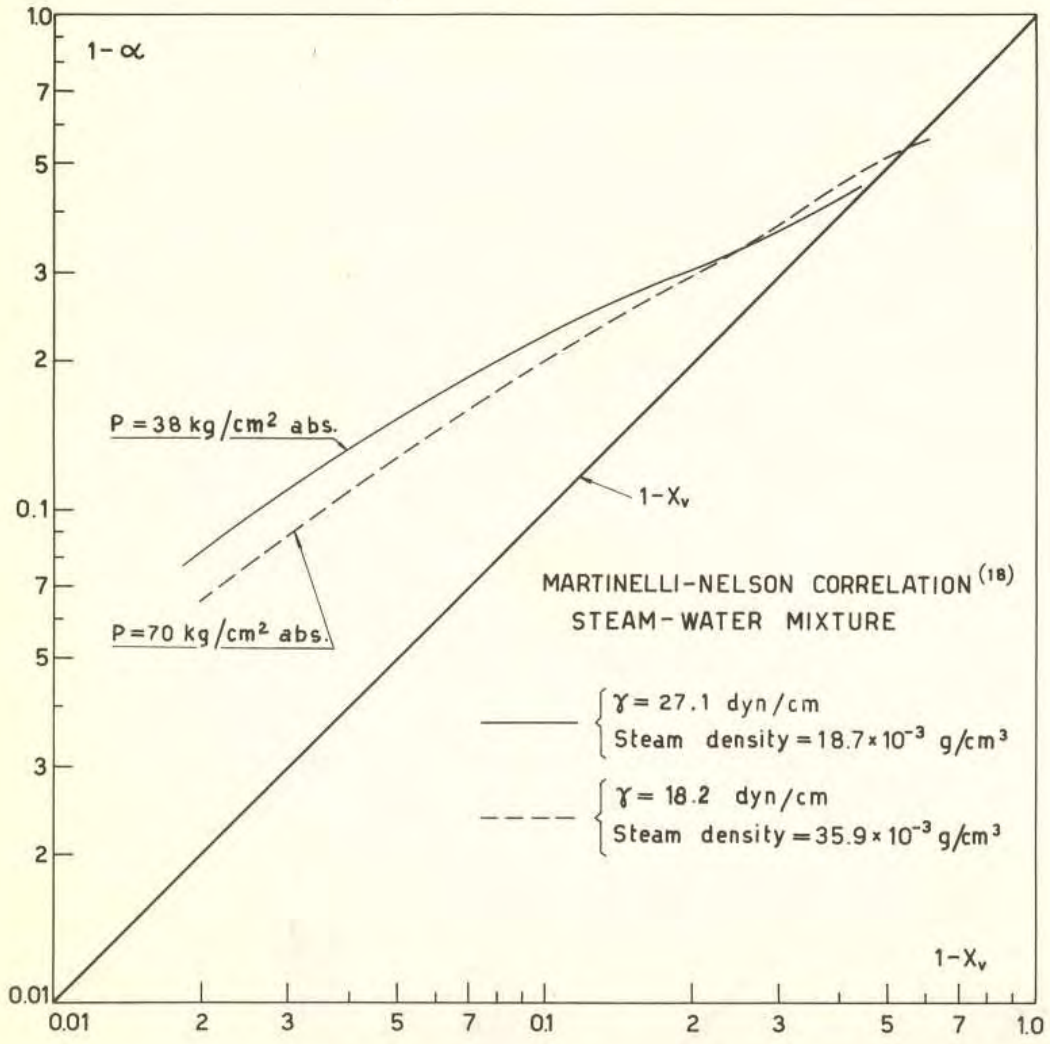

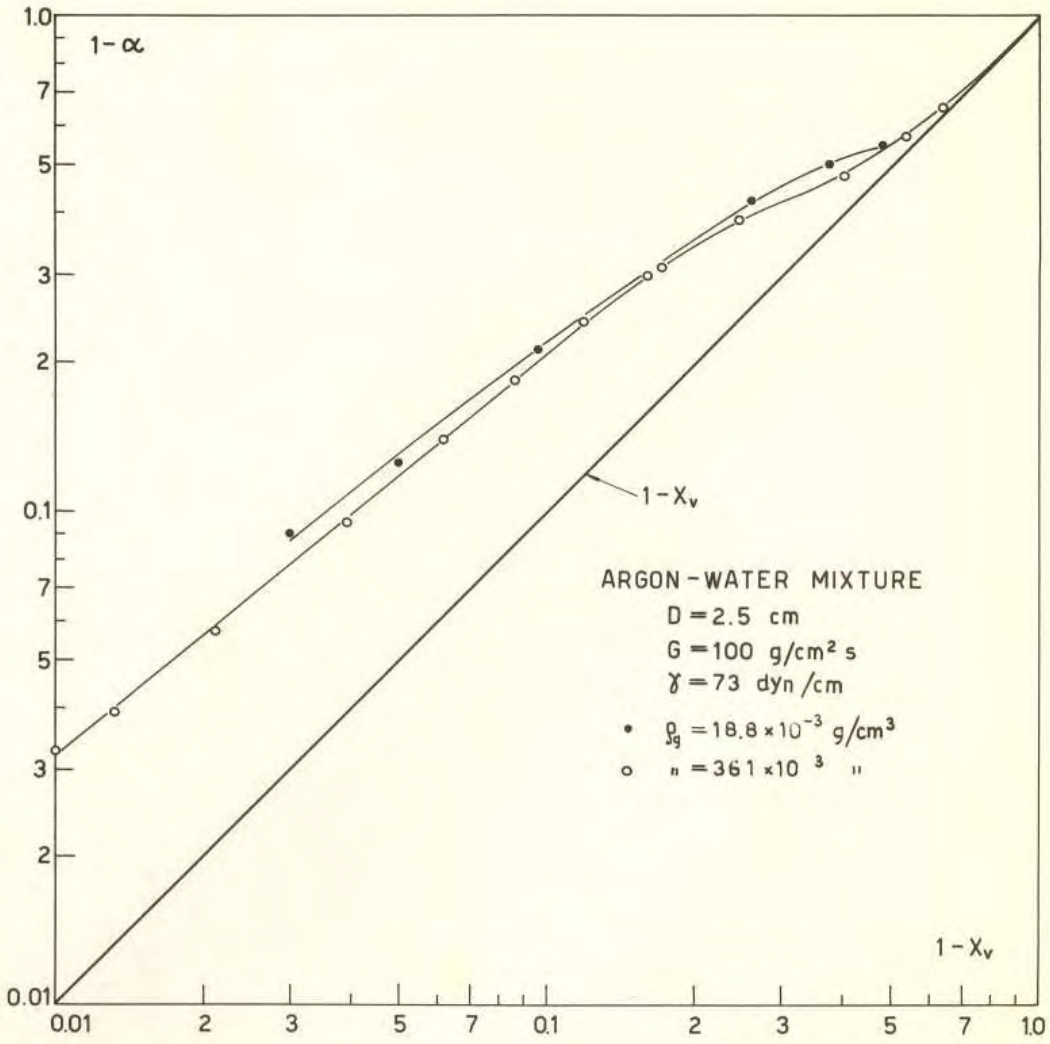

Fig. 18 - Effect of Pressure as predicted by Martinelli - Nelson correlation for steam-water mixture and without the effect of surface tension (CISE data at various ρ_g).

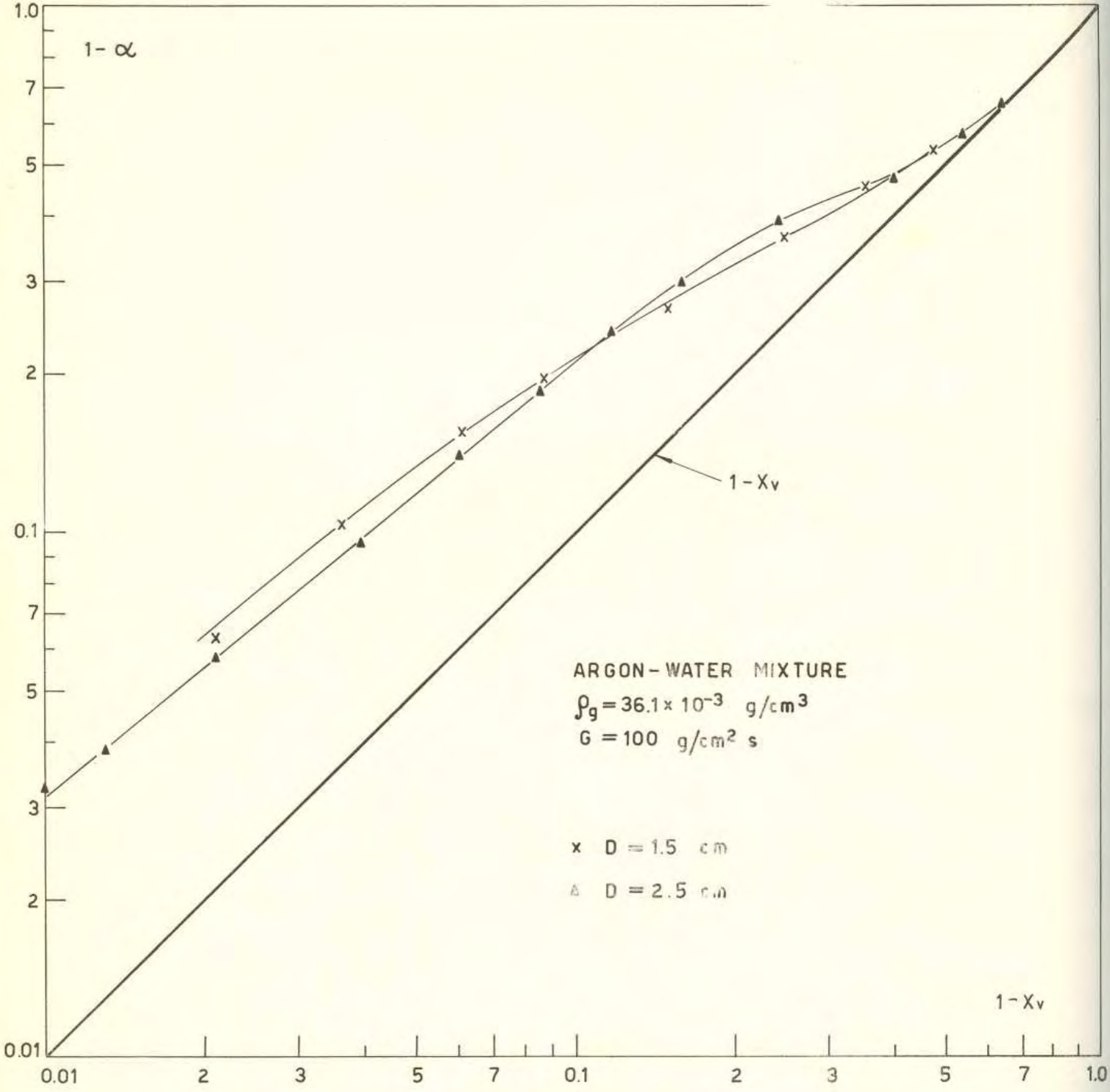

Fig. 19 - Influence of diameter on liquid volume fraction.

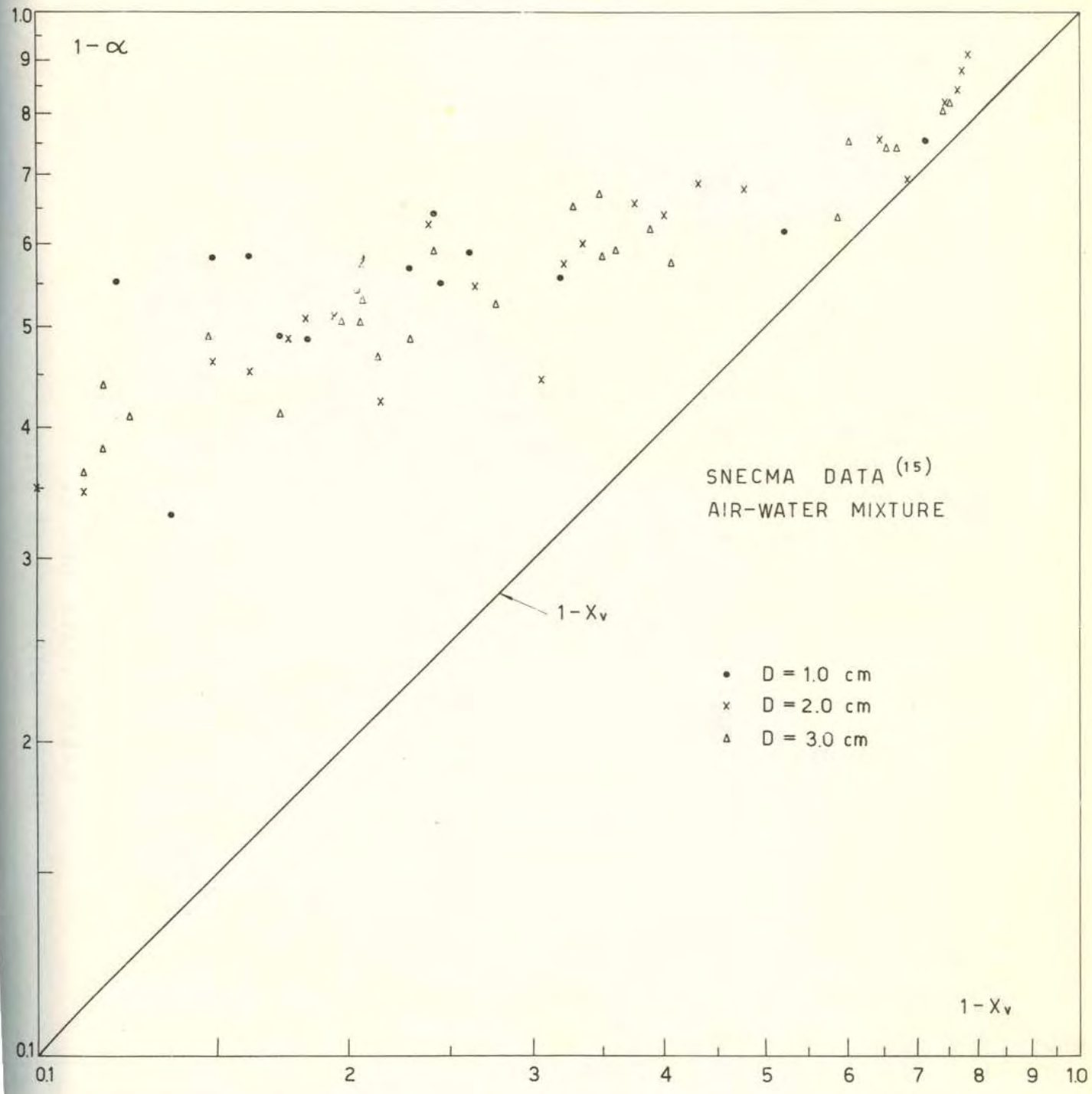

Fig. 20 - Liquid volume fraction data of SNECMA reduced to the same G (150 g/cm^2 s) and ρ_g(1.5 x 10^{-3} g/cm^3) by utilizing the correlation of par. 5.2.

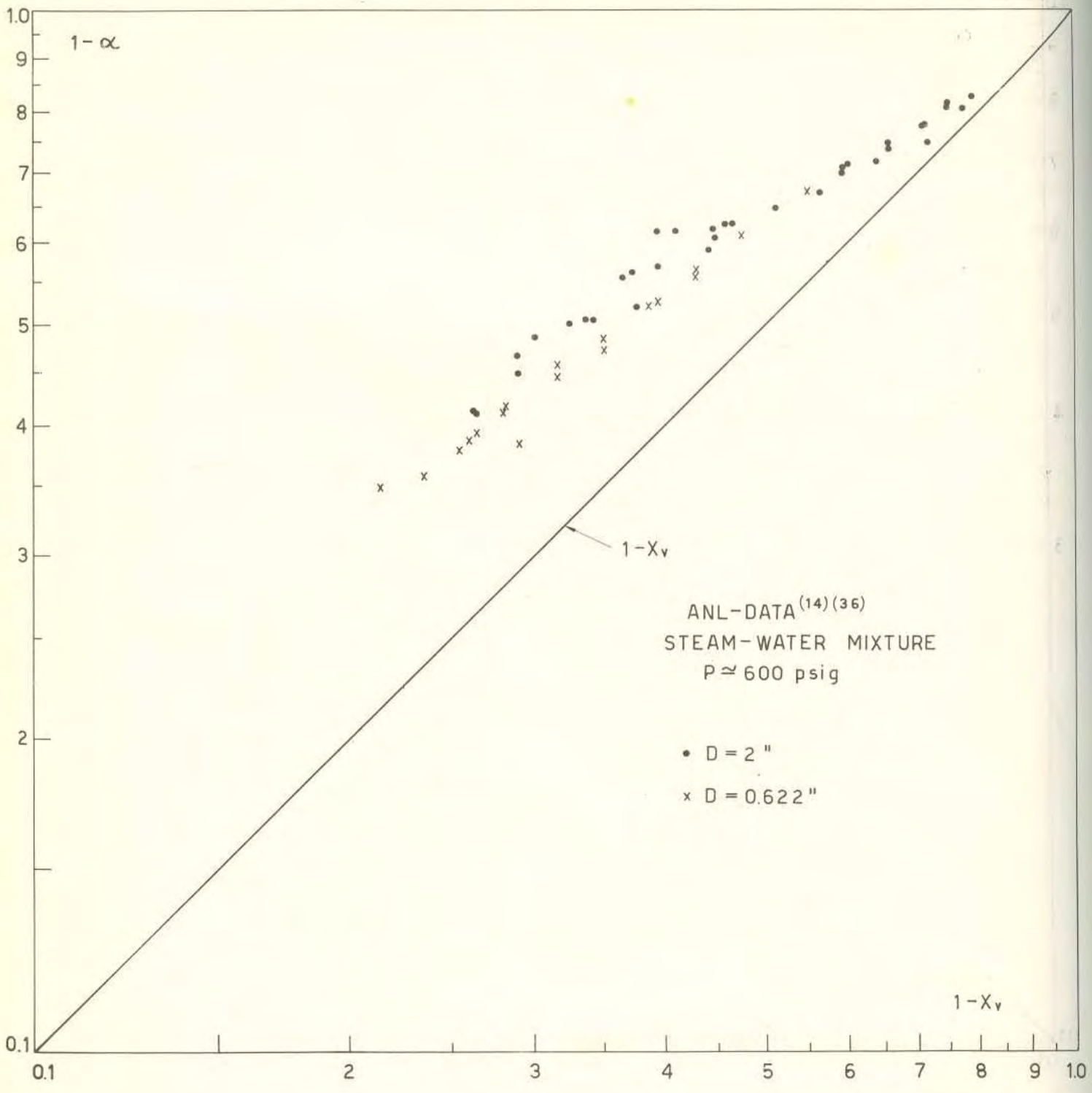

Fig. 21 - Effect of diameter on liquid volume fraction from experimental ANL data reduced to the same G (50 g/cm^{2}s) by utilizing the correlation of par 5.2.

RUSSIAN INTERPOLATED DATA[8]

STEAM-WATER MIXTURE

P = 40 kg/cm² abs.

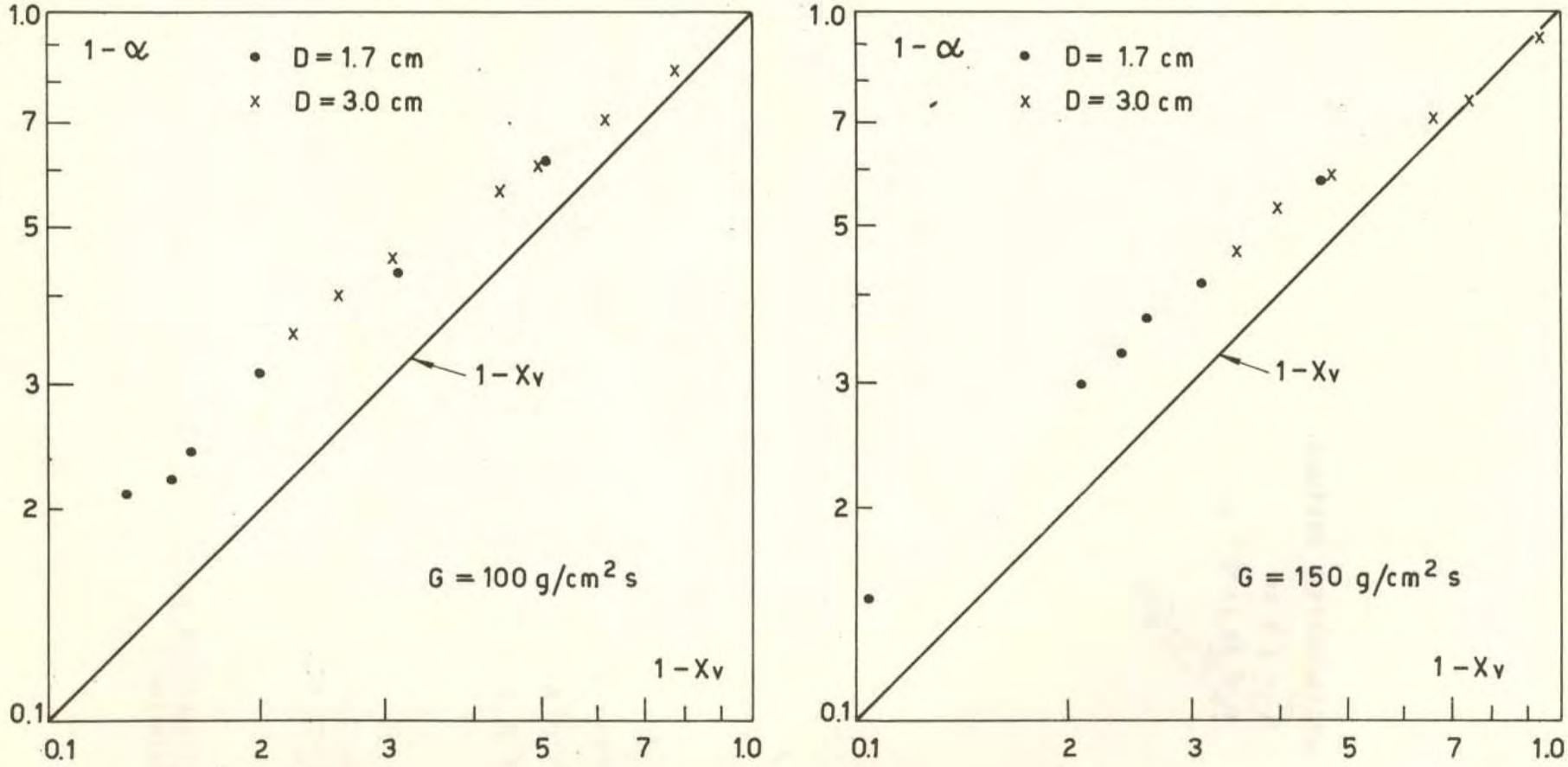

Fig. 22 - Effect of diameter on liquid volume fraction from russian experimental data (interpolated).

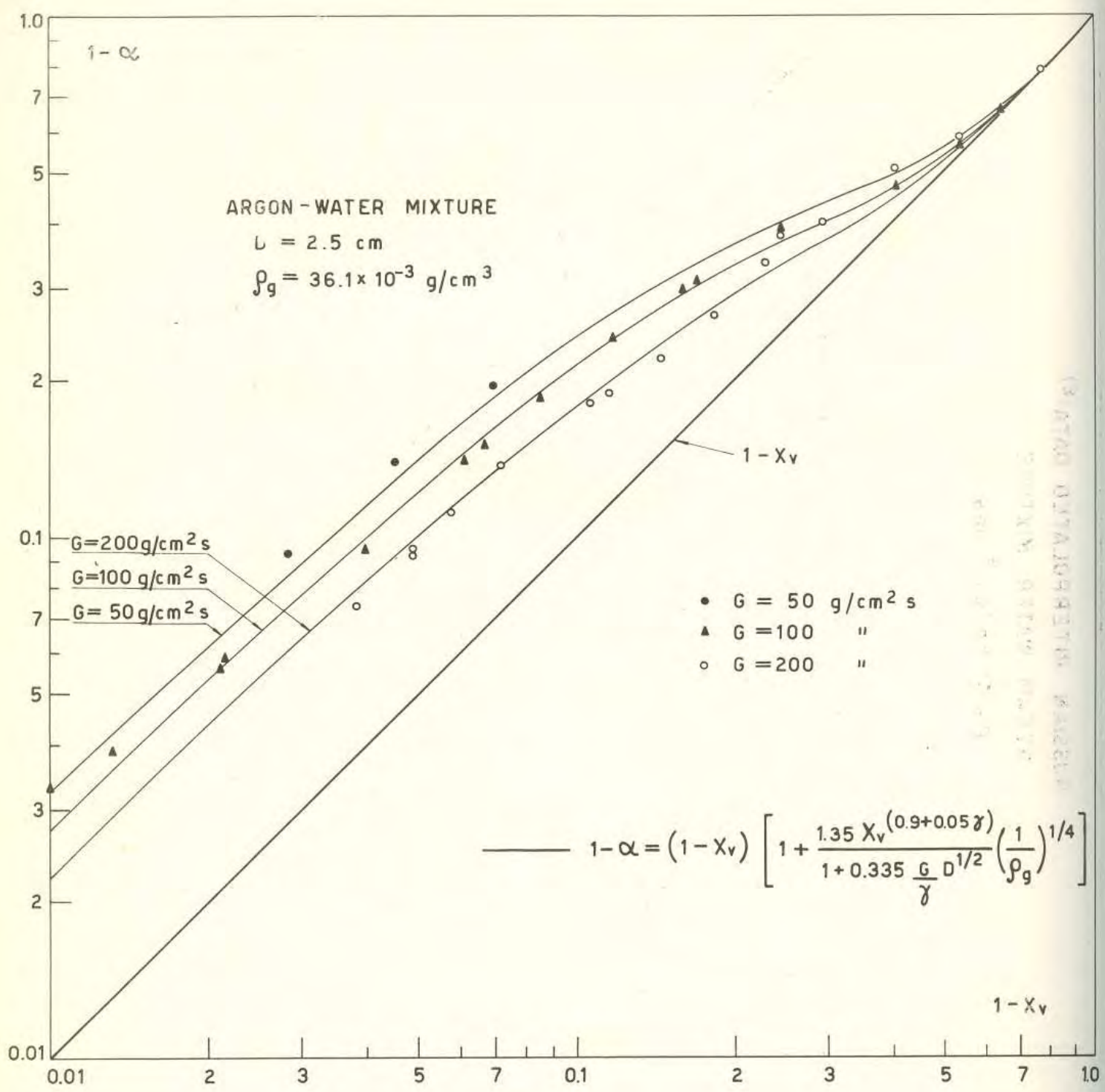

Fig. 23 - Experimental trend of CISE data (interpolated) against that predicted by the present correlation.

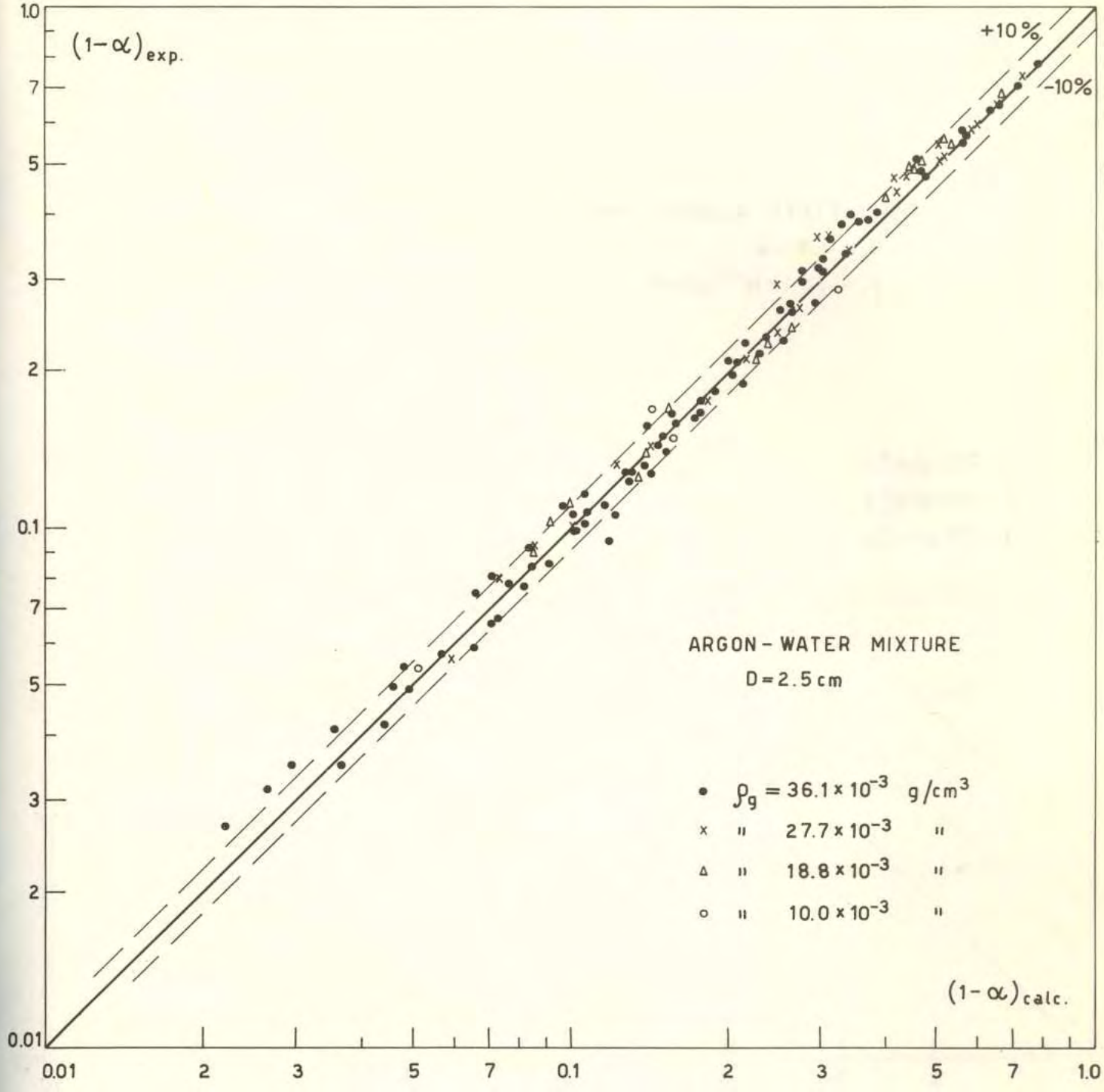

Fig. 24 - CISE experimental data checked against the Present correlation for argon-water mixture.

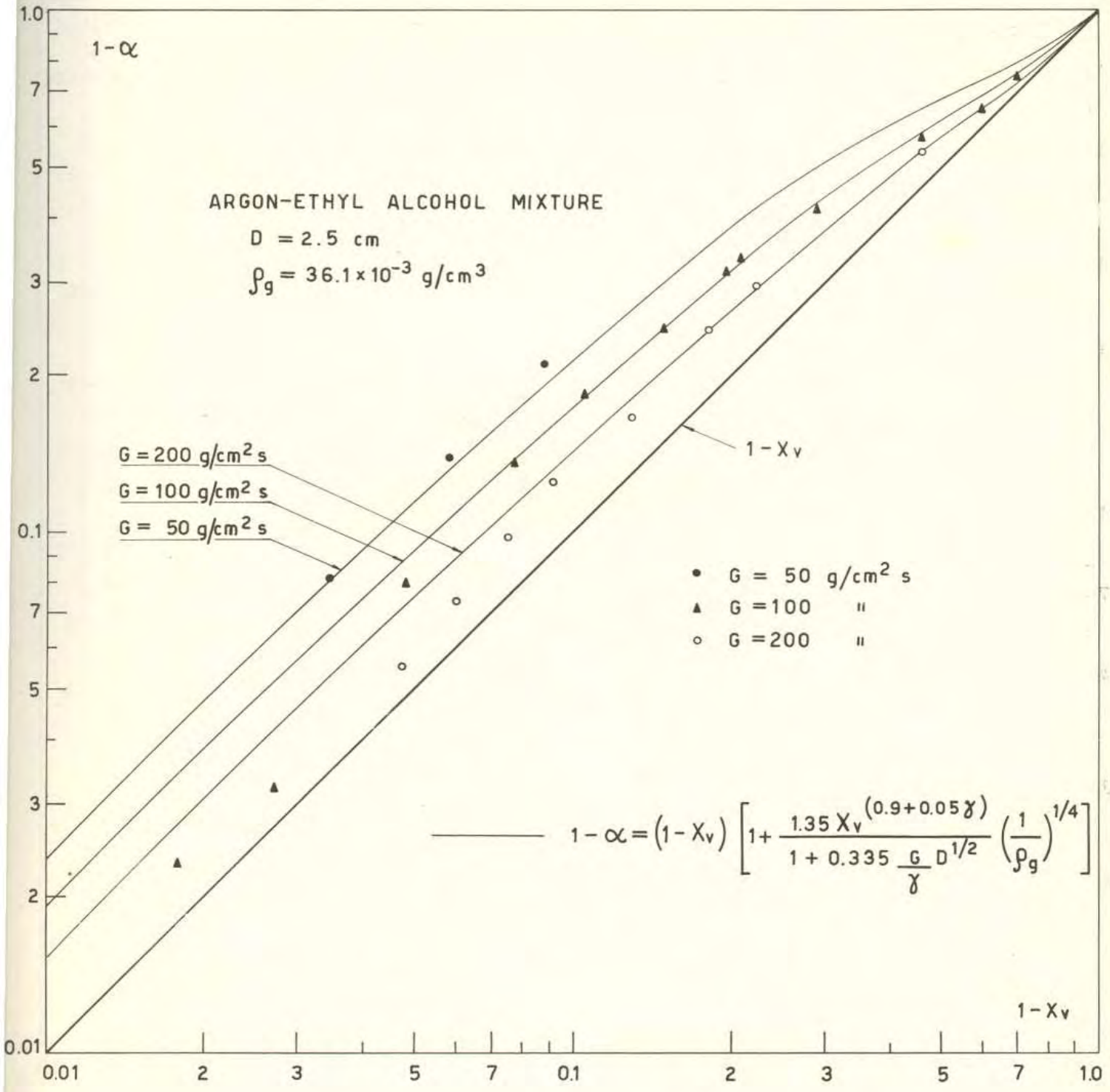

Fig. 25 - Experimental trend of CISE data (interpolated) against that predicted by the present correlation.

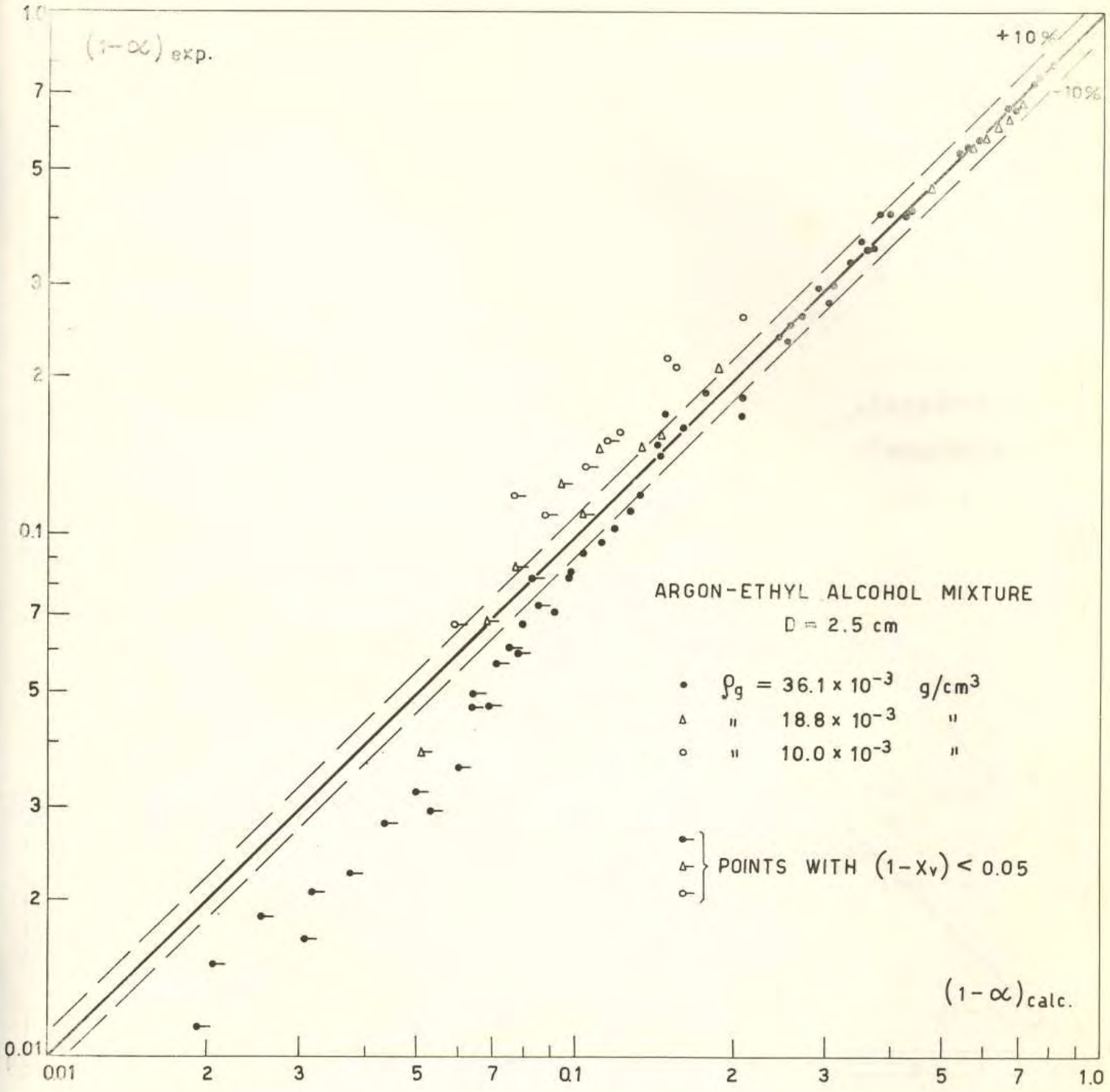

Fig. 26 - CISE experimental data checked against the present correlation for argon-ethyl alcohol mixture.

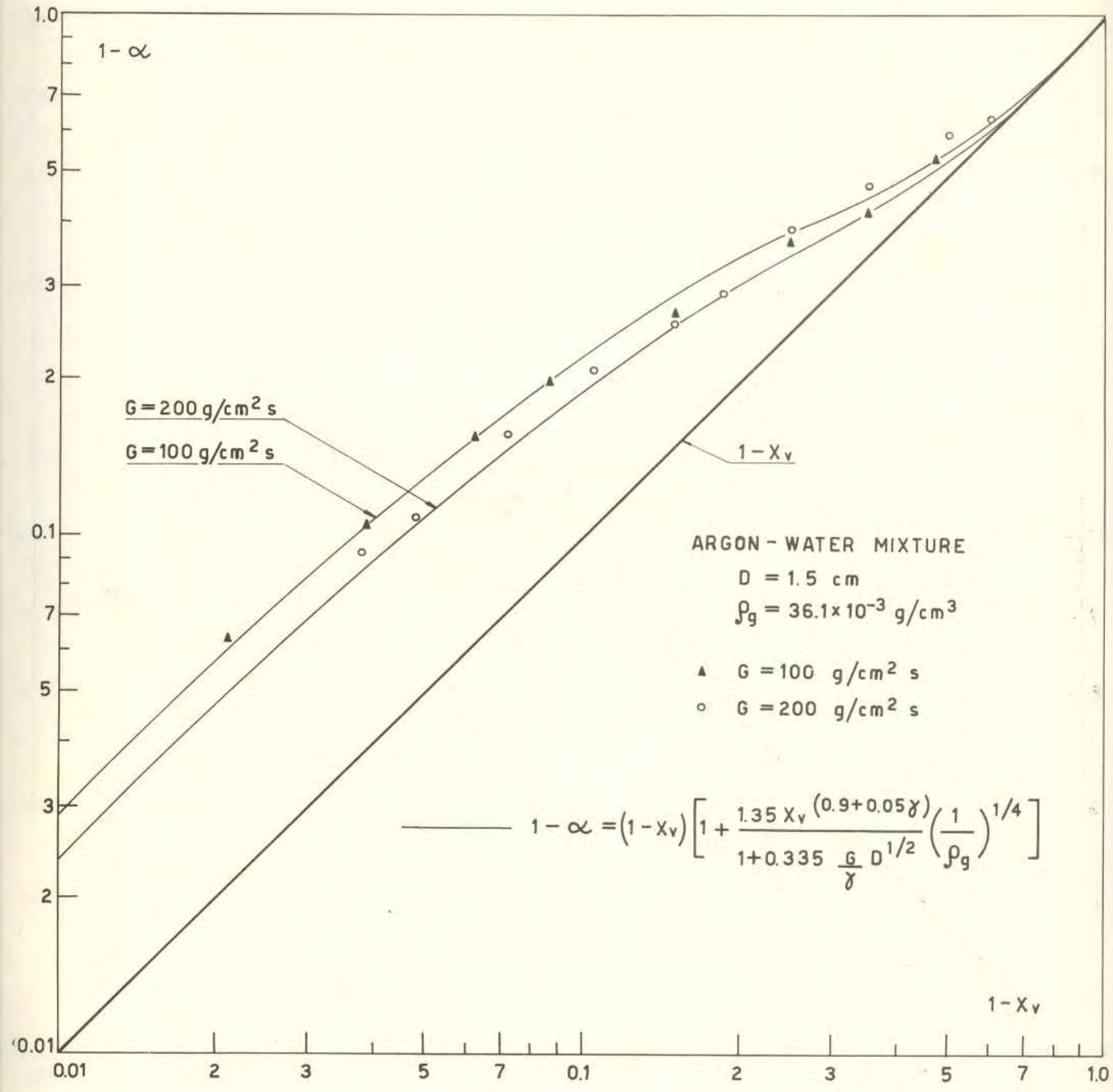

Fig. 27 - Experimental trend of CISE data (interpolated) against that predicted by the present correlation.

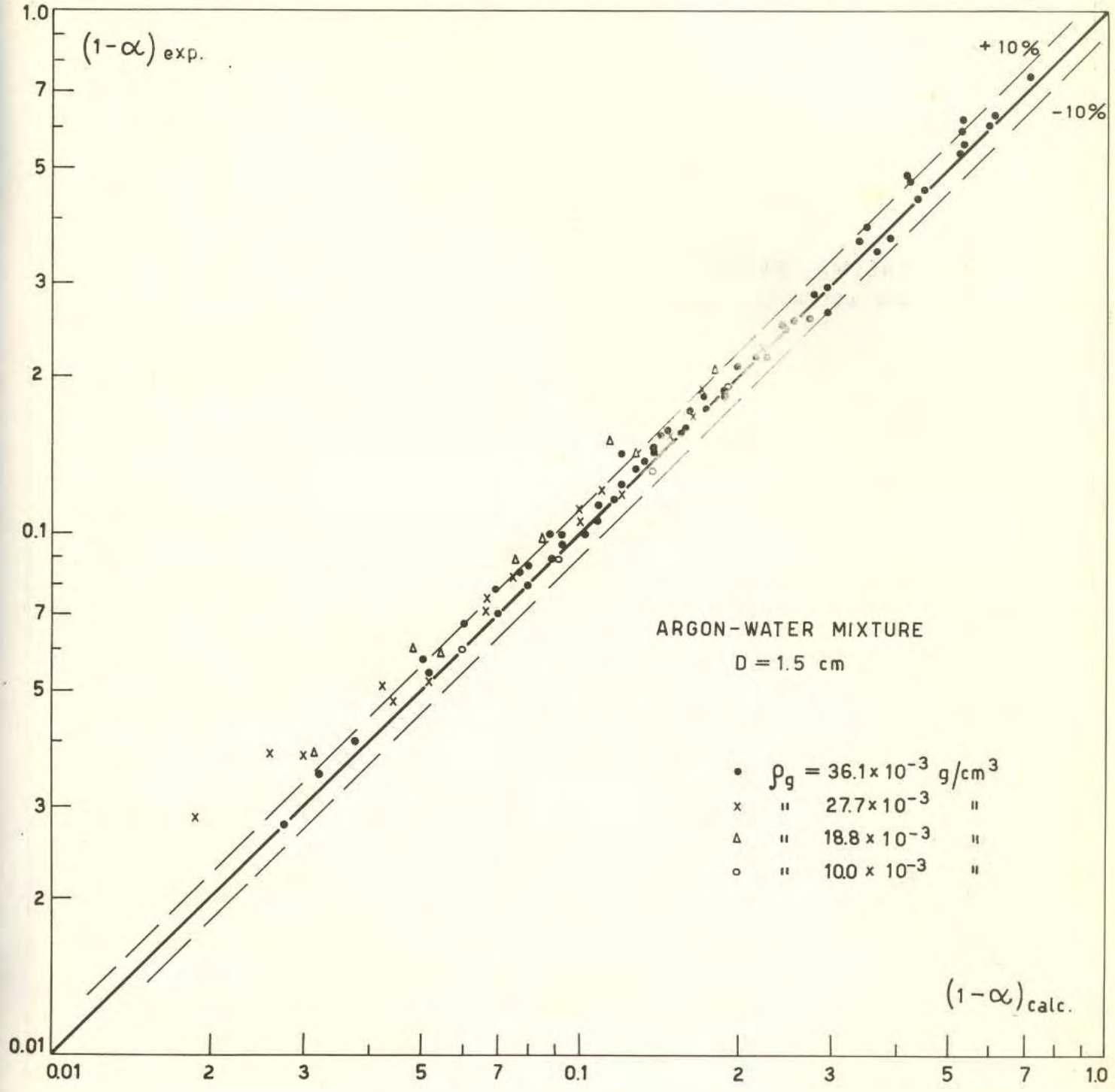

Fig. 28 - CISE experimental data checked against the present correlation for argon-water mixture.

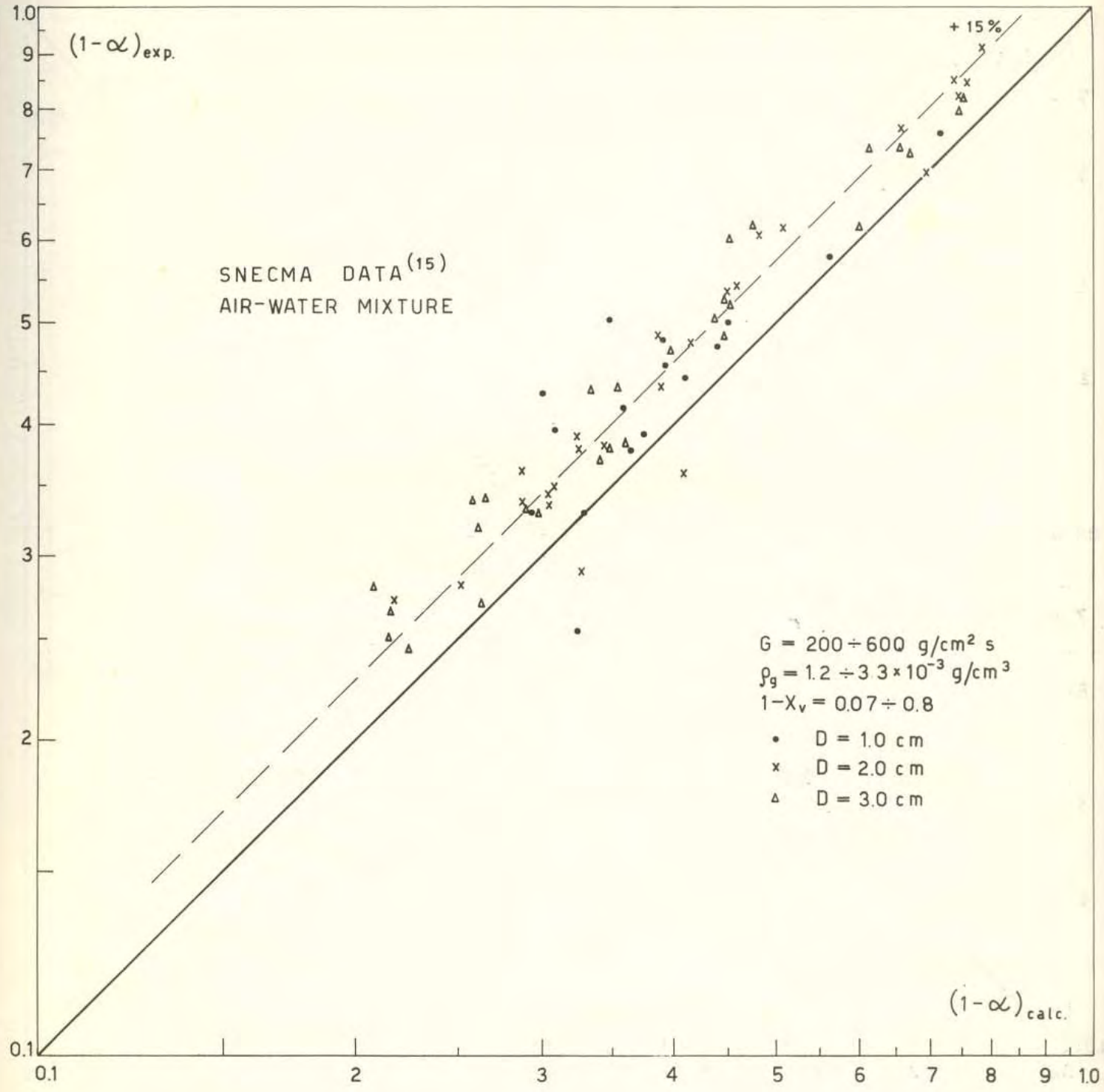

Fig. 29 - SNECMA experimental data checked against the Present correlation for air-water mixture.

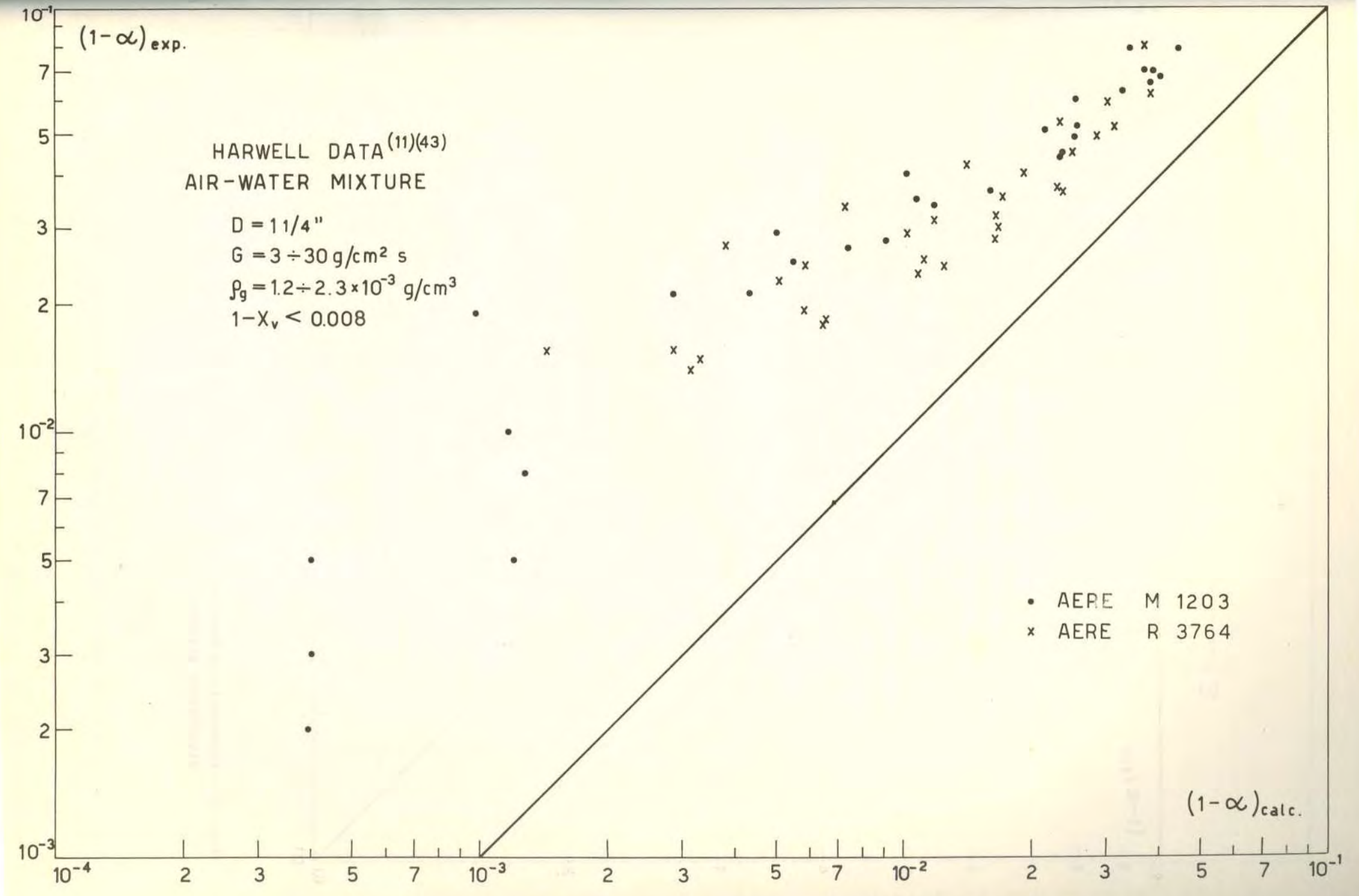

Fig. 30 - Harwell experimental data checked against the present correlation for air-water mixture.

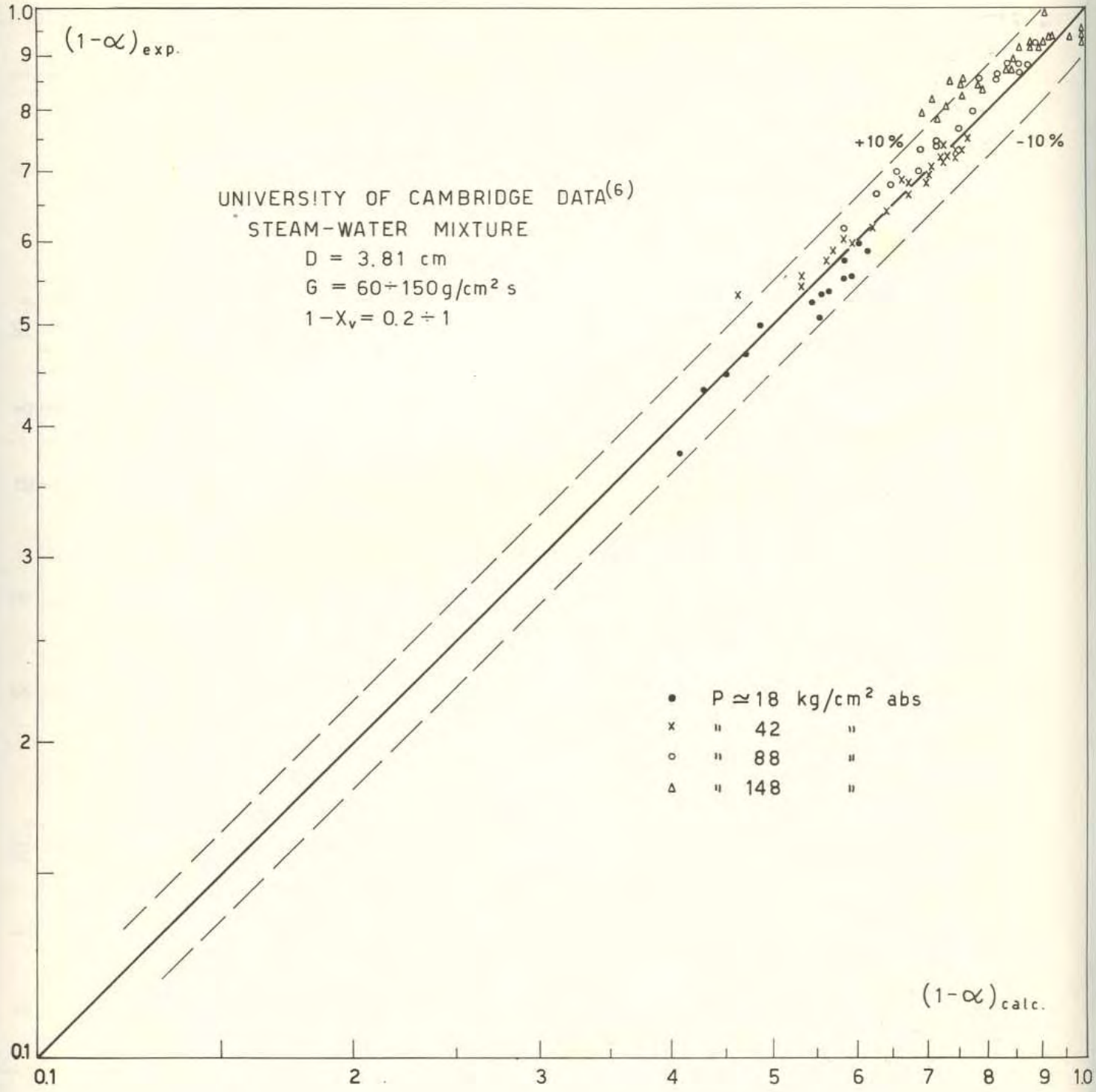

Fig. 31 - University of Cambridge experimental data checked against the present correlation for steam-water mixture.

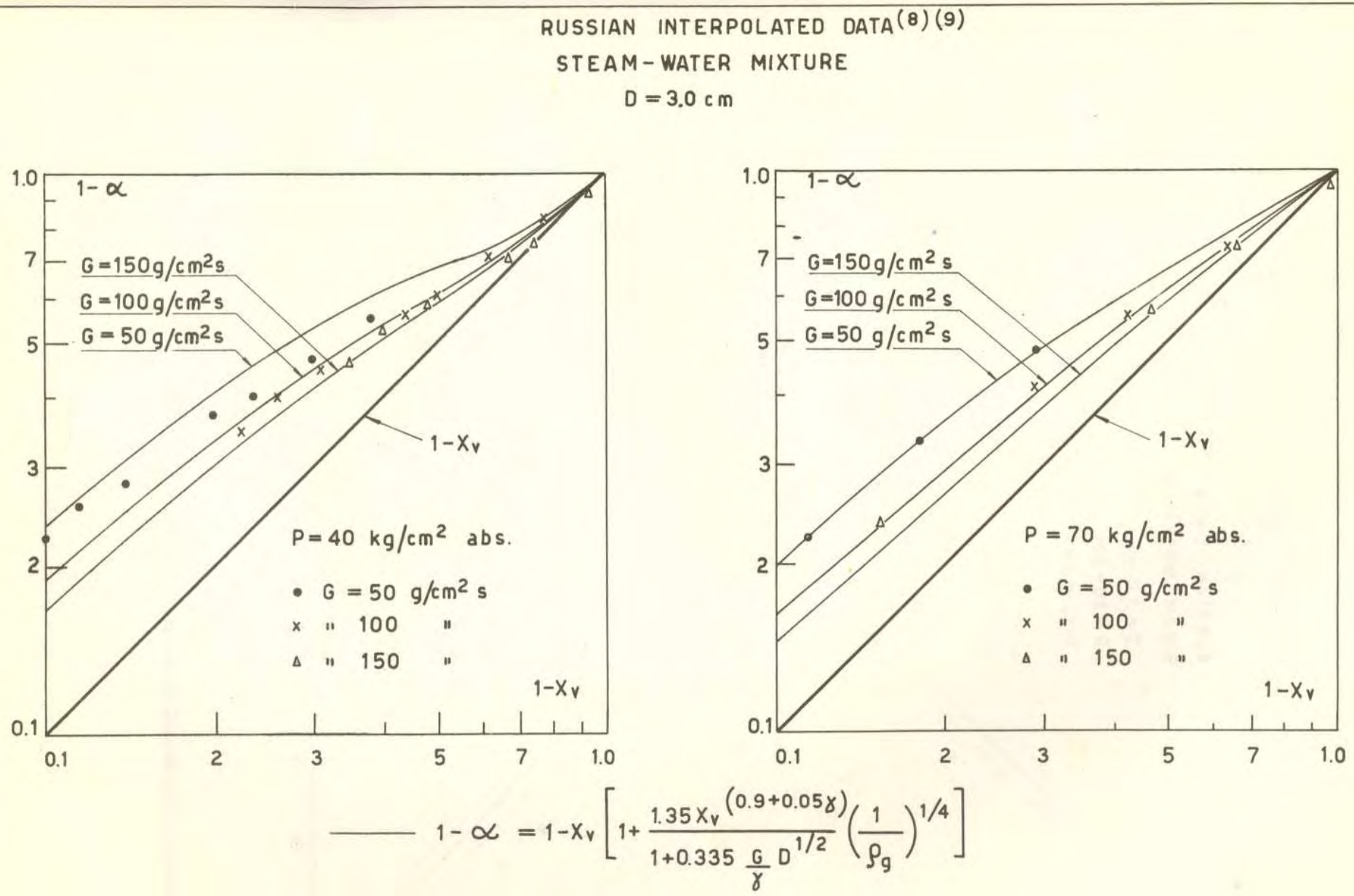

$$1-\alpha = 1-X_v\left[1+\frac{1.35\,X_v^{(0.9+0.05\gamma)}}{1+0.335\,\frac{G}{\gamma}\,D^{1/2}}\left(\frac{1}{\rho_g}\right)^{1/4}\right]$$

Fig. 32 - Experimental trend of russian data (interpolated) against that predicted by the present correlation.

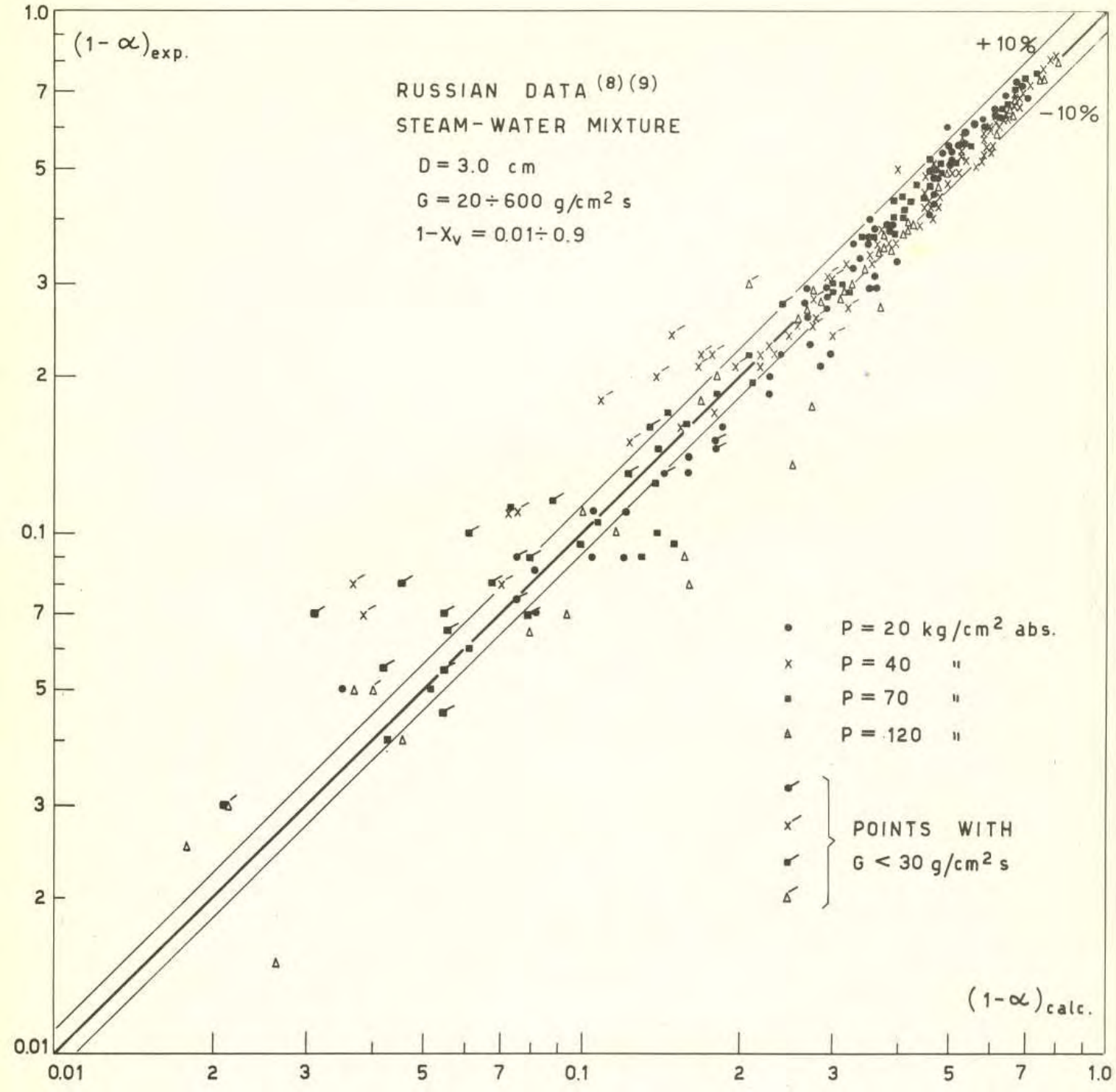

Fig. 33 - Russian experimental data checked against the present correlation for steam-water mixture.

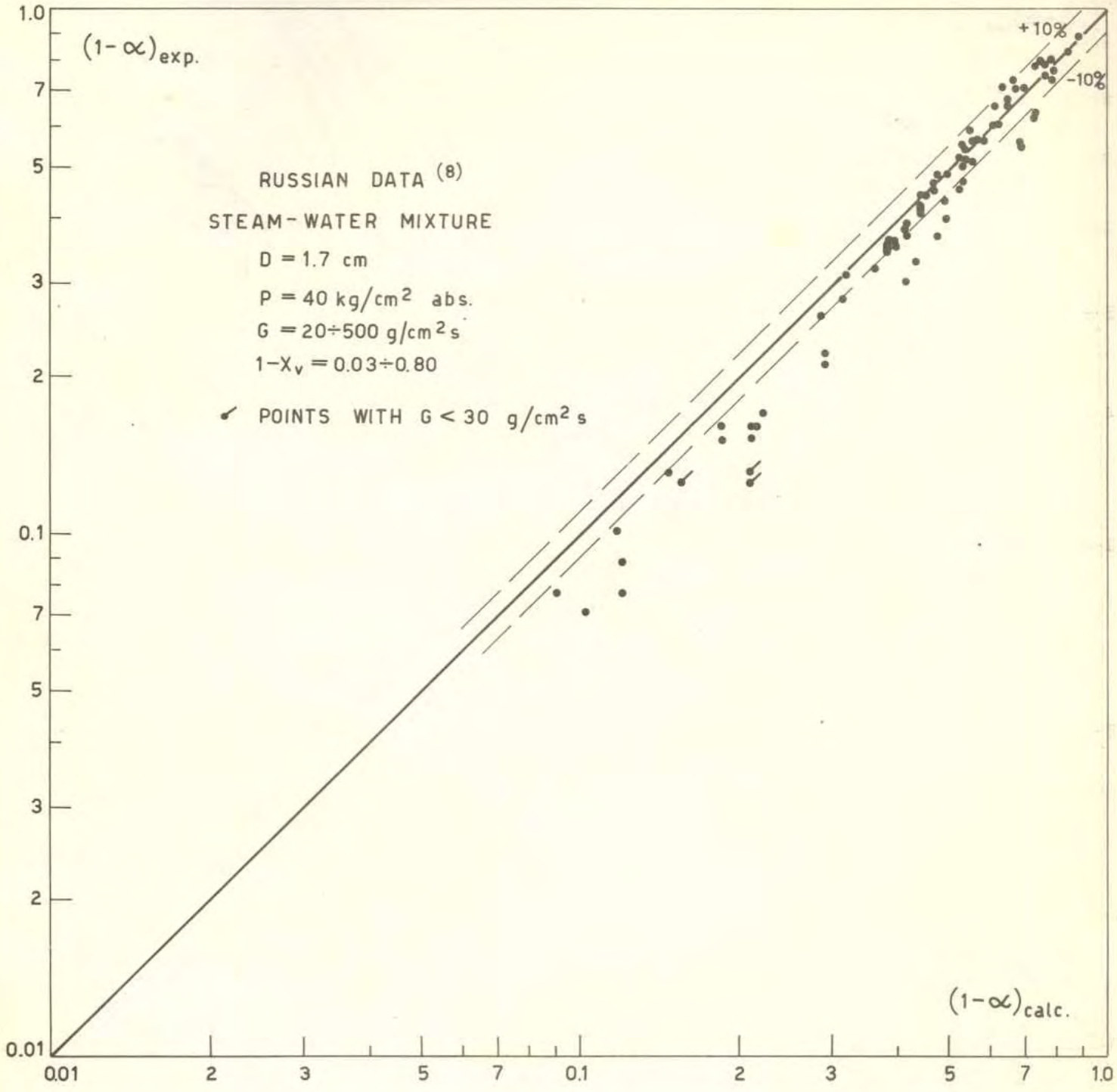

Fig. 34 - Russian experimental data checked against the present correlation for steam-water mixture.

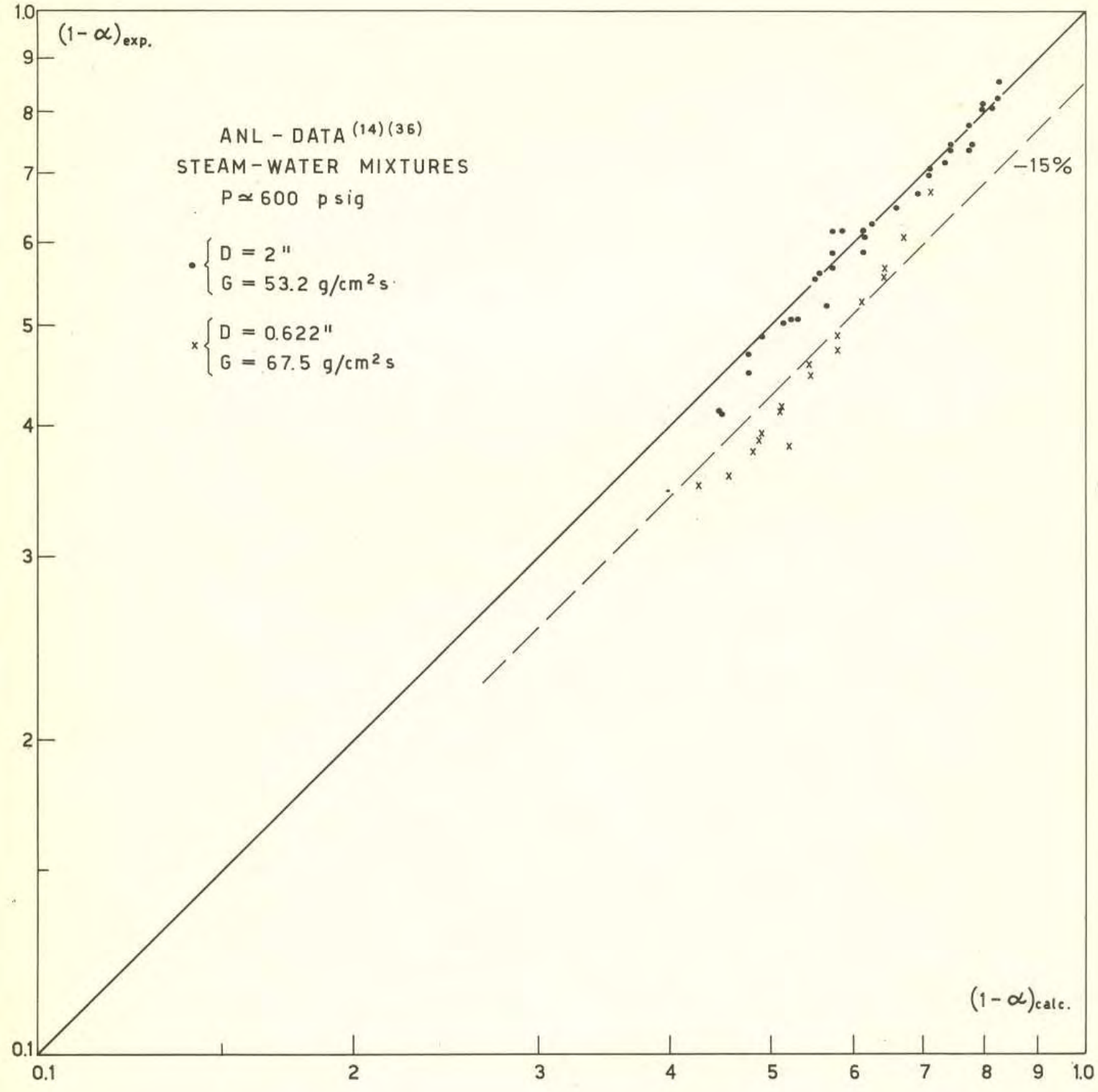

Fig. 35 - ANL experimental data checked against the Present correlation for steam-water mixture.

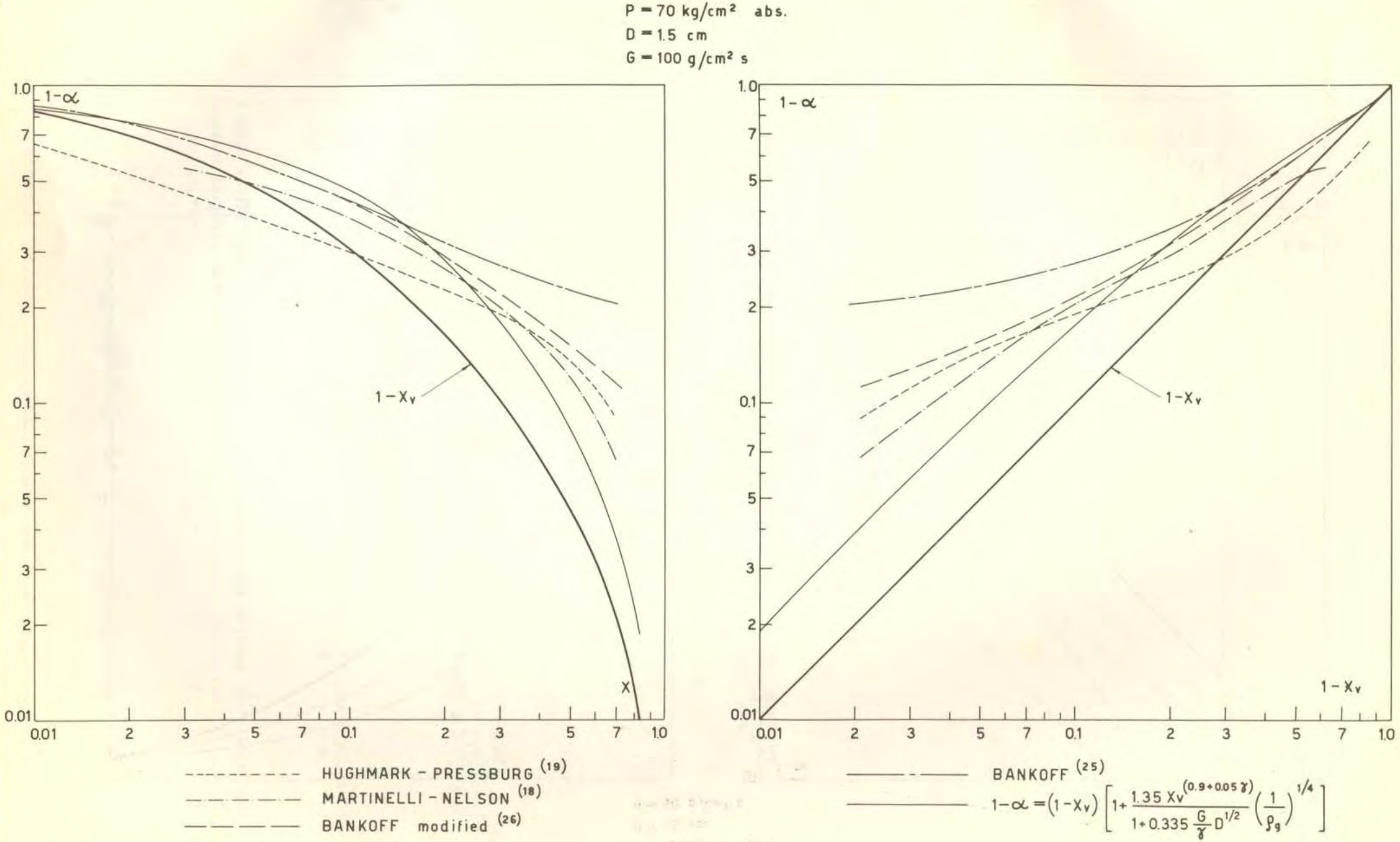

Fig. 36 - Comparison among various correlation for steam-water mixture.

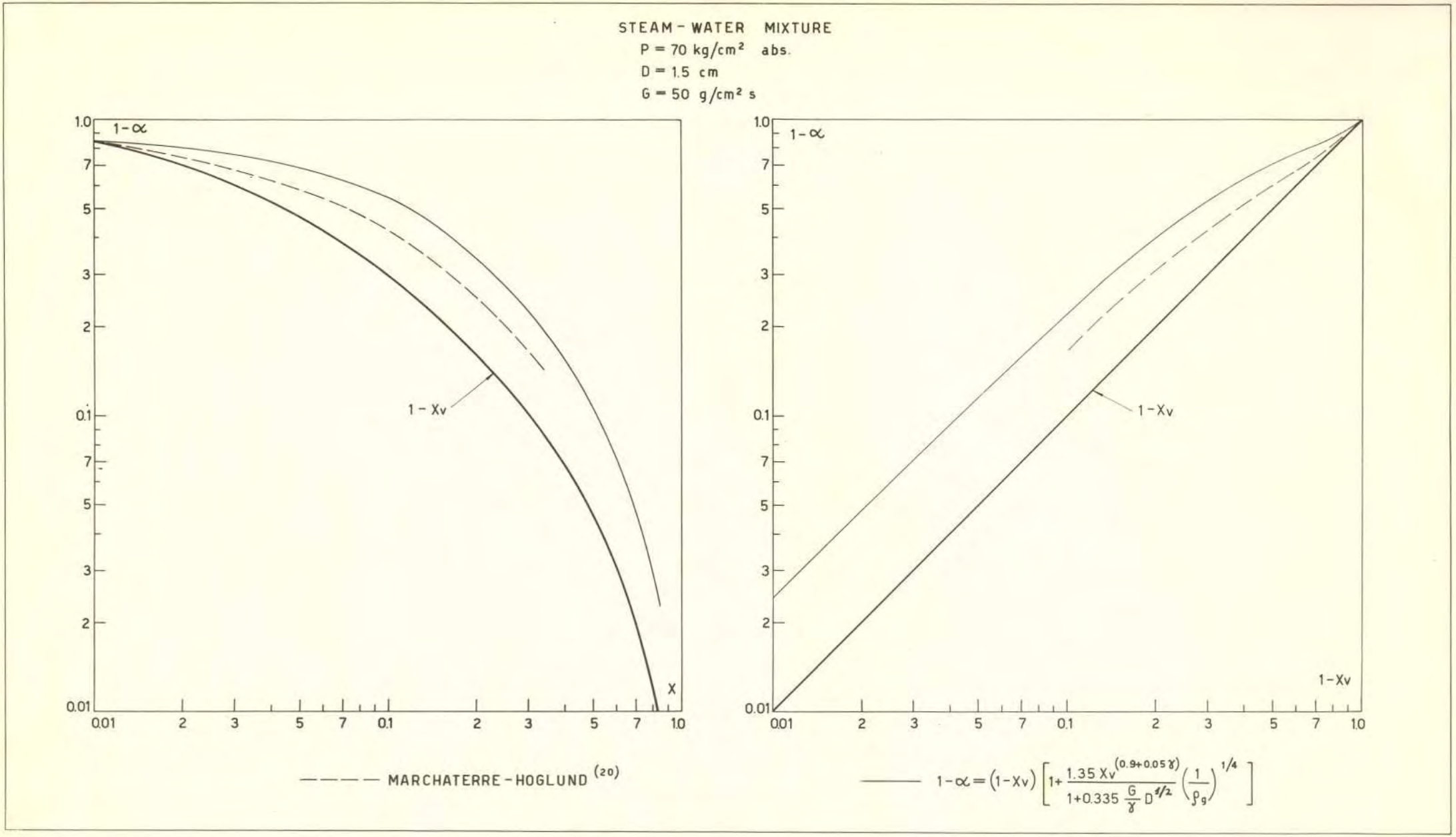

Fig. 37 - Comparison among various correlation for steam-water mixture.

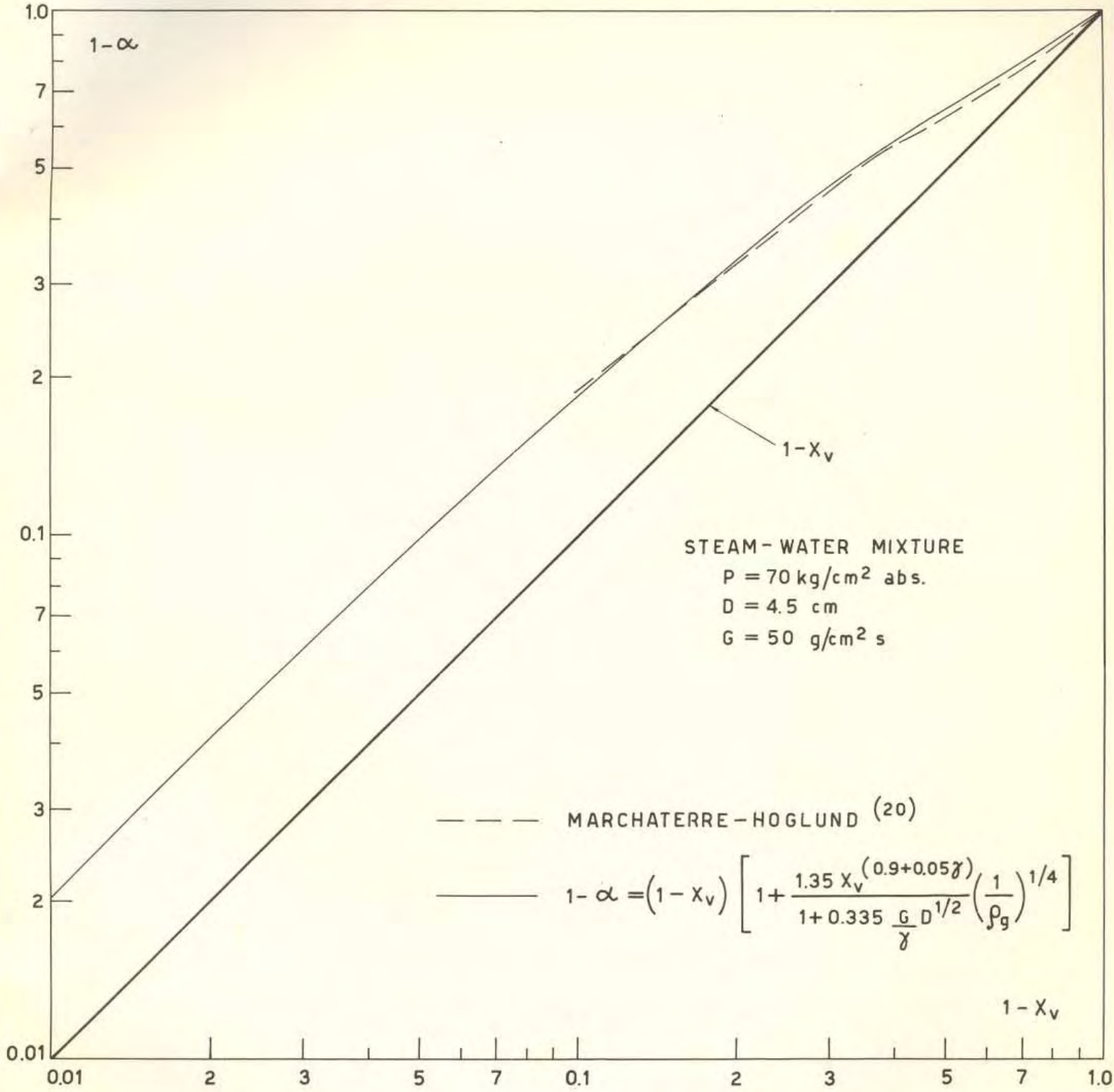

Fig. 38 - Liquid volume fraction as predicted by Marchaterre and Hoglund correlation and the present correlation at D = 4.5 cm.

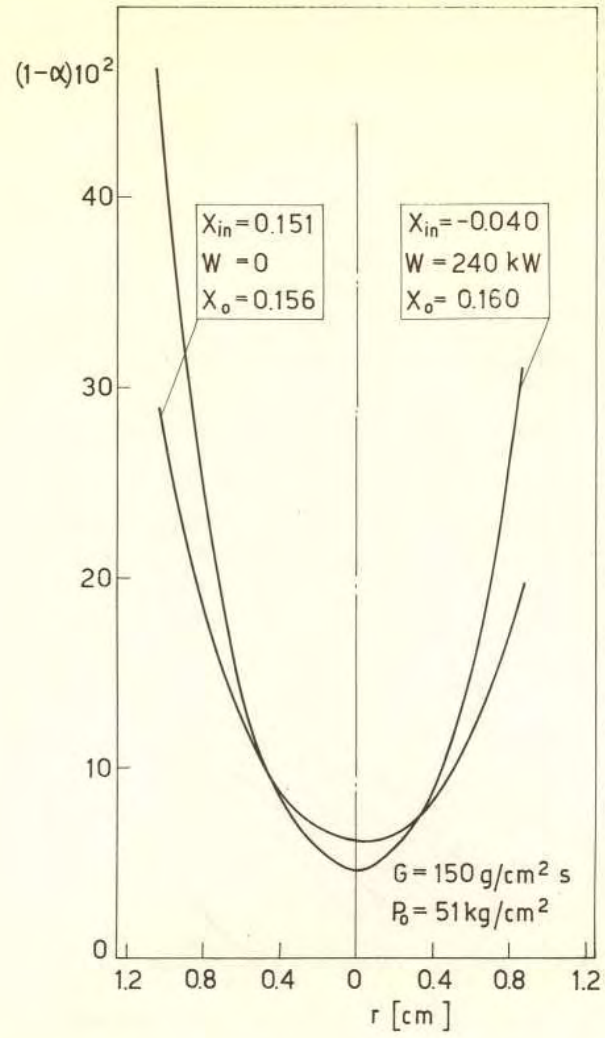

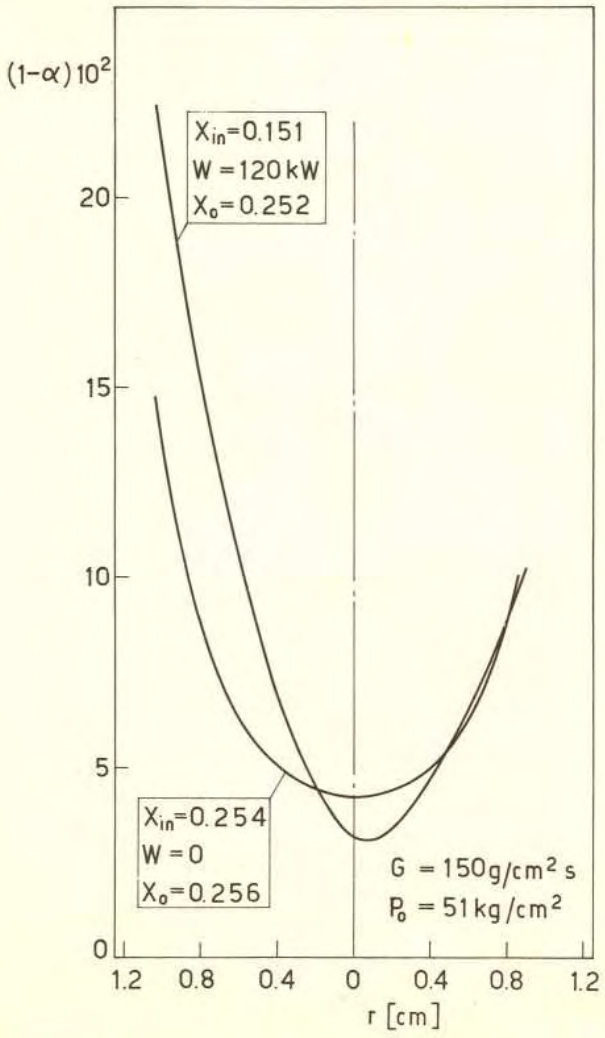

Fig. 39 - Influence of heat transfer on liquid volume fraction with steam-water mixture. Profiles with the same quality at the probe cross section.